ZINC-DEPENDENT POTASSIUM CHANNEL MODULATION MEDIATES NEURONAL APOPTOSIS

By

Patrick Timothy Redman

B.S. Neuroscience, Allegheny College, 2002

Submitted to the Graduate Faculty of the Department of Neurobiology

University of Pittsburgh School of Medicine

in partial fulfillment

of the requirements for the degree of

Doctor of Philosophy

University of Pittsburgh

2008

UNIVERSITY OF PITTSBURGH

Department of Neurobiology

This dissertation was presented

By

Patrick Timothy Redman

It was defended on

October 17, 2008

and approved by

Edwin S. Levitan, Ph.D.
Professor
Department of Pharmacology
and Chemical Biology
Committee Chair

Teresa G. Hastings, Ph.D.
Associate Professor
Department of Neurology

Donald B. DeFranco, Ph.D.
Professor
Department of Pharmacology
and Chemical Biology

Stephen D. Meriney, Ph.D.
Associate Professor
Department of Neuroscience

Michael M. Tamkun, Ph.D.
Professor
Department of Biological
Sciences
Outside Examiner

Elias Aizenman, Ph.D.
Professor
Department of Neurobiology
Major Advisor

ZINC-DEPENDENT POTASSIUM CHANNEL MODULATION MEDIATES NEURONAL APOPTOSIS

Patrick Timothy Redman, Ph.D.

University of Pittsburgh, 2008

Advisor: Elias Aizenman, Ph.D.

The liberation of zinc from intracellular stores during pathophysiological conditions, especially those in which reactive oxygen and nitrogen species have been implicated, is central to the progression of neuronal injury. In addition, cellular efflux of a second ionic species, potassium, is similarly responsible for facilitating apoptotic cell death downstream of the initial oxidant-induced zinc liberation. Potassium efflux is mediated by Kv2.1-encoded potassium channels in apoptotic neurons. Here, I have characterized several critical molecular components that link zinc liberation to the loss of cytoplasmic potassium following oxidative injury. First, electrophysiological and viability studies using Kv2.1 channel mutants identified a p38 phosphorylation site at serine 800 (S800) that is required for Kv2.1 membrane insertion, potassium current enhancement, and cell death. In addition, a phospho-specific antibody for S800 detected a p38-dependent increase in Kv2.1 phosphorylation in apoptotic neurons, and reveals phosphorylation of S800 in immunopurified channels incubated with active p38. Next, I present data indicating that an N-terminal tyrosine of Kv2.1 (Y124), which is targeted by src, is also critical for the apoptotic current surge. These latter studies suggest that Y124 works in concert with the C-terminal serine (S800) target of p38 MAPK to regulate Kv2.1-mediated current enhancement. While zinc was previously shown to activate p38 and src, I demonstrate here that this metal inhibits cytoplasmic protein tyrosine phosphatase ε (Cyt-PTPε), which targets Y124 and antagonizes the actions of src. Therefore, I have identified two requisite phosphorylation sites on Kv2.1, at Y124 and S800, that cooperatively mediate apoptotic potassium current enhancement. Importantly, disruption of either phosphorylation event is neuroprotective. The work presented here provides a more complete understanding of neuronal apoptotic processes by revealing the intracellular signaling events linking intracellular zinc liberation and cytoplasmic potassium efflux.

FOREWARD

This dissertation would not have been possible without the support and guidance of a number of very important people. I would first like to thank all the members of my dissertation committee for providing me with important advice, as well as a different perspective on how to look at my work. I would especially like to thank Dr. Terri Hastings, who accepted me into her lab for the first laboratory rotation of my graduate school career, and has remained as a fantastic advisor since. In addition, I would like to especially thank my dissertation chair, Dr. Edwin Levitan, not only for access to his laboratory when conducting experiments, but most importantly for pushing me to be a better scientist.

I would also like to thank all of the members of the Aizenman Lab whom I was fortunate enough to get to know while my time here. Specifically, thank you Karen Hartnett, Mia Jefferson, Kai He, Mandar Aras, Megan Knoch and Becky Henderson. You have all provided me with indispensible technical assistance, whether it is how to properly treat neurons, or how to properly deliver a seminar talk. You have also been great friends, and have made my time both inside and outside the lab a lot of fun.

Most importantly, I'd like to thank my advisor Elias Aizenman. Elias is a great scientist, wonderful mentor, an endless source of positivity, and has also been a great friend. I could not have had a better graduate training experience.

Finally, I'd like to thank my parents, Timothy and Janet, and my brother, Colin, for their unconditional love and support. You have all inspired me in ways too many to describe. I love you all very much.

TABLE OF CONTENTS

LIST OF FIGURES

SUPPLEMENTARY FIGURES

1. INTRODUCTION

1.1 Overview

Zinc is a ubiquitous, essential metal required for normal cell function, including the regulation of protein structure and function (Frederickson et al., 2005), and modulation of neurotransmission (Frederickson and Bush, 2001). Zinc also has an important role as an ionic second messenger (Pearce et al., 2000; Yamasaki et al., 2007). Although Zn^{2+} is present in all eukaryotic cells, the concentration of Zn^{2+} in the mammalian brain is particularly high (~150μM) (Weiss et al., 2000). Intracellular free, or "chelatable" Zn^{2+} concentrations, however, are in the picomolar to low nanomolar levels under normal conditions, because of the precise regulation of this metal by ionic transport mechanisms, its compartmentalization in organelles, and the presence of a large number of metal binding proteins (Frederickson et al., 1989; Sensi et al., 1997). Nonetheless, pathological conditions that are accompanied by the generation of reactive oxygen and nitrogen species (ROS, RNS) can severely disrupt intracellular Zn^{2+} homeostasis, producing excess free intracellular Zn^{2+} and triggering the activation of cell death cascades in neurons and other cells (Choi and Koh, 1998; Aizenman et al., 2000a; Pal et al., 2004; Capasso et al., 2005).

Another essential ion under tight cellular regulation is potassium. K^+ is the single most abundant free intracellular cation (~140mM), while its extracellular concentration is relatively low (~4mM). This concentration gradient is maintained primarily by the Na^+/K^+-ATPase pump, with contributions from various other ionic transport mechanisms (Panayiotidis et al., 2006).

This concentration gradient drives the efflux of intracellular potassium when permeable routes for ionic movement, such as voltage-gated K^+ channels, are made available. Importantly, increasing evidence supports the notion that these gateways for K^+ efflux are indispensable mediators of the execution phase of neuronal apoptosis (Yu, 2003a). When the intracellular K^+ concentration decreases during pathophysiological conditions, cell death programs can be completed (Bortner and Cidlowski, 2007). Until recently, dysregulation of either Zn^{2+} or K^+ were often considered in isolation within the context of neuronal injury. However, it is now known that the sequential disruption in the homeostatic regulation of both these ions is part of a continuum along a common apoptotic signaling pathway (Pal et al., 2004). In this dissertation, I sought to more completely characterize the intracellular signaling events connecting Zn^{2+} and K^+ dysregulation that regulate oxidant-induced neuronal apoptosis.

1.2 Apoptosis.

Apoptosis is a form of programmed cell death in multicellular organisms associated with distinct biochemical signaling events. Apoptosis was originally described in anatomical terms (Kerr et al., 1972), as these biochemical signaling events lead to characteristic morphological changes including cell shrinkage, membrane blebbing, chromatin condensation, loss of cell attachment, and DNA fragmentation (Taylor et al., 2008). The regulated signaling network and the resulting morphological changes normally serve to dispose of unwanted cells in a manner that elicits minimal damage to the immediate extracellular environment and neighboring cells. This is achieved by signaling to phagocytes via the externalization of the plasma membrane associated phosphatidylserine (Martin et al., 1995). Recruited phagocytes then serve to engulf

and remove apoptotic cell remains, protecting the nearby extracellular environment (Kerr et al., 1972). Efficient removal of apoptotic debris distinguishes this form of cell death from necrosis, which is generally regarded as an acute traumatic insult leading to a disruption in membrane integrity and release of cellular contents into the extracellular space. Thus, one overall objective of apoptosis is to avoid necrotic cell lysis, as it inevitably leads to an inflammatory immune response, and further exacerbation of the initial injury. Because the wide variety of cell injury processes can result in both traditional apoptotic and necrotic morphologies, it is critical to characterize the biochemical signaling events when defining a particular form of cell death. For instance, our laboratory has described both caspase-dependent (McLaughlin et al., 2001) and caspase-independent (Du et al., 2002; Zhang et al., 2007) cell death pathways resulting from the liberation of intracellular Zn^{2+} by two distinct injurious stimuli. Since the term "apoptosis" was coined (Kerr et al., 1972), research has characterized a wide range of apoptotic biochemical signaling cascades, some conserved and some unique to specific pathophysiological circumstances.

Much attention has been given to cell death signaling events mediated by mitochondria, as many pro- and anti-apoptotic signaling molecules function within this organelle to ultimately determine cell fate. For instance, the so-called "intrinsic" pathway is initiated by severe cellular stressors such as growth factor withdrawl, DNA damage and endoplasmic reticulum (ER)-stress (Taylor et al., 2008). The intrinsic pathway is primarily regulated by the actions of the β cell lymphoma (BCL-2) protein family. The BCL-2 family is made up of three subfamilies (either pro- or anti-apoptotic) containing between one and four BCL-2 homology (BH) domains (Taylor et al., 2008). When the injurious stimulus is sufficient to overcome inhibition by the anti-

apoptotic BCL-2 family members, pro-apoptotic proteins, such as BAK and BAX, have been proposed to form oligomeric channels in mitochondrial outer membranes, presumably permitting the release of cytochrome c into the cytoplasm (Riedl and Salvesen, 2007). Cytochrome c then binds the cytoplasmic protein Apaf-1, forming the cell death signaling complex known as the apoptosome, which is necessary for activation of caspase 9 (Riedl and Salvesen, 2007). Caspase 9, in addition to caspase 2, 8 and 10 function as initiator caspases, or cysteine proteases that cleave effector caspases. Effector caspases are normally present in the cytoplasm as inactive precursor proteins, or pro-caspases, but are activated following proteolytic cleavage of the pro-peptide domain. Effector caspases (3, 6, and 7) then cleave other cellular substrates such as the actin cytoskeleton, nuclear envelope, and cell adhesion sites, resulting in apoptosis (Taylor et al., 2008). In contrast to the intrinsic pathway, the "extrinsic" pathway is activated when death-promoting ligands, such as Fas ligand (FasL) or Tumor necrosis factor α (TNFα), bind to membrane resident death receptors. Following ligand binding, adaptor proteins associated with the receptors recruit and promote activation of caspase 8, which can bypass the mitochondria and activate caspase 3 and 7 directly. Regardless of which pathway is initiated, the bulk of death-inducing proteolytic events observed during apoptosis are carried out by activated caspase 3, caspase 6 and caspase 7 (Creagh et al., 2003). Furthermore, not only have extrinsic and intrinsic pathways been shown to converge in certain cell death paradigms, but various forms of caspase-independent cell death have also been described (Taylor et al., 2008). In this thesis, I will describe the contribution of Kv2.1-encoded K^+ channels downstream of intracellular Zn^{2+} liberation during caspase dependent neuronal apoptosis (McLaughlin et al., 2001) via a relatively unexplored regulatory mechanism of cell death.

1.3 Oxidative stress and neurotoxicity.

Despite the variety of biochemical signaling cascades implicated in neuronal injury, there is considerable evidence suggesting that oxidative stress is a critical component of apoptotic cell death. Oxidative stress results from the excess production of reactive oxygen species (ROS) due to dysregulation in the normal balance between cellular oxidant production and anti-oxidant mechanisms. ROS are a family of oxygen containing molecules, some of which have an unpaired electron, and can be particularly damaging to cellular components such as proteins, lipids and DNA. ROS include superoxide anion ($O_2^{\cdot -}$), hydoxyl radical ($OH^{\cdot}$), and hydrogen peroxide (H_2O_2). Superoxide also damages cellular components by readily reacting with nitric oxide (NO) to form the highly reactive peroxynitrite ($ONOO^-$), a member of the reactive nitrogen species (RNS) family. Similar to studies of apoptosis, investigations of ROS- and RNS-mediated neuronal injury have also widely implicated mitochondria, as deficits in the energy generating electron transport chain are linked to ROS generation. Indeed, ROS production is a defining characteristic of several Parkinson's disease animal models, such as exposure to rotenone or 1-methyl-4-phenyl-1,2,3,6-tetrahydrophyridine (MPTP) (Mattson, 2000). Together, oxidative and nitrative stress can trigger cellular injury and apoptosis, and have been implicated in the pathogenesis of many additional acute and chronic neurodegenerative conditions, including stroke, epilepsy, Alzheimer's disease and amyotrophic lateral sclerosis (Shibata and Kobayashi, 2008). Indeed, treatment with antioxidants such as glutathione, ascorbic acid and superoxide dismutase is sometimes sufficient to protect neurons in *in vitro* and *in vivo* models of ischemia (Mattson, 2000), and in *in vitro* models of Alzheimer's disease, Parkinson's disease and

amyotrophic lateral sclerosis (Di Matteo and Esposito, 2003). The mechanism by which particular cellular populations in these disease states are vulnerable to oxidative stress is an area of current, intense investigation. It is important to mention, however, that ROS are not always associated with injury, and that they also participate in signaling processes important for normal physiological responses, including proliferation and survival (Tonks et al., 2006).

1.4 Oxidative liberation of intracellular Zn^{2+}.

Of the total Zn^{2+} content in the brain, only 10% is free or chelatable and is restricted to a population of glutamate-containing synaptic vesicles (Frederickson et al., 1989). The majority of the cellular Zn^{2+} is complexed to proteins such as metallothionein (MT), Zn^{2+} finger-containing transcription factors (Frederickson et al., 2005; Maret and Krezel, 2007), and other functional proteins, like kinases and phosphatases (Korichneva, 2006). Nonetheless, Zn^{2+} can be liberated from some of these stores by either oxidative stimuli or NO-related species (Maret, 1994; Aizenman et al., 2000b; Frederickson et al., 2002; Frederickson et al., 2004). Moreover, products of lipid peroxidation have also been recently shown to trigger intracellular Zn^{2+} release, thereby linking a common oxidative stress product directly to Zn^{2+}-mediated signaling (Hao and Maret, 2006). Maret and Vallee (1998) have pointed out that MT-bound Zn^{2+} is readily released by thiol oxidants, because of MT's relatively negative redox potential (-366 mV). Hence, even though this metalloprotein has a relatively high affinity for Zn^{2+} (K_d=1.4 x 10^{-13} M), oxidants acting as cellular signals can rapidly and effectively induce the transfer of Zn^{2+} from MT to other proteins with lower affinities for this metal (Maret, 2006). Under injurious oxidant conditions however, the liberated Zn^{2+} becomes a significant trigger for neuronal injury (Pal et al., 2004).

1.5 Role of Zn^{2+} in neuronal injury.

Zn^{2+} has been referred to as the "calcium of the twenty-first century" (Frederickson et al., 2005), as many of the roles of Zn^{2+} in the central nervous system have just begun to be fully appreciated, including its newly recognized function as a second messenger (Pearce et al., 2000; Yamasaki et al., 2007). Nonetheless, Zn^{2+}-mediated neurodegeneration studies now span nearly two decades since this metal was first shown to be directly toxic to neurons (Yokoyama et al., 1986; Choi et al., 1988). In nearly all of the initial studies in this field, neuronal cell death was proposed to be mediated by the influx of synaptically released Zn^{2+} into cells (Weiss et al., 1993). Zn^{2+}-induced injury was shown to be blocked by antagonists of potential entry sites for this metal, such as Ca^{2+}-permeable voltage- and glutamate-gated ion channels, as well as by cell-impermeant metal chelators (Colvin et al., 2003). The balance between the physiological and pathophysiological actions of Zn^{2+} closely resembles those which have been described for Ca^{2+} (Choi, 1995). Zn^{2+}, like Ca^{2+}, is a selective ligand for a metabotropic receptor (Hershfinkel et al., 2001; Hershfinkel et al., 2007), can be sequestered by intracellular organelles such as mitochondria (Sensi et al., 2003), is bound to metal chaperone proteins such as metallothionein (MT) (Maret, 2006) and is regulated by plasma membrane transporters (Sekler et al., 2007), all of which work in unison to maintain intracellular Zn^{2+} homeostasis, similar to Ca^{2+} regulation (Colvin et al., 2003). Additionally, like Ca^{2+}, Zn^{2+} is an important component of several molecular signaling pathways (Frederickson et al., 2005). Interestingly, a recent study suggested that some of the previously proposed neurotoxic mechanisms of intracellular Ca^{2+} dysregulation may be actually due to Zn^{2+} (Stork and Li, 2006).

Cellular Zn^{2+} influx has been associated with neuronal damage resulting from ischemia, trauma and epilepsy, among other disorders. Free (chelatable) Zn^{2+} is present in synaptic vesicles (Frederickson et al., 1989; Frederickson et al., 1992), and is generally believed to be synaptically released and enter postsynaptic neurons (Weiss et al., 2000). Despite these reports, some controversy exists, as reports have also provided evidence suggesting that vesicular Zn^{2+} might not be released into the synapse (Kay, 2003; Lavoie et al., 2007). Also, intracellular Zn^{2+} accumulation and neurotoxicity is sustained in mice lacking vesicular Zn^{2+} (Lee et al., 2000; Lee et al., 2003), demonstrating synaptic Zn^{2+} is not the only death-inducing source of this metal. Regardless of the origin of Zn^{2+}, the significance of Zn^{2+}-mediated neuronal injury is best exemplified by the observation that Zn^{2+} chelation is neuroprotective in *in vivo* models of neuronal injury, including ischemia (Calderone et al., 2004; Choi et al., 2006) and head trauma (Suh et al., 2000).

1.6 Mechanisms of Zn^{2+} neurotoxicity.

The mechanisms by which an increase in intracellular free Zn^{2+} induces neuronal cell death in neurodegenerative disorders are not completely understood. Zn^{2+} is redox inactive (Maret, 2006) and, as such, is likely to be relatively non-toxic by itself. Several mechanisms have therefore been suggested to account for the toxic actions of this metal. (Manev et al., 1997) first proposed that Zn^{2+} can enter mitochondria and induce the release of oxygen-derived free radicals. Zn^{2+} also affects several key components of mitochondrial function (Kleiner, 1974), in addition to inducing permeability transition (Wudarczyk et al., 1999; Jiang et al., 2001),

inhibiting mitochondrial movement (Malaiyandi et al., 2005), and activating mitochondrial multi-conductance channels associated with cell death signaling molecules (Bonanni et al., 2006). Furthermore, Zn^{2+} can inhibit glycolysis and deplete nicotinamide adenine dinucleotide (NAD^{+}), an essential coenzyme that regulates cellular redox reactions (Sheline et al., 2000). Although each of these studies has contributed significantly to our understanding of Zn^{2+} toxicity, the specific signaling pathways that contribute to Zn^{2+}-induced injuries are incomplete, and remain important and critical areas of study.

Zn^{2+}-associated cellular injury has been implicated in both caspase-dependent and independent cell death pathways (Kim et al., 1999; McLaughlin et al., 2001; Du et al., 2002; Bossy-Wetzel et al., 2004). The activation of these divergent pathways has been linked to the intensity of Zn^{2+} exposure (Kim et al., 1999). Other factors, such as regulation of Zn^{2+}-dependent transcription factors (Park and Koh, 1999), activation of kinases (Noh et al., 1999; McLaughlin et al., 2001; Du et al., 2002) and generation of reactive oxygen species (Noh and Koh, 2000), as well as the release of apoptosis-inducing molecules (Jiang et al., 2001) and activation of death induction proteins (Bonanni et al., 2006), likely determine the cellular processes by which neurons die following Zn^{2+} exposure. Importantly, Zn^{2+} can also *prevent* apoptosis under certain circumstances (Fraker and Telford, 1997), and the depletion of this metal can be deleterious to cells (Ahn et al., 1998).

1.7 Potassium channels and apoptosis.

Potassium channels are integral proteins that selectively permit potassium ions to cross the cell membrane. Potassium channels are comprised of pore-forming α subunits that assemble into homo- or hetero-tetramers and are sometimes associated with auxillary regulatory β subunits (Trimmer and Rhodes, 2004). Over 100 genes encoding K^+ channel α subunits have been identified, making them the most diverse group of ion channels in the mammalian genome (Trimmer and Rhodes, 2004). Despite this diversity, all K^+ channels share a homologous pore loop domain that is responsible for K^+ ion selective permeability (Choe, 2002). Potassium channels are widely expressed and contribute to a variety of neuronal functions, including establishing cellular resting potential and repolarization during an action potential.

There are four major classes of K^+ channels: Ca^{2+}-activated (K_{Ca}), inward rectifying (K_{ir}), tandem pore domain (K_{2P}), and voltage gated (Kv), characterized as such according to their structure and function (Choe, 2002). Calcium-activated potassium channels permeate K^+ ions in response to intracellular Ca^{2+} and contain one pore and six transmembrane domains (Burg et al., 2006). Inward rectifier channels contain two transmembrane domains, one pore domain, and pass K^+ current more easily into the cytoplasm than into the extracellular space, contributing to a cells resting membrane potential (Burg et al., 2006). Tandem pore domain channels or "leak channels" contain four transmembrane domains and two pore domains, are constitutively open and contribute to the negative resting membrane potential of neurons (Burg et al., 2006). Voltage-gated (Kv) K^+ channels contain six transmembrane domains (S1-S6), one pore domain, and are permeable to K^+ ions in response to changes in transmembrane voltage (Burg et al.,

2006) detected by the voltage-sensing S4 domain (Cha et al., 1999). The N-terminal tetramerization or T1 domain is a common component in all Kv channels, and is required for assembly of individual subfamily-specific α subunits and formation of functional channels (Papazian, 1999). In addition to channel assembly, the T1 domain is the site of β auxillary subunit binding in Kv1 and Kv4 channels, which regulates channel gating, trafficking and subcellular localization (Li et al., 2006). Certain Kv channels can adopt an inactivated conformation in which K^+ ion movement is blocked despite a change in membrane voltage. Two primary types of inactivating Kv channels have been identified. While rapidly inactivating (A-type) channels display millisecond inactivation, delayed rectifying channels take seconds to inactivate (Pongs et al., 1999). Several mechanisms of inactivation have been recognized. C- and P-type inactivation is correlated with a structural rearrangement of the α subunit C-terminals, while N-type inactivation is mediated by "ball and chain" domains of the amino terminal of certain α and β subunits (Pongs et al., 1999).

1.7.1 Kv2.1

Voltage-gated potassium channels play a critical role in cell function by governing processes such as maintaining proper ionic gradients and regulating cellular excitability. There are 12 subfamilies of Kv channels, encoded by distinct genes (Gutman et al., 2005), that are composed of the aforementioned six transmembrane and one pore forming domain in addition to N- and C-terminal cytoplasmic tails (Long et al., 2005). Kv2.1, a product of the human *KCNB1* gene, is the primary delayed-rectifying K^+ channel expressed in most neurons. In cortical and hippocampal neurons, Kv2.1 α homotetramers are localized in large somatodendritic clusters

(Trimmer, 1991). Kv2.1 does not generally participate in neuronal repolarization during single action potentials due to an elevated voltage-dependent activation threshold and slow activation kinetics (Du et al., 2000; Surmeier and Foehring, 2004). Instead, under normal conditions Kv2.1 activates slowly following depolarization and functions to suppress neuronal excitability during repeated, high frequency synaptic stimulation (Misonou et al., 2005).

Both Kv2.1 intracellular termini play important roles in regulating channel function, as phosphorylation and dephosphorylation events on the intracellular termini have been shown to modulate Kv2.1 gating and subcellular localization. A number of serine, threonine and tyrosine kinases are known to target and modify Kv2.1 channels. The majority of well described phosphorylation and dephosphorylation events reported for Kv2.1 had been shown to strongly influence channel gating and neuronal excitability (Park et al., 2006), but not apoptosis. Following an apoptotic insult, alterations in the voltage-dependence of membrane-resident channels have not been observed, a phenomenon that has been reported by others to accompany non-lethal neuronal injury (Misonou et al., 2004; Misonou et al., 2005a). In those cases, calcineurin-dependent dephosphorylation of multiple intracellular sites on Kv2.1 participate in the graded regulation of channel activation. The dynamic regulation of calcineurin-sensitive sites on Kv2.1 is responsible for suppressing neuronal firing during periods of high activity (Misonou et al., 2005b), as dephosphorylation of these sites lowers the voltage threshold for channel activation (Mohapatra et al., 2007). This hyperpolarizing shift in Kv2.1 activation has been proposed to be a neuroprotective response to excitotoxic injury induced by epileptic seizures and ischemic insults (Misonou et al., 2005b).

An association between the Kv2.1 C-terminal and an undefined retention protein is hypothesized to regulate the clustered subcellular distribution in neurons (O'Connell et al., 2006). Interestingly, single Kv2.1 channels are remarkably mobile within channel clusters, and sometimes randomly move between individual clusters (Tamkun et al., 2007), indicating that a sustained physical association between Kv2.1 and an unknown scaffolding protein does not govern clustering. In addition, calcineurin dephosphorylation of the intracellular termini regulates the cluster dispersion accompanying high frequency neuronal activity (Misonou et al., 2004). Accordingly, it has been proposed Kv2.1 clusters are maintained by an actin cytoskeleton perimeter fence, which contains channel retention proteins that can only associate with Kv2.1 when the C-terminal calcineurin-sensitive sites are phosphorylated (Tamkun et al., 2007). Following dephosphorylation, the protein associated is disrupted and Kv2.1 channels are able to freely travel beyond the cytoskeleton boundary. In addition to phosphorylation-dependent membrane localization and channel gating, phosphorylation is also known to affect Kv channel trafficking, and likely participates in surface delivery of Kv2.1 to channel containing clusters (O'Connell et al., 2006). The phosphorylation-dependent trafficking of other Kv channels has been demonstrated with Kv1.2 following PKA activation in *Xenopus* oocytes (Huang et al., 1994) and hERG channels following PKC activation (Cockerill et al., 2007). In this dissertation, I detail multiple Kv2.1 intracellular phosphorylation reactions and their effect on channel trafficking and K^+ efflux during oxidant-induced neuronal apoptosis.

1.7.2 Potassium efflux and apoptosis.

The enhancement of voltage-gated K^+ channel activity in injured cells, resulting in K^+ efflux, has been shown to be a crucial element in apoptotic neuronal death (Yu, 2003a). Indeed, several models of apoptosis have demonstrated K^+ efflux as a required event in the cell death process (Bortner and Cidlowski, 2007). In most instances, the molecular mechanism by which the K^+ current enhancement and/or K^+ efflux is achieved has yet to be elucidated. Regardless, increased K^+ efflux seems to be a critical component for cell death in many pathological circumstances. Interestingly, blocking K^+ efflux via channel *inhibition*, can also sometimes lead to apoptosis (Lauritzen et al., 1997). For instance, Drosophila *Ether-a-go-go* (EAG) K^+ channels have been shown to *inhibit* apoptosis and increase proliferation (Hegle et al., 2006). However, the anti-apoptotic actions in this instance were attributed to intracellular cell survival signaling cascades initiated by a voltage-dependent conformational change in the channel, but not ion flux, as non-conducting mutants channels were also protective. Furthermore, certain K^+ channels have been shown to facilitate tumor progression and proliferation in cell lines, as pharmacological inhibition of K^+ channels blocks these effects (Pardo et al., 2005).

It has been proposed that the enhancement of K^+ currents during apoptosis leads to a decrease in the concentration of this cation in the cytoplasm (Yu et al., 1999). In fact, the intracellular K^+ concentration in some apoptotic cells has been estimated to be as low as 30-50 mM. This decrease in intracellular K^+ acts as a permissive apoptotic signal in both traditional intrinsic and extrinsic pathways of apoptosis (Bortner and Cidlowski, 2004), as caspases and apoptotic nucleases are activated most efficiently at significantly reduced potassium

concentrations (Hughes and Cidlowski, 1999). Moreover, reduced intracellular K^+ is a prerequisite for other apoptotic processes, including cell volume decrease, cytochrome c release and alterations in mitochondrial membrane potential (Yu, 2003a), while normal intracellular K^+ levels hinder oligomerization of Apaf-1 and assembly of the apoptosome (Cain et al., 2001). It must also be noted that inhibition of both Na^+/K^+-ATPase and potassium leak channels has been shown to contribute to reduced intracellular K^+ concentrations during apoptosis (Yu, 2003a; Brevnova et al., 2004). Interestingly, depleting intracellular K^+ alone is sometimes sufficient to induce apoptosis, as demonstrated in granule neurons, T-lymphocytes and rodent tumor cell lines following K^+ channel overexpression or K^+-selective ionophore treatment (Yu, 2003). Thus, maintaining physiological intracellular potassium levels by blocking K^+ channels or increasing the extracellular K^+ concentration effectively attenuates cell death in many models of neuronal apoptosis (Yu et al., 1997; Yu et al., 1998; Yu et al., 1999; Wang et al., 2000; McLaughlin et al., 2001; Xiao et al., 2001; Bossy-Wetzel et al., 2004; Wei et al., 2004; Redman et al., 2006).

1.8 The zinc-potassium continuum in apoptosis.

Cell death pathways linking intracellular Zn^{2+} liberation and enhanced K^+ currents may be widespread (Pal et al., 2004). Our laboratory has provided a direct link between these two phenomena following the release of Zn^{2+} by thiol oxidants (McLaughlin et al., 2001) and peroxynitrite (Pal et al., 2004; Zhang et al., 2004). More recently we have also reported that neurons exposed to microglia-derived ROS and RNS have observable Zn^{2+} release and a very pronounced K^+ current surge preceding cell death (Knoch et al., 2008). While the requirement of Zn^{2+} liberation and K^+ efflux have been demonstrated for neuronal cell death (McLaughlin et al.,

2001; Pal et al., 2003), in this dissertation, I describe important molecular signaling events connecting the two phenomena. Specifically, I will discuss the contribution of three Zn^{2+}-dependent signaling enzymes: p38 MAPK, src, and the cytoplasmic form of protein tyrosine phosphatase epsilon (Cyt-PTPε), and their contribution to the Kv2.1-mediated apoptotic K^+ current surge.

1.9 Signaling enzymes connecting Zn^{2+} liberation to K^+ efflux.

1.9.1 p38 MAPK

Mitogen activated protein kinases (MAPKs) are serine/threonine kinases that transduce environmental signals into cellular responses such as initiation of gene expression, differentiation and cell survival/death. MAPK activation is achieved via dual phosphorylation of conserved threonine and tyrosine residues by upstream MAPK kinases (MKKs), which are activated by upstream MAPK kinase kinases (MAPKKKs). Four families of MAPKs: ERK1/2, ERK5, JNKs and p38 have been characterized. Mammalian p38 MAPKs are activated by a variety of cellular stressors including exposure to inflammatory cytokines, UV radiation, osmotic stress, and oxidative stress (Cuenda and Rousseau, 2007). There have been four p38 MAPKs identified in mammals: p38α, p38β, p38γ, and p38δ, all of which are encoded by different genes (Cuenda and Rousseau, 2007). p38α was the first isoform discovered and was originally characterized as a 38 kDa protein that displayed increased tyrosine phosphorylation following both endotoxin and hyperosmolarity insults (Han et al., 1994). p38α and p38β are are widely expressed, but very abundant in the brain and heart (Han et al., 1996), while p38γ is most highly expressed in

skeletal muscle and p38δ is primarily expressed in the testis, pancreas kidney and small intestine (Cuenda and Rousseau, 2007). Each isoform is similarly transiently activated via dual tyrosine/threonine phosphorylation, although differential activation of the individual isoforms within a single cell is likely to result from a specific stimulus. Following activation, p38 phosphorylates both cytosolic and nuclear targets, including transcription factors and other proteins involved in cell cycle progression, chromatin remodeling, mRNA stability, and cytoskeletal reorganization (Cuenda and Rousseau, 2007). Due to its originally described role in regulating the production of the inflammatory cytokines IL-1 and TNF-α (Lee et al., 1994), p38 has long been implicated the progression of neurodegenerative processes (Cuenda and Rousseau, 2007). However, the exact mechanism by which p38 mediates an apoptotic cellular response is unknown.

Incubation of metallothionein, an important intracellular metal binding protein, with the cell-permeant thiol oxidant 2,2'-dithiodipyridine (DTDP) results in the oxidation of all 20 cysteines contained in the protein and release of all bound Zn^{2+} atoms (Maret and Vallee, 1998). Our laboratory utilized DTDP to induce the release of Zn^{2+} from intracellular metal binding proteins in cortical neurons *in vitro* (McLaughlin et al., 2001). We observed that DTDP-liberated Zn^{2+} was an upstream mediator of neuronal apoptosis via a p38 kinase-dependent process (McLaughlin et al., 2001; Aras and Aizenman, 2005; Zhang et al., 2007). Our studies have described in detail an apoptotic cell death pathway that is activated by the liberated metal in neurons: the intracellular release of Zn^{2+} is followed by generation of reactive oxygen species (ROS) from mitochondria (Sensi and Jeng, 2004) and 12-lipoxygenase (12-LOX) (Zhang et al., 2004). 12-LOX is an important enzyme in the arachadonic acid (AA) metabolism pathway

(Kudo and Murakami, 2002) and is the primary LOX expressed in the brain (Shimizu and Wolfe, 1990). ROS are a byproduct of AA production via 12-LOX under normal conditions (Dikalov and Mason, 2001), and an oxidative cellular environment enhances 12-LOX activity (Shornick and Holtzman, 1993), further increasing ROS and facilitating Zn^{2+}-release.

ROS generation leads to the activation of p38 via the upstream apoptosis signal-regulating kinase 1 (ASK-1) (McLaughlin et al., 2001; Aras and Aizenman, 2005). ASK-1 is a member of the MAPKKK family which activates p38 by phosphorylating the upstream kinases MKK3/MKK6 (Ichijo et al., 1997). During normal conditions, ASK1 is inhibited by thioredoxin (Trx) via a physical association (Matsukawa et al., 2004). Trx is a redox-regulatory protein that is vulnerable to ROS-induced modifications. During cell stress, ROS induce the liberation of ASK1, which subsequently becomes activated following oligomerization and autophosphorylation (Liu and Min, 2002). Importantly, the generation of ROS likely provides a feedback-like stimulus for additional Zn^{2+} release from metallothionein and other metalloproteins in addition to activating ASK-1. The activation of p38 is followed by an enhancement of delayed rectifying, Kv2.1-mediated K^+ currents, and finally caspase activation (Pal et al., 2003).

This enhancement of K^+ currents is mediated by the N-ethylmaleimide-sensitive factor attachment protein receptor (SNARE)-dependent membrane insertion of Kv2.1-encoded channels following p38 activation (Pal et al., 2006; Redman et al., 2007), rather than an alteration in membrane resident channel activity. Thus, p38 may be directly phosphorylating Kv2.1 leading to plasma membrane insertion. Phosphorylation-dependent surface delivery is an effect that has been demonstrated in other ion channel populations (Hayashi et al., 2000; Yang et

al., 2007). Importantly, another member of the MAPK family, ERK1/2, has been shown to directly phosphorylate Kv4.2 resulting in a downregulation of dendritic K^+ currents in CA1 hippocampal pyramidal neurons (Yuan et al., 2002). However, whether this change in currents results from channel trafficking has not been demonstrated (Adams et al., 2000).

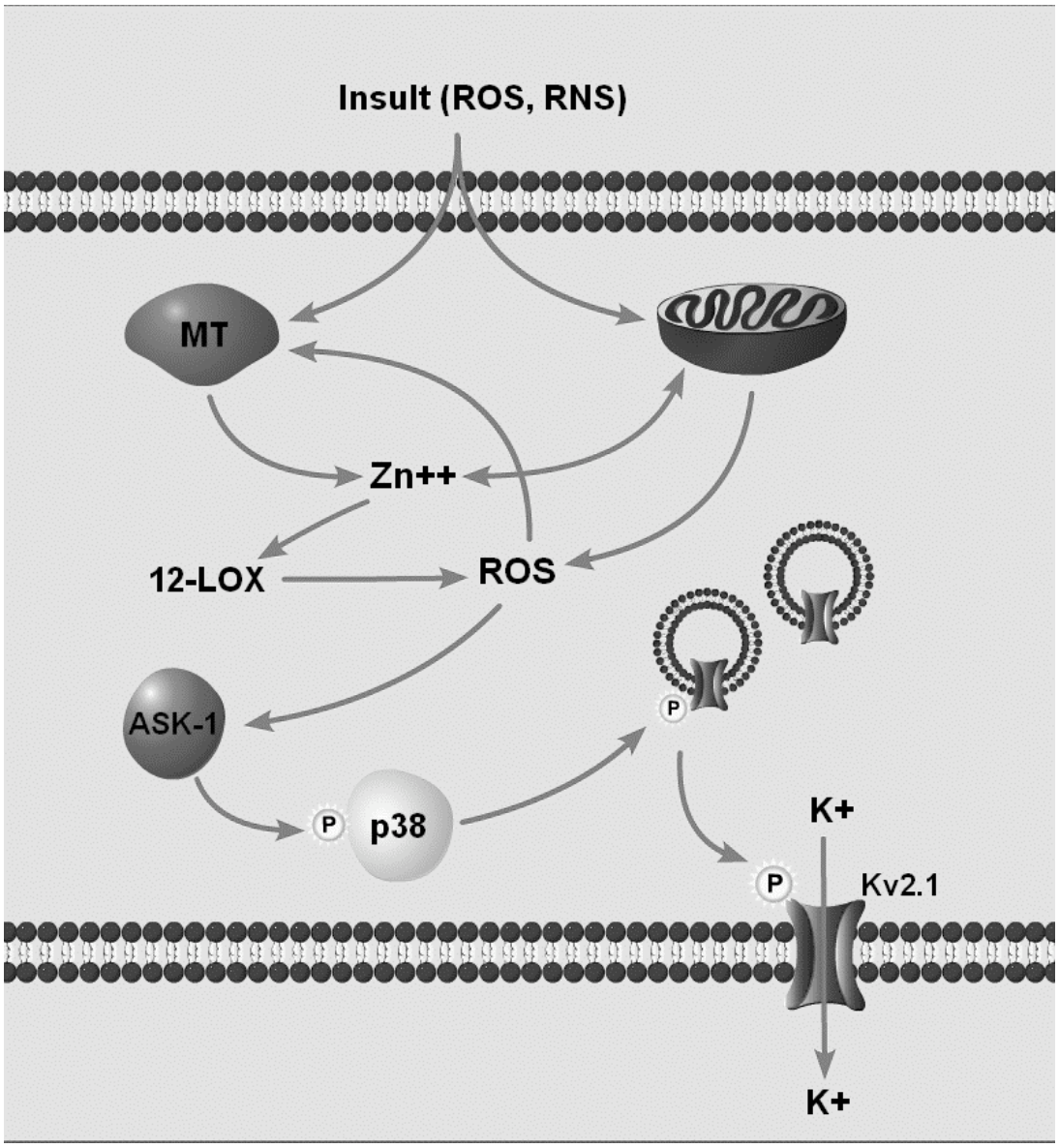

Figure 1. Schematic diagram of proposed pathway linking ROS/RNS-mediated liberation of intracellular Zn^{2+} and a subsequent enhancement of Kv2.1-mediated K^+ currents. Increases in intracellular Zn^{2+} lead to activation of p38 via a ROS-dependent activation of ASK-1. Kv2.1 channels are inserted in the cell membrane following activation of p38. Channel membrane insertion is a SNARE-dependent process.

1.9.2 Src

The Src family of tyrosine kinases consists of 8 distinct proteins involved in a wide variety of cellular signaling processes regulating viability, proliferation, migration and differentiation (Ingley, 2008). Src was the first protein tyrosine kinase to be discovered (Levinson et al., 1978) and has traditionally been associated with cancer cell transformation and the progression of human malignancies (Ishizawar and Parsons, 2004). However, it has now been repeatedly shown that src can affect cell function via non-oncogenic mechanisms. For instance, src, which is highly expressed in the brain (Soriano et al., 1991), affects nervous system function by contributing to synaptic plasticity (Maness et al., 1988), neuronal differentiation (Ingraham et al., 1989), neurite extension (Maness et al., 1988) and astrocytic gap junction closure (Lau, 2005). Interestingly, src is also known to play an instrumental role in glutamate-induced neuronal cell death (Khanna et al., 2002), as both src depletion (Paul et al., 2001) and pharmacological inhibition of src activity (Lennmyr et al., 2004) is sufficient to reduce injury following an ischemic insult. Because glutamate toxicity contains both excitotoxic and oxidative stress components, it is important to note that inducible src activity has been shown to be a critical component of the oxidant-dependent pathway of glutamate toxicity (Khanna et al., 2002). In this paradigm, glutamate treatment of immature neurons lacking N-methyl-D-aspartate (NMDA) receptors generates ROS primarily via inhibition of the glutamate/cystine antiporter (Murphy et al., 1989). This inhibition blocks cellular uptake of cystine, a precursor of the antioxidant glutathione, which subsequently leads to ROS-mediated damage. Further relevant to the present study, src is also activated by cytosolic Zn^{2+} (Wu et al., 2002; Huang et al., 2008), a previously mentioned component in oxidant-induced neuronal injury.

Src family tyrosine kinases share similar domain arrangements (N-terminal "unique", SH2, SH3 and catalytic domains) that regulate both substrate targeting and enzymatic activity (Martin, 2001). Src normally assumes a closed or "autoinhibited" inactive state mediated by a dual phosphorylation site. Phosphorylation of the C-terminal tyrosine 527 leads to inactivation via an intramolecular interaction with the SH2 domain, guiding the SH3 domain to interact with the "linker" that connects SH2 and catalytic domains (Martin, 2001). The nature of src autoinhibition allows for multiple mechanisms of enzymatic activation, such as dephosphorylation of tyrosine 527 by a protein tyrosine phosphatase, binding of the SH2 domain to another phospho-tyrosine that competes with tyrosine 527, and competitive binding of a domain similar to the "linker" to SH3 (Ingley, 2008). Following disruption of the intramolecular interaction by any of these mechanisms, phosphorylation of the catalytic domain tyrosine 416 then facilitates enzyme activation (Tatosyan and Mizenina, 2000). Phosphorylation of the inhibitory tyrosine 527 is mediated by the kinase Csk (Tatosyan and Mizenina, 2000), a cytoplasmic enzyme susceptible to direct Zn^{2+} inhibition (Huang et al., 2008).

Src has been shown to phosphorylate Kv2.1 at intracellular N-terminal tyrosine 124 (Y124), leading to upregulation of channel activity (Tiran et al., 2003) during non-injurious conditions. In those studies, Y124 phosphorylation was observed not to affect Kv2.1 gating properties (Tiran et al., 2003; Tiran et al., 2006), suggesting src may be regulating the number of membrane resident channels via changes in trafficking, as our group has observed with Kv2.1 surface delivery during neuronal apoptosis (Pal et al., 2006). Accordingly, here I will

characterize the effect of Y124 phosphorylation by src on the apoptotic K^+ current surge observed during neuronal cell death.

1.9.3 Protein Tyrosine Phosphatase ε

Protein phosphorylation can be reversed through the catalytic activity of protein phosphatases. Specifically, tyrosine phosphorylation via tyrosine kinases is countered by the actions of protein tyrosine phosphatases (PTPs). Protein tyrosine kinases and protein tyrosine phosphatases are represented in the human genome by 90 genes and 107 genes, respectively (Tonks, 2006). The majority of active tyrosine phosphatases are either tyrosine-specific or target both phosphoserine and phosphothreonine in addition to phosphotyrosine residues. Classical PTPs have been defined by either one or two catalytic domains containing the signature motif HCX_5R, in which the cysteine residue located in the core of the catalytic domain is critical for enzymatic function (Tonks, 2006). This critical cysteine forms a covalent bond with the phosphate via nucleophilic attack followed by a break in the substrate phospho-tyrosine bond and release of the dephosphoyrlated substrate. The cysteine-phosphate bond is then hydrolyzed, releasing the phosphate and reactivating the phosphatase (Berman-Golan et al., 2008).

The classical PTPs include two major structurally distinct subgroups: transmembrane receptor like proteins (RPTPs) and cytosolic, non-transmembrane PTPs. RPTPs contain a ligand-binding extracellular domain, a transmembrane domain and either one or two cytosolic phosphatase domains termed D1 and D2. Studies have shown that in PTPs with two cytosolic domains, the catalytic activity resides primarily in the proximal D1 domain, while the distal D2

domain is either weakly or entirely inactive, and serves largely a regulatory role (Buist et al., 1999). Non-receptor PTPs are characterized by a single catalytic domain flanked by protein sequences that determine both phosphatase activity and subcellular localization (Tonks et al., 2006). Both RPTPs and non-receptor PTPs are regulated at the protein level by proteolysis, ligand-induced dimerization, reversible oxidation of the catalytic cysteine residue and phosphorylation (Berman-Golan et al., 2008). PTPs are also inhibited by endogenous Zn^{2+} following oxidative injury (Ho et al., 2008), Zn^{2+} itself in cell free preparations (Brautigan et al., 1981; Haase and Maret, 2003, 2005) and following cellular exposure to exogenous Zn^{2+} (Haase and Maret, 2003, 2005; Kim et al., 2006; Tal et al., 2006).

Protein tyrosine phosphatase epsilon (PTPε) was originally characterized as an RPTP containing a typical transmembrane domain and two cytoplasmic catalytic domains (Elson and Leder, 1995). Since then, a cytoplasmic form of PTPε (Cyt-PTPε) has been described that is structurally similar to RPTPε, but without a transmembrane domain (Elson and Leder, 1995). Both PTPε isoforms are produced from a unique mRNA species transcribed from a single gene (*PTPre*) by alternative promoters (Tanuma et al., 1999). A third and fourth forms of PTPε, p67 and p65, are produced from internal initiation of translation from a region common to both mRNA isoforms (p67) and calpain-mediated cleavage of the three larger PTPε isoforms (p65) (Gil-Henn et al., 2000). The only structural difference between these four PTPε isoforms is in their amino termini, rendering RPTPε membrane bound, Cyt-PTPε localized to the cytoplasm, nucleus and plasma membrane, and p67 and p65 localized exclusively to the cytoplasm (Gil-Henn et al., 2000). In addition to transcriptional, translational, and proteolytic regulation, PTPε is also controlled by dimerization (Toledano-Katchalski et al., 2003), association with tubulin

(Sines et al., 2007), or via phosphorylation state (Berman-Golan et al., 2008). Regulatory mechanisms, such as oxidation and Zn^{2+} inhibition, and their impact on neuronal apoptosis will be discussed in greater detail later in the dissertation.

Cyt-PTPε has been shown to dephosphorylate Kv2.1 at intracellular N-terminal tyrosine 124 (Y124), countering the upregulation of channel activity mediated by src during non-injurious conditions (Tiran et al., 2003). Y124 phosphorylation state does not affect Kv2.1 gating properties (Tiran et al., 2003; 2006), suggesting Cyt-PTPε and src regulate the number of membrane resident channels via changes in trafficking. In my work, I will describe how, during apoptosis, Zn^{2+} regulates Cyt-PTPε, its known physiological substrate the delayed-rectifier voltage-gated potassium channel Kv2.1, and hence neuronal apoptosis.

1.10 Thesis Goals

The goal of my dissertation was to characterize an important signaling pathway regulating neuronal apoptosis. Although Zn^{2+} and K^+ dysregulation have been shown to contribute to neuronal cell death, the intracellular signaling processes connecting the two phenomena have not been established. Because earlier studies from our lab indicated that the Kv2.1-mediated apoptotic K^+ current surge was dependent on p38 activity, and a putative p38 phosphorylation site was identified at S800 using a proteomic and biochemical based phosphorylation prediction program, I first investigated the effect of direct p38 phosphorylation of Kv2.1 on the apoptotic process. The results from these experiments are presented in Chapter 1. This chapter represents the contents of a manuscript that has been published (Redman et al.,

2007). Next, I examined the effect of a second Kv2.1 phosphorylation site on apoptosis, at Y124, which is known to be oppositely modulated by src and Cyt-PTPε under normal conditions. The results from these experiments are presented in Chapter 2. This chapter comprises a manuscript currently under review. Finally, Zn^{2+} liberation is required for oxidant-induced p38 activity and known to affect src activity. However, although some evidence implicates Zn^{2+}-inhibition of tyrosine phosphatase activity, no direct demonstration of Zn^{2+}-mediated Cyt-PTPε inhibition has been shown following oxidative injury. Thus, I investigated the role of intracellular Zn^{2+} liberation in Cyt-PTPε inhibition. The results from these studies are also presented in Chapter 2. The present findings, taken together with previous experiments, suggest a concurrent, Zn^{2+}-dependent disruption in tyrosine phosphatase activity and enhancement of src and p38 activity during apoptosis, thereby ensuring the phosphorylation of both Y124 and S800. With this dissertation, I detail how separate Zn^{2+}-dependent signaling pathways converge at Kv2.1 to mediate the apoptotic K^+ current surge and neuronal death. In addition, I have included another related study in the appendix describing the role of Kv2.1-mediated K^+ efflux in dopamine-transporter dependent 6-hydroxydopamine neurotoxicity. This study has also been published (Redman et al., 2006).

2. Apoptotic surge of potassium currents is mediated by p38 phosphorylation of Kv2.1

2.1 Abstract

Kv2.1, the primary delayed rectifying potassium channel in neurons, is extensively regulated by phosphorylation. Previous reports have described Kv2.1 phosphorylation events affecting channel gating and the impact of this process on cellular excitability. Kv2.1, however, also provides the critical exit route for potassium ions during neuronal apoptosis via p38 MAPK-dependent membrane insertion, resulting in a pronounced enhancement of K^+ currents. Here, electrophysiological and viability studies using Kv2.1 channel mutants identify a p38 phosphorylation site at serine 800 (S800) that is required for Kv2.1 membrane insertion, K^+ current surge, and cell death. In addition, a phospho-specific antibody for S800 detects a p38-dependent increase in Kv2.1 phosphorylation in apoptotic neurons, and reveals phosphorylation of S800 in immunopurified channels incubated with active p38. Consequently, phosphorylation of Kv2.1 residue S800 by p38 leads to trafficking and membrane insertion during apoptosis, and remarkably, the absence of S800 phosphorylation is sufficient to prevent completion of the cell death program.

2.2 Introduction

Enhancement of voltage-gated K^+ channel activity, resulting in K^+ efflux, is an essential step in neuronal apoptosis (Yu, 2003b). Blocking K^+ channels, or increasing the extracellular K^+ concentration, effectively attenuate cell death in many apoptotic models (Bortner et al., 1997; Hughes et al., 1997; Yu et al., 1997; Zaks-Makhina et al., 2004; Grishin et al., 2005), including oxidant exposure in cortical and midbrain dopaminergic neurons (Aizenman et al., 2000b; McLaughlin et al., 2001; Bossy-Wetzel et al., 2004; Redman et al., 2006). With the use of dominant negative mutant subunits, Kv2.1, the major component of the delayed rectifier K^+ current in neurons (Murakoshi and Trimmer, 1999; Malin and Nerbonne, 2002), was identified as the channel responsible for mediating the apoptotic K^+ current surge in cortical neurons (Pal et al., 2003). During oxidant-induced neuronal apoptosis, the liberation of intracellular Zn^{2+} from metal binding proteins (Aizenman et al., 2000b) leads to the activation of p38 mitogen-activated protein kinase (MAPK), which precedes and is necessary for the characteristic K^+ current surge (McLaughlin et al., 2001; Bossy-Wetzel et al., 2004). This enhancement of K^+ currents is due to a SNARE-dependent insertion of new Kv2.1-encoded channels (Pal et al., 2006), rather than an alteration in the properties of existing surface channels, such as a change in activation kinetics (Yu et al., 1997). In spite of this information, the molecular process connecting p38 activation and the apoptotic membrane insertion of Kv2.1 K^+ channels had heretofore remained undefined.

Here, we combine several experimental approaches to establish a direct link between active p38 and Kv2.1 during apoptosis after a sequence-based prediction model (Obenauer et al., 2003) was used to identify a putative phosphorylation site for the MAPK on the C-terminal of

the channel. First, alanine substitution of serine 800 (S800) in Kv2.1 completely abolished the apoptotic enhancement of K^+ currents. Second, a cysteine-containing mutant of Kv2.1 and a thiol-reactive covalent inhibitor were used to demonstrate that S800 is critical for membrane insertion of the channel during apoptosis. Third, expression of phospho-mimetic mutant channels resulted in significant increases in basal K^+ current densities. Fourth, a phospho-specific antibody directed at S800 detected a p38-dependent increase in phospho-Kv2.1 levels in apoptotic neurons, and revealed phosphorylation of immunopurified Kv2.1, but not of Kv2.1(S800A), incubated with active p38. Most significantly, Kv2.1(S800A) did not support apoptosis mediated by the wild-type channel in a recombinant expression system. This study establishes that p38-mediated phosphorylation of Kv2.1 is necessary and sufficient for its apoptotic trafficking and completion of the cell death program.

2.3 Materials and Methods

Plasmids and site-directed mutagenesis. The mammalian expression vector encoding wild-type Kv2.1 was the gift of J. Trimmer (UC Davis). The poly-myc tagged Kv2.1 plasmid was from K. Takimoto (U. Pittsburgh). The FLAG tagged dominant negative Kv2.1(W365, Y380T) plasmid was provided by J. Nerbonne (Wash U., St. Louis). S. Korn (NIH/NINDS) provided the Kv2.1(I379C) vector. Mutagenesis of these cDNAs was performed using the QuickChange XL kit (Stratagene, La Jolla, CA) according to manufacturer's directions. Primers containing the desired mutations (S800A, S800D, S800E) were obtained from Integrated DNA Technologies (Coralville, IA). Mutations were confirmed by sequencing. A plasmid

encoding enhanced green fluorescent protein (pCMVIE-eGFP; Clontech, Palo Alto, CA) was used for the identification of positively transfected cells.

Tissue culture. Chinese hamster ovary (CHO) cells were plated at a density of 5.6 x 10^4 cells per well on coverslips in 24 well plates 24 hr prior to transfection. Cells were treated for 4 hr in serum free medium (F12 nutrient medium with 10 mM HEPES) with a total of 1.2 μl Lipofectamine (Invitrogen, Carlsbad, CA) and 0.28 μg DNA per well (0.14 μg of both eGFP and potassium channel cDNA). Cells were briefly washed in Minimal Essential Medium with Earle's salts containing 25 mM HEPES and 0.01% bovine serum albumin (MHB). Following transfection, cells were maintained in F12 medium containing fetal bovine serum (FBS) at 37°C, 5% CO_2 for 48 hr prior to recordings.

Cortical neurons were prepared from embryonic day 16 rat embryos and grown in 6-well plates according to (McLaughlin et al., 2001). Cultures were exposed to drug treatment procedures at 25-29 d *in vitro*. Cells were briefly washed in MHB and maintained in D2C growth medium until harvesting. Cells were harvested 3hr post-treatment in lysis buffer (1% Triton X-100, 0.1% SDS, 0.25% Na deoxycholate, 50 mM HEPES, 150 mM NaCl, protease inhibitor cocktail (Roche diagnostics), pH 7.5) after two washes with PBS. Cell lysate samples were combined in a 1:1 ratio with reducing sample prep buffer and incubated for 5 min at 100ºC in order to denature proteins prior to gel electrophoresis.

Drug treatment. The apoptotic stimulus for the electrophysiological experiments in CHO cells consisted of a 5 min treatment with 25 μM DTDP at 37°C, 5% CO_2.

The DTDP containing solution was then removed and replaced with fresh F12 medium containing 10 μM 1-3-boc-aspartyl (Ome)-fluoromethyl-ketone (BAF), a broad-spectrum cysteine protease inhibitor. BAF was necessary to maintain cells viable for electrophysiological recordings since Kv2.1-expressing cells are highly susceptible to DTDP-induced apoptosis (Pal et al., 2003). Cells were subsequently maintained in BAF containing medium and electrophysiological recordings were performed approximately 3 hr following oxidative injury. For channel insertion experiments, cells were first treated with 4 μM of the membrane impermeant thiol reagent (2-trimethylammoniumethyl) methanethiosulfate (MTSET) (Zhang et al., 1996; Sun et al., 2004) for 10 min to covalently block all Kv2.1(I379C) or Kv2.1(I379C, S800A) channels present on the plasma membrane surface prior to the usual DTDP exposure (Pal et al., 2006). The apoptotic stimulus for the biochemical experiments on rat primary cortical neurons consisted of a 10 min treatment with 100 μM DTDP at 37ºC, 5% CO_2 (Aizenman et al., 2000b; McLaughlin et al., 2001). Cortical neurons were pre-treated with either vehicle or the specific p38 MAPK inhibitor SB-293063 (SB; 20 μM for 10 min).

Electrophysiological measurements. Current recordings were performed on eGFP positive cells using the whole-cell patch clamp configuration technique, as described previously (McLaughlin et al., 2001). We observed that 97% of GFP-positive CHO cells co-transfected with Kv2.1 had measurable K^+ currents. The intracellular electrode solution contained (in mM): 100 K-gluconate, 10 KCl, 1 $MgCl_2$, 1 $CaCl_2$ x $2H_2O$, 10 HEPES; pH adjusted to 7.2 with concentrated KOH; 0.22 mM ATP was added and the osmolarity was adjusted to 280 mOsm with sucrose. The extracellular solution contained (in mM): 115 NaCl, 2.5 KCl, 2.0 $MgCl_2$, 10 HEPES, 0.1 BAPTA, 10 D-glucose, 0.1 tetrodotoxin; pH was adjusted to

7.2. Measurements were obtained under voltage clamp conditions with an Axopatch 1-D amplifier (Axon Instruments, Foster City, CA) and pClamp software (Axon instruments) using 2-3 MΩ electrodes. Recording electrodes were pulled from 1.5 mm borosilicate glass (Warner Instruments, Hamden, CT) with a model P-97 mechanical pipette puller (Sutter Instruments, Novato, CA). Series resistance was partially compensated (80%) in all cases. Currents were filtered at 2 kHz and digitized at 10 kHz with Digidata (Axon Instruments) software. Potassium currents were evoked with incremental 15 mV voltage steps to +35 from a holding potential of –70 mV. To determine current density values, steady-state current amplitudes were measured at 80 msec after the initiation of the + 5 mV step and normalized to cell capacitance. All data are expressed as mean ± S.E.M. and statistical analysis was performed using InStat software (GraphPad, San Diego, CA).

Generation of phospho-specific antibody. To generate an antibody specific for the phosphorylated p38 MAP kinase consensus sequence of Kv2.1 (pKv2.1; Supporting Fig. 2), we synthesized the peptide C-KNHFESSPLPTS(p)PKFLR (Tufts University Core Facility, Boston, MA). The high-pressure liquid chromatography purified peptide was conjugated to keyhole limpet hemocyanin (Pierce Chemical Co., Rockford, Illinois) with Sulfo-Link (44895; Pierce) following the manufacturer's protocol. Antiserum was generated in New Zealand white rabbits at Covance (Princeton, New Jersey). Following pre-bleed screening, animals were initially injected with 1.5 mg immunogen, followed by 3 monthly boosts of 0.75 mg and 3 monthly boosts of 0.5 mg. The crude serum was affinity purified using an Immunopure (A) IgG Purification Kit (Pierce) according to the methods described by the manufacturer, and the resulting product was used in the experiments reported here. A commercially available Kv2.1

polyclonal antibody (Alomone Labs, Jerusalem, Israel), which was not targeted to the p38 site, was used as a control in immunoblots.

Cell-free kinase assay. Poly-myc-Kv2.1 and poly-myc-Kv2.1(S800A) expressed protein from transfected CHO cells were immunoprecipitated by incubating cell lysates with an anti-myc-tag rabbit polyclonal antibody (40 μg/μl) (MBL International Corp., Woburn, MA) followed by protein A/G PLUS-Agarose immunoprecipitation reagent (Santa Cruz Biotechnology Inc., Santa Cruz, CA). The immunopurified substrate was incubated in 15 μl of kinase buffer (in mM: 25 HEPES, pH 8.0, 2 DTT and 0.1 vanadate), 15 μl of Mg/ATP (50 mM MgCl and 50 μM ATP) and 50 μg activated p38α ((Roche Protein Expression Group, Indianapolis, IN) for 1hr at 30˚C. Reactions containing kinase buffer alone and kinase buffer + Mg/ATP were used as controls. The reaction was stopped with sample preparation buffer (625 mM Tris, 25% glycerol, 2% SDS, 0.01% bromophenol blue and 5% β-mercaptoethanol) and incubated at 100°C for 5 min prior to SDS-PAGE and immunoblotting. Immunoblotting was performed with the pKv2.1 antibody (1:12,000) and with a commercially available polyclonal Kv2.1 antibody (1:3000) (Alomone Labs, Jerusalem, Israel).

Electrophoresis and immunoblotting. Sodium dodecyl sulphate–polyacrylamide gel electrophoresis was carried out by standard procedures using the Mini Protean 3 System (Bio-Rad, Hercules, CA). Equal amounts of cell lysate were separated by reducing 6% or 10% SDS-PAGE gels. Separated protein bands were transferred onto a 0.2 μm nitrocellulose membrane (Bio-Rad). The membranes were then blocked with 1% Bovine Serum Albumin (BSA) in PBS with 0.05% Tween 20 (PBST) at room temperature for 1 hr, and probed

with appropriate primary antibodies diluted in PBST. Blots were then incubated with goat secondary antibody conjugated to horseradish peroxidase at room temperature for 1 hr. Blots were visualized using SuperSignal CL-HRP Substrate System (Pierce, Rockford, IL) and exposed to BioMax films (Kodak, CT). In the cortical culture experiments, optical density measurements (Scion Image software, NIH) were taken of both pKv2.1 immunoreactive bands, normalized to their respective Kv2.1 immunoreactive bands and the resulting values were pooled.

Viability Assays. Chinese hamster ovary (CHO) cells were plated and transfected with eGFP and pRBG4 vector plus Kv2.1, Kv2.1(S800A) or Kv2.1(W365C/Y380T) according to the protocol described above, with 0.28 μg DNA added per well (0.14 μg:0.13 μg: 0.0028 μg; eGFP: empty vector: potassium channel cDNA). Twenty-four hr following transfection, cells were exposed to either 30 μM DTDP or vehicle for 15 min at 37ºC, 5%CO_2. Twenty-four hr following treatment, counts of GFP positive cells were obtained by a person blinded to the experimental treatment groups from 15 fields with a 20X objective per coverslip; 3 coverslips were counted per condition in 3 independent experiments.

2.4 Results

2.4.1 S800 in Kv2.1 is necessary for the apoptotic surge in K^+ currents.

Scansite (http://scansite.mit.edu), a program that predicts protein phosphorylation sites based on proteomic and biochemical data (Obenauer et al., 2003), was utilized to search for potential MAPK targets in Kv2.1 (GenBank NM_013186). A medium-stringency scan revealed a single serine residue at position 800 (Fig. 2a) as a potential phosphorylation target for both p38 and extracellular signal regulated kinase (ERK). However, the Scansite score for this sequence suggested a substantially better match for p38 than for ERK. S800 resides in the serine and threonine-rich intracellular C-terminal tail of the protein (Fig. 2a), where other phosphorylation sites exist (Park et al., 2006). We thus examined the role of S800 in the up-regulation of K^+ currents during oxidant-induced apoptosis in a recombinant expression system.

Whole-cell electrophysiological recordings were performed on Chinese Hamster Ovary (CHO) cells transiently expressing either wild-type Kv2.1 channels or a non-phosphorylatable mutant, Kv2.1(S800A). CHO cells have no endogenous voltage-gated K^+ channels (Yu and Kerchner, 1998), but can be induced to readily undergo oxidant-induced apoptosis after expressing Kv2.1 (Pal et al., 2003), and, like neurons, show a pronounced K^+ current enhancement during this process (Pal et al., 2006). Recordings were obtained under control conditions and following treatment with the oxidant apoptogen 2,2'-dithiodipyridine (DTDP; (Aizenman et al., 2000b; Pal et al., 2006). Electrophysiological measurements were routinely performed 3 hours following oxidant exposure, a time when a robust K^+ current surge is well

established (McLaughlin et al., 2001; Pal et al., 2003; Pal et al., 2006). As shown previously (Pal et al., 2006), currents mediated by wild-type Kv2.1-encoded channels were substantially enhanced following the apoptotic stimulus (Fig. 2b, left). In contrast, no current surge was observed in CHO cells expressing Kv2.1(S800A) following the oxidant treatment (Fig. 2b, right), indicating that S800, a putative target for p38-mediated phosphorylation, is required for the increase in K^+ currents during apoptosis.

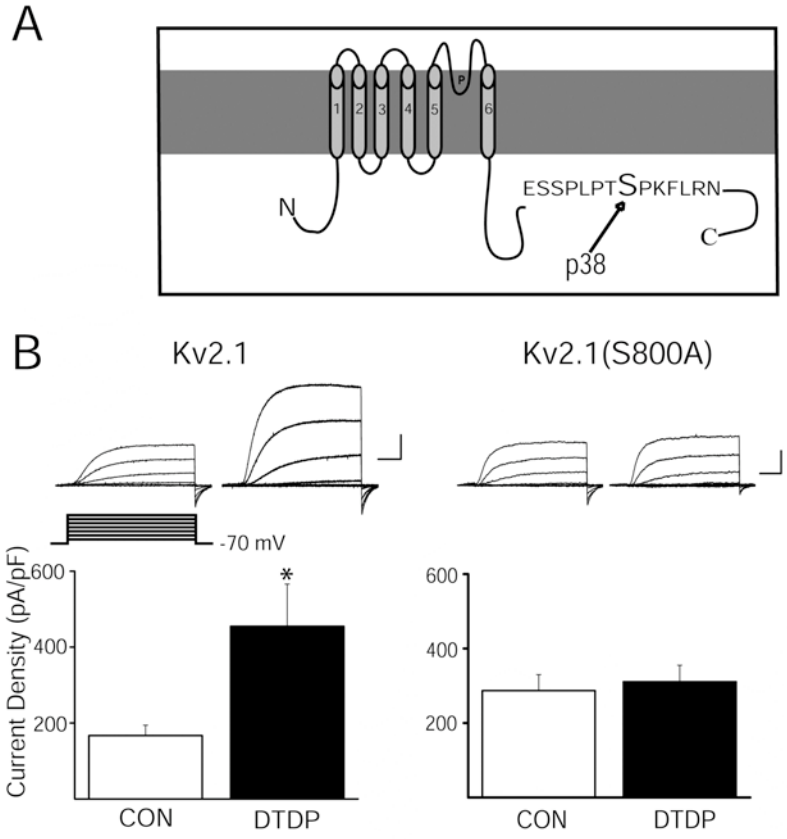
A
1
2
3
4
5
P
6
N
ESSPLPTSPKFLRN
C
p38
B
Kv2.1
Kv2.1(S800A)
-70 mV
Current Density (pA/pF)
600
400
200
*
CON
DTDP
600
400
200
CON
DTDP

Figure 2. Serine 800 of Kv2.1 is critical for apoptosis associated K^+ current enhancement. (a) Schematic of Kv2.1 showing the putative p38 phosphorylation site on the cytoplasmic C-terminus. (b) Top left: Representative whole-cell K^+ currents from Kv2.1-expressing CHO cells recorded under control and DTDP treatment conditions. Currents were obtained 48 hr post transfection and evoked by sequential 15 mV voltage steps to +35 mV from a holding potential of –70 mV. Calibration: 5 nA, 15 msec. Bottom left: Mean ± s.e.m. K^+ current densities from Kv2.1-expressing CHO cells under control (n = 25) and DTDP (n = 12) treatment conditions (* $p<0.05$; *t* test). Currents were induced with a voltage step to +5 mV from a holding potential of –70 mV and normalized to cell capacitance. Top right: Representative whole cell K^+ currents from Kv2.1(S800A) expressing CHO cells recorded under control and DTDP treatment conditions. Bottom right: Mean ± s.e.m. K^+ current densities from Kv2.1(S800A)-expressing CHO cells recorded under control (n = 24) and DTDP (n = 24) treatment conditions.

2.4.2 S800 is required for apoptogen-induced membrane insertion of Kv2.1.

The apoptotic surge in K^+ current observed in both cortical neurons and CHO cells is the result of trafficking and SNARE-dependent exocytotic insertion of new Kv2.1 channels into the plasma membrane (Pal et al., 2006). New channel membrane insertion was detected by utilizing the cysteine-containing K^+ channel mutant Kv2.1(I379C) (Kurz et al., 1995). The presence of this mutation allows the channel to be functionally blocked by the membrane impermeant thiol reagent (2-trimethylammoniumethyl) methanethiosulfate (MTSET) (Zhang et al., 1996; Sun et al., 2004). Virtually all previously existing surface Kv2.1(I379C) channels can therefore be silenced following a 5-10 min exposure to MTSET. With existing plasma membrane Kv2.1 channels permanently blocked, the insertion of new channels is easily detected electrophysiologically by the appearance of new currents under MTSET-free conditions (Pal et al., 2006). This assay, which has the distinct advantage of detecting the insertion of new functional channels, has been previously validated by parallel biotinylation studies (Pal et al., 2006).

In order to investigate the role of S800 in the apoptotic insertion of new channels, the double mutant Kv2.1(I379C, S800A) was generated. Whole-cell recordings first confirmed the preservation of functional silencing by MTSET in this double mutant channel (Fig. 3a). Next, CHO cells expressing either Kv2.1(I379C) or Kv2.1(I379C,S800A) were exposed to MTSET for 10 min to block all existing surface channels. The cells were then exposed to oxidant to trigger the apoptotic cascade. Electrophysiological recordings 3 hours later revealed the presence of K^+ currents in Kv2.1(I379C)-expressing cells (Fig. 3b), similar to what was reported earlier (Pal et

al., 2006). However, little or no current could be measured in CHO cells expressing Kv2.1(I379C,S800A), indicating a lack of apoptotic membrane insertion of these mutant channels (Fig. 3b). This result not only accounts for the lack of Kv2.1(S800A)-mediated apoptotic current surge observed earlier, but demonstrates that phosphorylation of S800 is necessary for Kv2.1 membrane insertion during the cell death program.

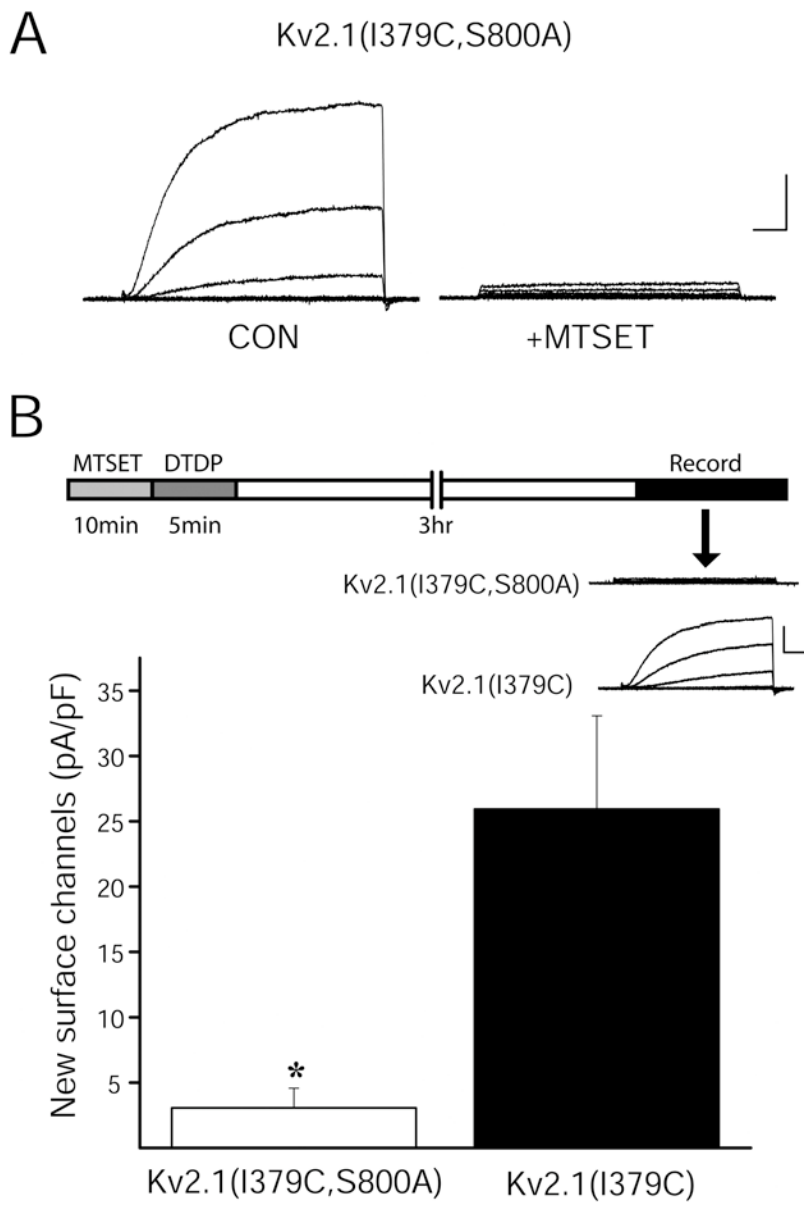
A
Kv2.1(I379C,S800A)
CON
+MTSET
B
MTSET
DTDP
Record
10min
5min
3hr
Kv2.1(I379C,S800A)
Kv2.1(I379C)
New surface channels (pA/pF)
35
30
25
20
15
10
5
*
Kv2.1(I379C,S800A)
Kv2.1(I379C)

Figure 3. S800A mutation blocks apoptogen induced membrane insertion of Kv2.1. (a) MTSET blocks Kv2.1(I379C) channel containing the Kv2.1(S800A) mutation. Calibration: 2nA, 10msec. (b) Top: Diagram representing the experimental protocol designed to measure the appearance of new K^+ channels during the apoptotic process. Shown are representative whole-cell K^+ currents obtained from Kv2.1(I379C) and Kv2.1(I379C,S800A) expressing CHO cells 3 hr after sequential treatment with MTSET and DTDP. Currents were evoked by sequential 15 mV voltage steps to +35 mV from a holding potential of –70 mV. Calibration: 1nA, 10msec. Bottom: Mean ± s.e.m. K^+ current densities recorded from Kv2.1(I379C) (n=17) and Kv2.1(I379C, S800A) (n=20) expressing CHO cells 3 hr after the sequential MTSET/DTDP treatments (*$p<0.01$; *t* test). These currents represent the newly inserted channels during apoptosis

2.4.3 Negatively charged amino acids at position 800 mimic the apoptotic surge. Recordings were performed from CHO cells transiently expressing two additional variants of Kv2.1 to test whether substitution of S800 with negatively charged residues would mimic the apoptotic increase in currents observed in wild-type channels. Indeed, basal current densities in untreated Kv2.1(S800D) and Kv2.1(S800E) mutant expressing cells displayed significantly enhanced amplitudes, comparable to those observed in DTDP-treated Kv2.1-expressing cells (Fig. 4). Oxidant treatment of cells expressing these mutations did not produce any additional current enhancement (not shown). Rather, a slight decrease in the currents was observed under these conditions, likely the result of cellular damage by the injurious stimulus. These results further support the role of S800 phosphorylation as a key mediator of the K^+ current surge during apoptosis.

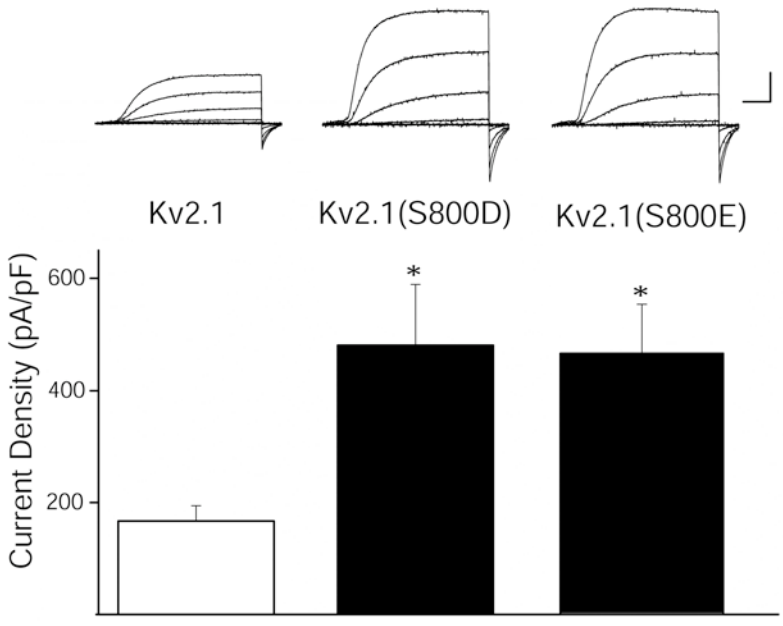
Kv2.1
Kv2.1(S800D)
Kv2.1(S800E)
Current Density (pA/pF)
600
400
200
*
*

Figure 4. Substitution of serine 800 with negatively charged amino acids mimics apoptotic K^+ current densities. Top: Representative whole-cell K^+ currents from Kv2.1, Kv2.1(S800D) and Kv2.1(S800E) expressing CHO cells. Currents were obtained 48 hr post transfection and evoked by sequential 15 mV voltage steps to +35 mV from a holding potential of –70 mV. Calibration: 5 nA, 15 msec. Bottom: Mean ± s.e.m. current densities from Kv2.1 (n=13), Kv2.1(S800D) (n = 17) and Kv2.1 (S800E) (n=14) expressing CHO cells; (*$p<0.05$; *t* test).

2.4.4 S800 phosphorylation is p38-dependent in neurons undergoing apoptosis. Biochemical studies were performed to detect phospho-S800 levels in primary cortical neurons following oxidative injury. Cell lysates were subjected to gel electrophoresis and the resulting blots were probed with a commercially available antibody directed against amino acids 841-857 of the C-terminus of Kv2.1 (Kv2.1; Alomone Labs, Jerusalem, Israel) or with an antibody that we generated against the phosphorylated form of S800 (pKv2.1; Supplemetary Fig. 1). Immunoblots probed with Kv2.1-directed antibodies revealed the presence of two major bands in cortical extracts: a diffuse band near 100 kDa and another, more compact band, at approximately 80 kDa (Supplementary Fig. 1; see also (Trimmer, 1993; Scannevin et al., 1996; Chung and Li, 2005). The diffuse band near 100 kDa likely represents multiple, non-p38 dependent phosphorylation states of the predicted full-length channel (Misonou et al., 2004; Park et al., 2006), while the 80 kDa band may reflect the presence of a protein generated by an alternative mRNA isoform (Trimmer, 1993; Roder and Koren, 2006) or a proteolytic fragment. Importantly, preincubation of the two antibodies with their respective immunizing peptides completely blocked both immunoreactive signals (Supplementary Fig. 2).

Phospho-S800 levels in cortical neuronal lysates were assessed using the pKv2.1 antibody under control conditions and following oxidative injury. We observed a significant increase in pKv2.1 immunoreactivity in cortical neurons undergoing apoptosis, compared to vehicle-treated controls (Fig. 5A,B). This was particularly apparent in the compact, 80 kDa band. Importantly, SB-239063, a selective p38 inhibitor (Barone et al., 2001; McLaughlin et al., 2001) prevented oxidant-mediated increases in pKv2.1 immunoreactivity (Fig. 5A,B). These

data confirm a p38-dependent increase in phospho-S800 levels in endogenous Kv2.1 channels from cortical neurons undergoing apoptosis.

2.4.5 Active p38 phosphorylates S800 in cell free assays. To determine whether p38 could phosphorylate Kv2.1, we performed a cell-free assay in which recombinantly-expressed, immunoprecipitated poly myc-tagged wild-type Kv2.1 (myc-Kv2.1; (Ren et al., 2003; Pal et al., 2006) was used as a substrate for purified, active p38. We observed that myc-Kv2.1 protein exposed to active p38 produced a phospho-specific immunoreactive band (Fig. 5C). Similar experiments performed with an S800A mutant of the myc-tagged Kv2.1 yielded no phospho-specific signal (Fig. 5C). These results indicate that active p38 can directly induce selective phosphorylation of residue S800 of Kv2.1.

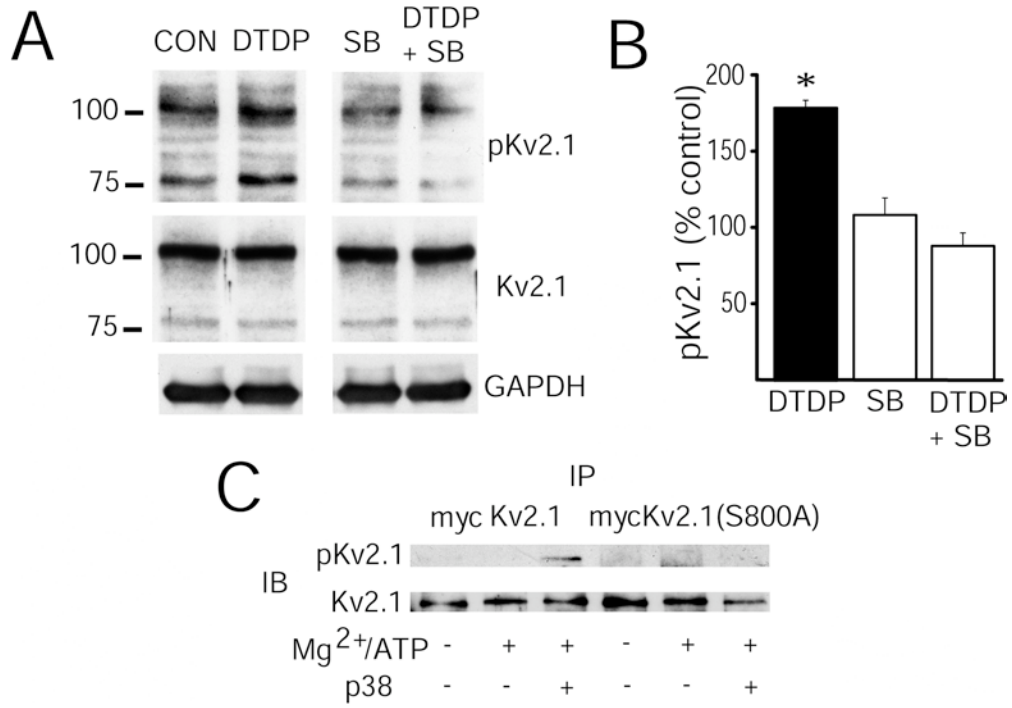
A
CON
DTDP
SB
DTDP + SB
100
75
pKv2.1
100
75
Kv2.1
GAPDH
B
pKv2.1 (% control)
200
150
100
50
*
DTDP
SB
DTDP + SB
C
IP
myc Kv2.1
mycKv2.1(S800A)
IB
pKv2.1
Kv2.1
Mg2+/ATP - + + - + +
p38 - - + - - +

Figure 5. A, DTDP-induced phosphorylation of Kv2.1-S800 is regulated by p38 MAPK in cultured cortical neurons. (Experiments completed by Kai He, Ph.D.) Cortical cultures were pre-treated with either vehicle or the specific p38 MAPK inhibitor SB293063 (SB; 20 μM for 10 min) and then incubated with either vehicle or DTDP (100 μM for 10 min). Immunoblots were probed with anti-pKv2.1 antibody (1:5000; top), a commercially available anti-Kv2.1 antibody (Alomone Labs, Jerusalem, Israel, 1:1000; middle) and an anti-GAPDH antibody (Novus Biologicals, Littleton, CO, 1:5000; bottom) to confirm equal protein loading between lanes. These data are representative of results from 3 independent experiments. **B,** Oxidative injury significantly increases S800 phosphorylation in cortical neurons *in vitro*. (Experiments completed by Kai He, Ph.D.) Optical density measurements of the phosphorylation level and its protein loading control at both the 100kDa and the 80 kDa band were quantified using Scion Image software. Values represent the mean ± s.e.m. normalized pKv2.1 signal (to Kv2.1 immunoreactivity) of both bands as a percentage of vehicle-treated control from 3 separate, independent experiments (*$p<0.01$; ANOVA/Dunnett). Note that the observed increase in S800 phosphorylation was effectively blocked with a p38 MAPK inhibitor. **C,** Serine 800 of Kv2.1 is phosphorylated by p38α in a cell-free kinase assay. Myc-Kv2.1 and Myc-Kv2.1(S800A) proteins were immunoprecipitated (IP) from CHO cell lysates and reacted at 30°C for 1hr with 15 μL of kinase buffer (in mM: 25 HEPES, pH 8.0, 2 DTT and 0.1 vanadate), 15 μL of Mg/ATP (50 mM MgCl and 50 μM ATP) and 50 μg activated p38α kinase. Reactions containing kinase buffer and Mg/ATP and kinase buffer alone were used as controls. Immunoblots (IB) were probed with the pKv2.1 antibody (1:12,000) and with the Kv2.1 antibody (1:3000; Alomone).

2.4.6 S800A mutation disrupts Kv2.1-mediated apoptosis. Unlike truncated or pore mutants of the channel (Pal et al., 2003), Kv2.1(S800A) does not function as a dominant interfering form in neurons undergoing apoptosis, but simply enhances the overall basal current amplitude without eliminating the contribution of endogenous channels (not shown). As such, the requirement for S800 phosphorylation in apoptosis was evaluated in Kv2.1-expressing CHO cells under oxidant exposure conditions that are normally sub-lethal to vector-expressing control cells (Pal et al., 2003). A 15 min exposure to 30 μM DTDP was sufficient to induce apoptosis in approximately 50% of wild-type Kv2.1 expressing cells (Fig. 6). However, the same oxidative insult was completely innocuous to CHO cells expressing Kv2.1(S800A) mutant channels. As a negative control, we assayed the viability of CHO cells expressing a non-conducting, double-pore mutant Kv2.1(W365C, Y380T) channel (Malin and Nerbonne, 2002). Similar to cells expressing Kv2.1(S800A), the oxidant was not toxic to cells expressing the double-pore mutant channels. These data demonstrate the requirement for functional Kv2.1 channels containing the phosphorylatable amino acid residue S800 to complete the apoptotic program.

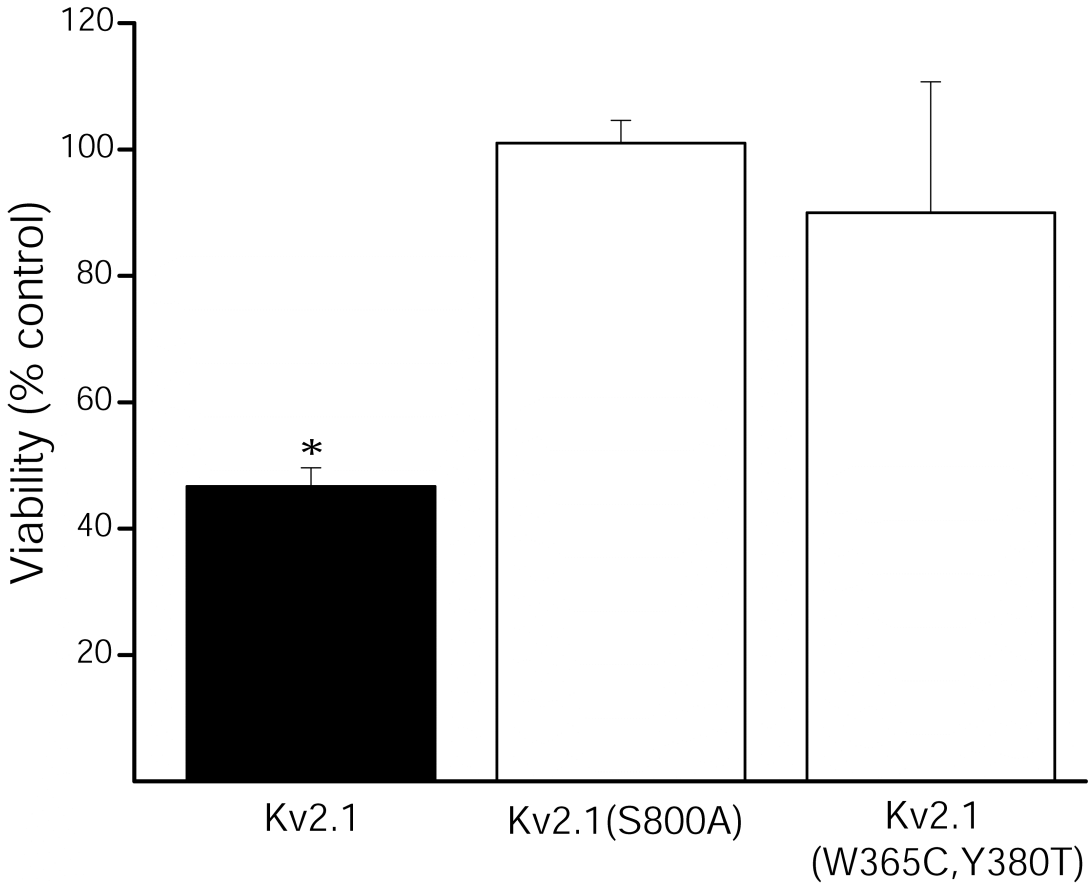
120
100
80
60
40
20
Viability (% control)
*
Kv2.1
Kv2.1(S800A)
Kv2.1
(W365C,Y380T)

Figure 6. S800A mutation blocks Kv2.1-mediated apoptosis. CHO cells were co-transfected with eGFP + pRBG4 vector and either Kv2.1, Kv2.1(S800A) or non-conducting Kv2.1(W365C, Y380T) and 24 hr later exposed to 30 μM DTDP (15 min). Viability was assayed 24 hr post-treatment by counting GFP positive cells and expressed as a percent of vehicle-treated control. Note that DTDP induced approximately 50% cell death in Kv2.1 expressing CHO cells but was not lethal to either Kv2.1(S800A) or Kv2.1(W365C, Y380T) expressing CHO cells. Values represent the mean ± s.e.m. viability from 3 separate, independent experiments (*$p<0.05$; ANOVA/Dunnett).

2.5 Discussion

The results presented in this study reveal an important and previously unrecognized mechanism of Kv2.1 regulation that has a critical impact on apoptosis. Kv2.1 is subject to extensive phosphorylation and dephosphorylation reactions, which alter the functional properties of this channel by influencing gating, and thereby, cell firing properties (Du et al., 2000; Park et al., 2006). We have found, however, a phosphorylation target for p38 on the C-terminal of Kv2.1 that is vital for the apoptotic surge of K^+ currents observed in apoptosis, as well as for completion of the cell death program. Interestingly, a paper by (Park et al., 2006) reported that S800 is a phosphorylation target, albeit by a then unidentified kinase. These authors further showed that S800 was not one of the several C-terminal sites subject to calcineurin-dependent dephosphorylation and did not participate in the graded regulation of Kv2.1 gating. We have found here that S800 is a unique p38 phosphorylation target on Kv2.1 that is required for channel trafficking and cell death.

Phosphorylation of S800 is not necessary, in and of itself, for normal Kv2.1 trafficking and plasma membrane insertion, as Kv2.1(S800A) mutant channels can be functionally expressed. Indeed, normal neurons overexpressing this construct simply have larger K^+ currents, which explains why this mutated form of Kv2.1 cannot function as a dominant interfering channel during neuronal apoptosis. Nonetheless, our studies in CHO cells reveal that under injurious situations this site is critical for *de novo* channel insertion, resulting in the current surge necessary for cytoplasmic K^+ loss and cell death.

Earlier studies revealed that the Kv2.1-mediated current surge during apoptosis is a result of the insertion of new channels into the plasma membrane (Pal et al., 2006), and the p38 MAPK signaling pathway is instrumental in this process (McLaughlin et al., 2001; Bossy-Wetzel et al., 2004; Pal et al., 2004). Interestingly, p38 activation by tumor necrosis factor α has also been implicated in the potentiation of tetrodotoxin-resistant Na^+ currents in sensory neurons, although a direct phosphorylation of the channel by p38 has not been documented (Jin and Gereau, 2006). The MAPK can phosphorylate Nav1.6 encoded Na^+ channels, but in this case the resulting interaction produces a decrease, rather than an increase, in Na^+ currents (Wittmack et al., 2005). In addition, another member of the MAPK family, ERK1/2, phosphorylates Kv4.2, a potassium channel responsible for A-type K^+ currents in neurons (Adams et al., 2000; Schrader et al., 2006), resulting in a downregulation of dendritic K^+ currents in CA1 hippocampal pyramidal neurons (Yuan et al., 2002). Collectively, this information indicates that MAPKs participate in cell signaling events that alter the contribution of voltage-gated ion channels to overall neuronal excitability. Our results demonstrate that p38 phosphorylation of Kv2.1 is required for an entirely different, but critical process: completion of the apoptotic program.

Several issues remain to be addressed. Primarily among them, the molecular mechanism linking p38-induced phosphorylation of Kv2.1 to the membrane insertion of this channel remains to be determined. We previously observed that cleavage and inactivation of the exocytotic SNARE proteins SNAP-25 and syntaxin was sufficient to prevent the apoptotic K^+ current surge (Pal et al., 2006). Importantly, both these proteins are known to directly interact with Kv2.1(Michaelevski et al., 2003): SNAP-25 with the cytoplasmic N-terminal (MacDonald et al., 2002), and syntaxin with two domains of the cytoplasmic C-terminal tail (Leung et al., 2003).

Overexpression of syntaxin and Kv2.1 inhibits channel surfacing and leads to a decrease in Kv2.1-mediated current density (Leung et al., 2003). It is thus tempting to speculate that p38 phosphorylation of Kv2.1 leads to changes in its association with syntaxin or other proteins, promoting, in turn, exocytosis of channel containing vesicles. In addition, Kv2.1 subunits consistently co-localize with cortical neuron subsurface cisterns, compressed stacks of smooth endoplasmic reticulum situated approximately 5-8 nm beneath the plasma membrane (Du et al., 1998). Thus, the possibility exists for cisternae to serve as a nearby holding area for channels destined for the plasma membrane (O'Connell and Tamkun, 2005), with p38 phosphorylation serving as the molecular switch necessary to free Kv2.1 from cisternal retention during apoptosis.

In summary, we have identified a putative p38 phosphorylation target residue on the C-terminal of Kv2.1. Importantly, mutation of S800 to a non-phosphorylatable residue is sufficient to disrupt the apoptotic cascade initiated by oxidative injury and block cell death. The work described here illustrates a critical mechanistic link between oxidant-induced Zn^{2+} release (Aizenman et al., 2000), p38 MAPK activation (McLaughlin et al., 2001; Bossy-Wetzel et al., 2004), the ensuing Kv2.1-mediated apoptotic K^+ current surge (Pal et al., 2003; Pal et al., 2006), and cell death. Thus, prevention of Kv2.1 phosphorylation by p38 is a potential novel therapeutic target for promoting neuronal survival during injurious oxidative stress conditions.

3. A Zn^{2+}-dependent dual phosphorylation checkpoint regulates the apoptotic surge of K^+ currents.

3.1 Abstract

Oxidant-liberated intracellular Zn^{2+} regulates neuronal apoptosis via an exocytotic membrane insertion of Kv2.1-encoded ion channels, resulting in a requisite enhancement of voltage-gated K^+ currents. In the present study, we show that an N-terminal tyrosine of Kv2.1 (Y124), which is targeted by src, is critical for the apoptotic current surge. Moreover, Y124 works in concert with a C-terminal serine (S800) target of p38 MAPK to regulate Kv2.1-mediated current enhancement. While Zn^{2+} was previously shown to activate p38, we demonstrate here that this metal inhibits cytoplasmic protein tyrosine phosphatase ε (Cyt-PTPε), which specifically targets Y124 and antagonizes the actions of src. Importantly, disruption of Y124 phosphorylation by a point mutation or by Cyt-PTPε over-expression protects cells from injury. Therefore, a dual tyrosine-serine phosphorylation checkpoint on Kv2.1 regulates neuronal survival by providing a converging input for two Zn^{2+}-dependent signal transduction cascades.

3.2 Introduction

K^+ efflux mediated by a surge of voltage-gated K^+ channel activity is a necessary component of neuronal apoptosis (Yu, 2003a). This current enhancement leads to reduced cytoplasmic K^+ concentrations (Yu et al., 1999), a permissive pro-apoptotic environment (Bortner and Cidlowski, 1999, 2007) as the catalytic activity of both caspases and apoptotic nucleases increases at low ionic strength (Hughes and Cidlowski, 1999). This effect is significant because inhibiting K^+ efflux effectively attenuates apoptotic cell death (Yu et al., 1997; Yu et al., 1998; Yu et al., 1999; Aizenman et al., 2000b; McLaughlin et al., 2001; Bossy-Wetzel et al., 2004).

Kv2.1, the primary delayed rectifying potassium channel in neurons (Murakoshi and Trimmer, 1999; Malin and Nerbonne, 2002), is the main channel responsible for the apoptotic K^+ current surge in rat cortical neurons (Pal et al., 2003). Following injury, the liberation of intracellular Zn^{2+} from metal binding proteins (Aizenman et al., 2000a) facilitates the generation of signaling reactive oxygen species (ROS) (Sensi and Jeng, 2004; Zhang et al., 2004) leading to the activation of p38 mitogen-activated protein kinase (MAPK) via the upstream kinase ASK-1 (McLaughlin et al., 2001; Aras and Aizenman, 2005). The subsequent enhancement of K^+ currents following Zn^{2+}-dependent p38 activation is mediated by the soluble *N*-ethylmaleimide-sensitive factor attachment protein receptor (SNARE)-dependent exocytotic plasma membrane insertion of new Kv2.1 channels (Pal et al., 2003; Pal et al., 2006; Redman et al., 2007). The

surface delivery of Kv2.1 during apoptosis requires the phosphorylation of intracellular C-terminal residue serine 800 (S800) by p38 MAPK (Redman et al., 2007).

Kv2.1-mediated K^+ currents can also be amplified during non-injurious conditions through direct phosphorylation of intracellular N-terminal residue tyrosine 124 (Y124) by src (Tiran et al., 2003; Tiran et al., 2006). Since elevations in cytoplasmic Zn^{2+}, linked to cell injury (Paul et al., 2001; Lennmyr et al., 2004), have been shown to activate src (Wu et al., 2002; Huang et al., 2008), we sought to investigate the requirement of converging src and p38 (Redman et al., 2007) phosphorylation events on apoptotic Kv2.1 trafficking and neuronal viability. We hypothesized that both intracellular termini contribute to the apoptotic K^+ current surge, as an interaction between these domains is required for channel surface delivery under normal conditions (Mohapatra et al., 2008). In addition, exocytotic SNARE proteins physically associate with the N- and C- terminal (MacDonald et al., 2002; Leung et al., 2003; Tsuk et al., 2005; Lvov et al., 2008; Tsuk et al., 2008), and SNARE cleavage blocks channel surface delivery during apoptosis (Pal et al., 2006). Results presented here demonstrate that Y124 on Kv2.1 is essential for the apoptotic surge of K^+ currents. In addition, disruption of Y124 phosphorylation strongly influences cell viability by modulating the effects of S800 on the current enhancement in a Zn^{2+}-dependent fashion.

3.3 Materials and Methods

Plasmids and site-directed mutagenesis. The mammalian expression vector encoding wild-type Kv2.1 was the gift of J. Trimmer (UC Davis). The Kv2.1(Y124F), Cyt-PTPε and Cyt-PTPε(D245A) plasmids were a gift from A. Elson (Weizmann Institute, Rehovot, Israel). Mutagenesis of these cDNAs was performed using the QuickChange XL kit (Stratagene, La Jolla, CA) according to manufacturer's directions. Primers containing the desired mutations (Y124F, Y124D, S800D) were obtained from Integrated DNA Technologies (Coralville, IA). Mutations were confirmed by sequencing. A plasmid encoding enhanced green fluorescent protein (pCMVIE-eGFP; Clontech, Palo Alto, CA) was used for the visual identification of positively transfected cells. We found that the Y124D mutation did not mimic the phosphorylation state at this site (results not shown).

Tissue culture and transfection. Chinese hamster ovary (CHO) cells were plated at a density of 5.6 x 10^4 cells per well on coverslips in 24 well plates 24 hr prior to transfection. Cells were treated for 4 hr in serum free medium (F12 nutrient medium with 10 mM HEPES) with a total of 1.2 μl Lipofectamine (Invitrogen, Carlsbad, CA) and 0.28 μg DNA per well (0.14 μg eGFP, 0.126 μg empty pRBG4 vector and 0.014 μg potassium channel cDNA). Following transfection, cells were maintained in F12 medium containing fetal bovine serum (FBS) at 37°C, 5% CO_2 for 24 hr prior to recordings.

Cortical neurons were prepared from embryonic day 16 rat embryos and grown in 6-well plates according to McLaughlin et al. (2001). Cultures (18-22 d *in vitro*) were transfected using

Lipofectamine 2000 (Invitrogen, Carlsbad, CA)(Ohki et al., 2001). Briefly, 1.5 μg of cDNA was diluted in 50 μl Opti-Mem medium and combined with 50 μl of Opti-Mem I medium containing 2 μl Lipofectamine 2000 reagent. Lipid-DNA complexes were allowed to form for 30 min at room temperature and then added to cortical cultures. Cells were then maintained at 37ºC, 5%CO_2 for 24-48h before drug treatment procedures and toxicity assays.

Drug treatment. The apoptotic stimulus for the electrophysiological experiments in CHO cells consisted of a 5 min treatment with 30 μM DTDP at 37°C, 5% CO_2. The DTDP containing solution was then removed and replaced with fresh F12 medium containing 10 μM 1-3-boc-aspartyl (Ome)-fluoromethyl-ketone (BAF), a broad-spectrum cysteine protease inhibitor. BAF was necessary to maintain cells viable for electrophysiological recordings since Kv2.1-expressing cells are highly susceptible to DTDP-induced apoptosis (Pal et al., 2003). Electrophysiological recordings were performed approximately 3 hr following oxidative injury. The apoptotic stimulus for the electrophysiological experiments in cortical neurons consisted of a 10 min treatment with 30 μM DTDP at 37°C, 5% CO_2. The DTDP containing solution was then removed and replaced with conditioned growth medium containing 10 μM BAF. For the src inhibition experiments, either 10 μM 4-Amino-5-(4-chlorophenyl)-7-(*t*-butyl)pyrazolo[3,4-d]pyrimidine (PP2) or 10 μM of the inactive structural analog 4-Amino-7-phenylpyrazol[3,4-d]pyrimidine (PP3) were included in the treatment solution and post-treatment medium.

Electrophysiological measurements. Current recordings were performed on eGFP positive CHO cells and cortical neurons using the whole-cell patch clamp configuration

technique, as described previously (McLaughlin et al., 2001). Ninety seven percent of GFP-positive CHO cells co-transfected with Kv2.1 had measurable K^+ currents. Ninety percent of GFP-positive neurons express co-transfected plasmids (Santos and Aizenman, 2002). The intracellular electrode solution contained (in mM): 100 K-gluconate, 10 KCl, 1 $MgCl_2$, 1 $CaCl_2$ x $2H_2O$, 10 HEPES; pH adjusted to 7.2 with concentrated KOH; 0.22 mM ATP was added and the osmolarity was adjusted to 280 mOsm with sucrose. The extracellular solution contained (in mM): 115 NaCl, 2.5 KCl, 2.0 $MgCl_2$, 10 HEPES, 0.1 BAPTA, 10 D-glucose, 0.1 tetrodotoxin; pH was adjusted to 7.2. Measurements were obtained under voltage clamp conditions with an Axopatch 1-D amplifier (Axon Instruments, Foster City, CA) and pClamp software (Axon instruments) using 2-3 MΩ electrodes. Recording electrodes were pulled from 1.5 mm borosilicate glass (Warner Instruments, Hamden, CT) with a model P-97 mechanical pipette puller (Sutter Instruments, Novato, CA). Series resistance was partially compensated (80%) in all cases. Currents were filtered at 2 kHz and digitized at 10 kHz with Digidata (Axon Instruments) software. Potassium currents were evoked with incremental 10 mV voltage steps to +80 mV from a holding potential of –80 mV. To determine current density values, steady-state current amplitudes were measured at 180 msec after the initiation of the -80 mV to +10 mV step and normalized to cell capacitance. All data are expressed as mean ± S.E.M. and statistical analyses were performed using InStat software (GraphPad, San Diego, CA).

Phosphatase Assay. CHO cells were lysed in buffer A (50mM Tris-HCl pH 7.5, 100mM NaCl, 1% NP-40) (Tiran et al., 2006) containing protease inhibitors (Complete Mini protease inhibitor cocktail, Roche Applied Science, Indianapolis, IN). FLAG-Cyt-PTPε expressed protein from transfected CHO cells was immunoprecipitated by incubating cell lysates

with an anti-FLAG rabbit polyclonal antibody (Sigma-Aldrich Inc., Saint Louis, MO) followed by protein A/G PLUS-Agarose immunoprecipitation beads (Santa Cruz Biotechnology Inc., Santa Cruz, CA). The immunoprecipitated complex was then washed 3 times with buffer A, two times in buffer B (100mM KCl, 0.5mM EDTA pH 8.2, 20mM Hepes pH 7.6, 0.4% NP-40, 20% Glycerol) and two times in buffer 54K (150 NaCl, 50mM Tris pH 7.9, 0.5% Triton X-100). FLAG-Cyt-PTPε was then eluted by incubating the beads in 2 equal volumes of elution buffer (50mM MES pH 7, 0.5mM DTT, 0.5 mg/ml BSA, 1 mg/mL FLAG peptide) (Sigma-Aldrich Inc., Saint Louis, MO) at 32º C for 3 min. Phosphatase from each elution step was pooled. Protein amounts were determined by a colorimetric protein assay (Bio-Rad, Hercules, CA). Phosphatase activity was then measured using a standard colorimetric malachite green phosphatase assay (Promega Corp., Madison, WI). Equal amounts of purified FLAG-Cyt-PTPε was incubated in 96-well plates with PTPε activity buffer (50mM MES pH 7, 0.5mM DTT, 0.5 mg/ml BSA) and two unique chemically synthesized phospho-tyrosine peptides (Promega Corp., Madison, WI; END(pY)INASL (Daum et al., 1993) and DADE(pY)LIPQQG (Zhang et al., 1993)) gently rocking at 32º C for 18 hr. The reaction was terminated by adding 50ul of the molybdate/additive mixture, incubated at room temp for 15 min and then optical density of each sample was measured at 600nm using a plate reader (1420 Victor^2 V Multilabel Counter, Perkin Elmer Life Sciences, Boston, MA). Activity was expressed as pmoles phosphate released normalized to total Cyt-PTPε protein added to the reaction. A standard activity curve was always performed with known amounts of free phosphate.

Viability Assays. Chinese hamster ovary (CHO) cells were plated and transfected with eGFP and pRBG4 vector plus Kv2.1 or Kv2.1(Y124F) according to the protocol

described above, with 0.28 μg DNA added per well (0.14 μg:0.13 μg: 0.0028 μg; eGFP: empty vector: potassium channel cDNA; 24-well plate). Twenty-four hr following transfection, cells were exposed to either 30 μM DTDP or vehicle for 15 min at 37ºC, 5%CO_2. Twenty-four hr following treatment, counts of GFP positive cells were obtained from 5 random fields with a 20X objective per coverslip; 3 coverslips were counted per condition in 3 independent experiments.

Cortical neurons were prepared from embryonic day 16 rat embryos and grown in 6-well plates according to McLaughlin et al. (2001). Neurons were transfected after 3 weeks *in vitro* with equal amounts of pUHC13-3 Luciferase and either pCDNA3 vector or Cyt-PTPε plasmids using Lipofectamine 2000 (Boeckman and Aizenman, 1996; Pal et al., 2003). A rat microglial cell line (Cheepsunthorn et al., 2001) was plated directly onto cortical neurons at a density of 50,000 cells/well 24hr following transfection. Microglia were stimulated with 10 U/ml interferon-γ (IFN-γ, Chemicon, Temecula, CA) and 1 μg/ml lipopolysaccharide (Knoch et al., 2008) and cells were subsequently maintained at 37ºC, 5% CO_2. Cell viability was measured 48hr later according to (Aras et al., 2008) using a luminescence reporter gene assay system (Perkin-Elmer, Boston, MA).

3.4 Results

3.4.1 Src inhibition blocks apoptotic K^+ current enhancement. We first examined whether src activity was required for K^+ current enhancement during oxidant-induced neuronal injury. Whole-cell electrophysiological measurements were obtained from cortical neurons following treatment with either vehicle or the oxidant apoptogen 2,2'-dithiodipyridine (DTDP) (Aizenman et al., 2000b; Pal et al., 2006). Recordings were performed approximately 3h after a 10 min DTDP (30 μM) exposure, a time when a prominent K^+ current enhancement is detected (McLaughlin et al., 2001; Pal et al., 2003; Pal et al., 2006; Redman et al., 2007). As previously demonstrated (McLaughlin et al., 2001; Pal et al., 2003; Pal et al., 2006; Redman et al., 2007), neurons treated with DTDP displayed significantly enhanced K^+ currents compared to vehicle-treated controls (Fig. 7A, B). Recordings were also obtained following treatment of cortical neurons with DTDP and either the selective src inhibitor PP2 (10μM) or its inactive structural analog PP3 (10μM). Apoptotic K^+ current enhancement was blocked in neurons co-treated with DTDP and PP2, while the apoptotic K^+ current surge remained in neurons co-treated with DTDP and PP3 (Fig. 7A, B). Additionally, treatment of cortical neurons with either PP2 or PP3 alone had no effect on baseline current densities (Fig. 7A, B). These results establish the requirement for src activity in the apoptotic neuronal K^+ current surge. Furthermore, these results, in combination with our previous work (McLaughlin et al., 2001; Bossy-Wetzel et al., 2004), show that both src and p38 signaling pathways converge upon Kv2.1 to mediate the apoptotic K^+ current enhancement.

a

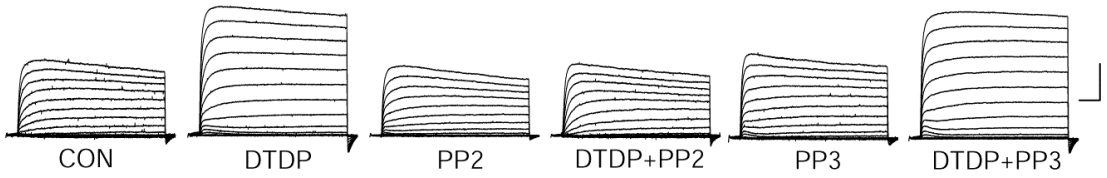
CON
DTDP
PP2
DTDP+PP2
PP3
DTDP+PP3

b

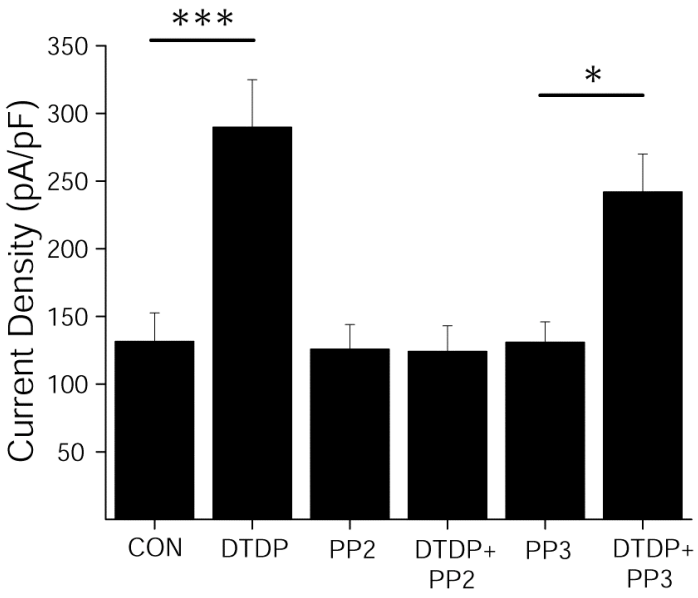
***
*
Current Density (pA/pF)
350
300
250
200
150
100
50
CON
DTDP
PP2
DTDP+ PP2
PP3
DTDP+ PP3

Figure 7. Src inhibition blocks the apoptotic K^+ current surge. *(a)* Representative whole-cell currents from cortical neurons recorded under control, DTDP (30μM), PP2 (10μM), DTDP + PP2, PP3 (10μM), and DTDP + PP3 treatment conditions. Currents were obtained 3h post injury and evoked by sequential 10 mV voltage steps to +80 mV from a holding potential of -80 mV. Calibration: 5nA, 25ms *(b)* Mean ± SEM current densities from cortical neurons recorded under control (n=13), DTDP (n=14), DTDP + PP2 (n=10), PP2 (n=10), PP3 (n=10), and DTDP + PP3 (n=10) treatment conditions. K^+ currents were evoked by a single voltage step to +10mV from a holding potential of -80mV and normalized to cell capacitance. (***P<0.001, *P<0.05; ANOVA/Bonferroni)

3.4.2 Y124 is critical for the apoptotic surge in K^+ currents. CHO cells express no endogenous voltage-gated K^+ channels (Yu and Kerchner, 1998), and undergo apoptosis following Kv2.1 expression after a normally sub-lethal oxidative injury (Pal et al., 2003). As with neurons, Kv2.1-expressing CHO cells display enhanced voltage-gated K^+ currents during the cell death program (Pal et al., 2006). Recordings were obtained from CHO cells transiently expressing either wild-type Kv2.1 or phenylalanine-substituted, Kv2.1(Y124F) mutant channels. Phenylalanine substitution was used to preclude phosphorylation at this site. Under normal conditions, CHO cells expressing Kv2.1(Y124F) channels exhibited K^+ current densities similar to CHO cells expressing wild-type Kv2.1 channels (Fig. 8A). Following DTDP exposure however, the K^+ current surge observed in wild-type Kv2.1-expressing cells was completely abrogated in cells expressing Kv2.1(Y124F) (Fig. 8B). Serine to aspartate-substituted Kv2.1(S800D) mutant channels have been shown to mimic the apoptotic K^+ current surge (Fig. 8C) (Redman et al., 2007). To further examine the requirement of Y124 in K^+ current enhancement, we obtained recordings from CHO cells expressing Kv2.1(Y124F, S800D) double mutant channels. Cells expressing Kv2.1(Y124F,S800D) channels displayed significantly reduced current densities compared to cells expressing Kv2.1(S800D) (Fig. 8C). Since phenylalanine substitution of Y124 blocks the K^+ current surge, we tested whether Y124 was required to support apoptosis in Kv2.1-expressing CHO cells. While DTDP treatment was sufficient to induce cell death in approximately 50% of wild-type Kv2.1-expressing cells, a significant, more than 2-fold increase in viability was observed in Kv2.1(Y124F)-expressing cells (Fig. 8D). Taken together, these data indicate that an intact Y124 is required for the apoptotic K^+ current surge and oxidant-induced cell death. Our results show that phosphorylation of S800 is not sufficient for the expression of this process. These findings also

suggest that under basal conditions Y124 may normally be phosphorylated by src, at least in CHO cells, as evident by the elevated current densities observed in uninjured Kv2.1(S800D)-expressing cells.

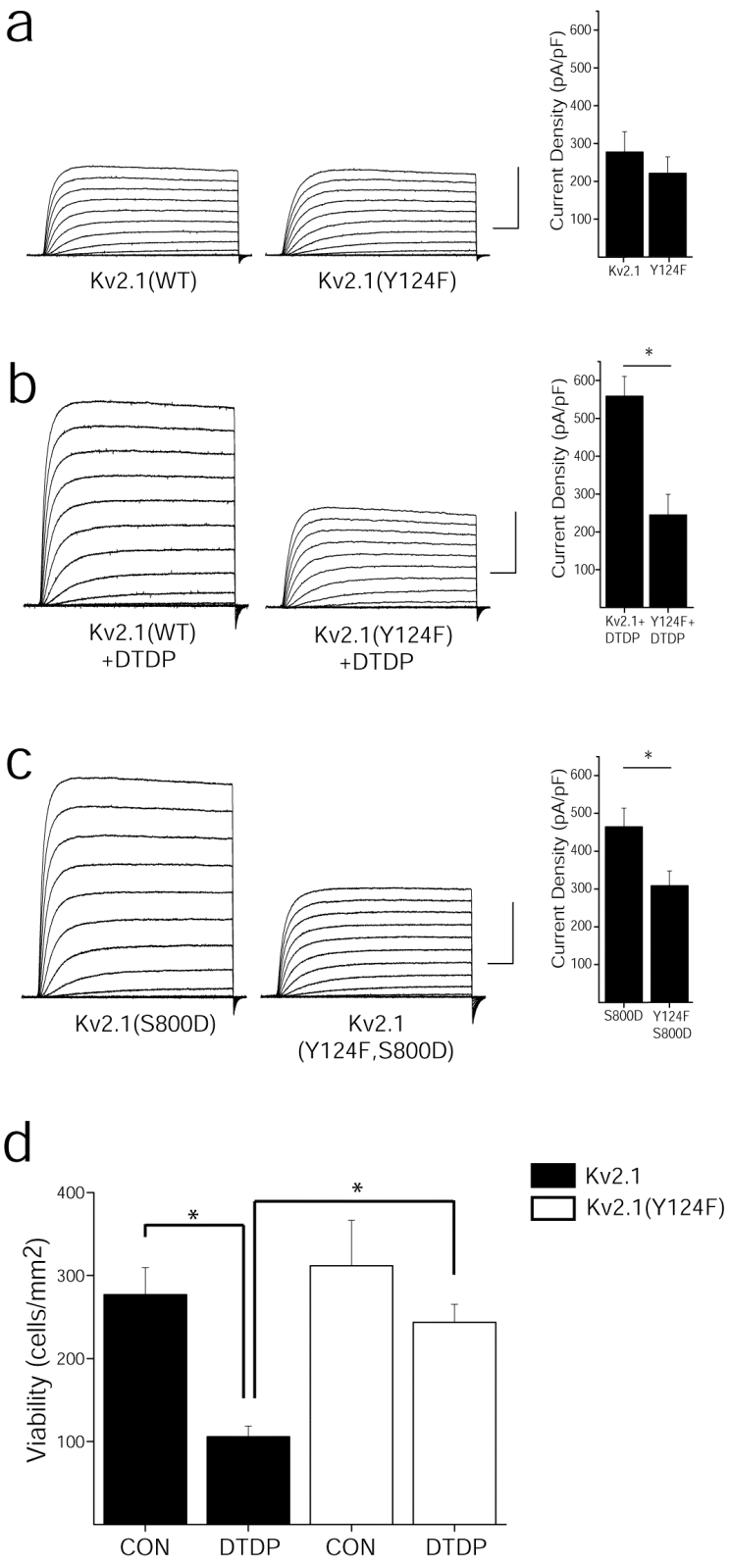
a
Kv2.1(WT)
Kv2.1(Y124F)
Current Density (pA/pF)
600
500
400
300
200
100
Kv2.1
Y124F
b
Kv2.1(WT)
+DTDP
Kv2.1(Y124F)
+DTDP
*
Kv2.1+
DTDP
Y124F+
DTDP
c
Kv2.1(S800D)
Kv2.1
(Y124F,S800D)
S800D
Y124F
S800D
d
Kv2.1
Kv2.1(Y124F)
Viability (cells/mm2)
400
300
200
100
CON
DTDP
CON
DTDP

Figure 8. Y124 is essential for the apoptotic K^+ current surge. *(a) (Left)* Representative whole-cell K^+ currents from wild-type Kv2.1- and Kv2.1 (Y124F)-expressing CHO cells. Currents were obtained 24h post-transfection and evoked by sequential 10 mV voltage steps to +80 mV from a holding potential of -80 mV. Calibration: 5nA, 25ms *(Right)* Mean ± SEM current densities from wild-type Kv2.1-expressing (n=15) and Kv2.1 (Y124F)-expressing CHO cells (n=10). *(b) (Left)* Representative whole-cell K^+ currents from wild-type Kv2.1- and Kv2.1(Y124F)-expressing CHO cells treated with DTDP. Calibration: 5nA, 25ms. *(Right)* Mean ± SEM current densities from wild-type Kv2.1- (n=12) and Kv2.1(Y124F)-expressing (n=9) CHO cells (*P<0.05; 2-tailed *t* test). *(c) (Left)* Representative currents from Kv2.1(S800D)- and Kv2.1(Y124F, S800D)-expressing CHO cells. Calibration: 5nA, 25ms. *(Right)* Mean ± SEM current densities from Kv2.1(S800D)-expressing (n=11) and Kv2.1(Y124F,S800D)-expressing (n=13) CHO cells (*P<0.05; 2-tailed *t* test). *(d)* Y124F mutation disrupts Kv2.1-mediated apoptosis. (Experiments performed by Elias Aizenman, Ph.D.). CHO cells were cotransfected with eGFP plus empty vector and either Kv2.1 or Kv2.1(Y124F) and 24h later exposed to 30μM DTDP (15min). Viability was assayed 24h post-treatment by counting GFP positive cells. Values represent the mean ± S.E.M. (n=3) and are representative of 3 separate, independent experiements (*P<0.05; ANOVA/Bonferroni).

3.4.3 Overexpression of Cyt-PTPε blocks apoptotic K^+ current surge. Cyt-PTPε dephosphorylates Y124, which can counteract enhanced Kv2.1 activity induced by src phosphorylation (Tiran et al., 2003; Tiran et al., 2006). Accordingly, we evaluated whether Cyt-PTPε overexpression would be sufficient to disrupt Y124 phosphorylation and inhibit the apoptotic K^+ current surge. We performed whole-cell recordings in CHO cells co-expressing Kv2.1 and Cyt-PTPε following vehicle and DTDP treatment. We observed that Cyt-PTPε expression strongly inhibited the DTDP-induced K^+ current surge (Fig. 9A), while co-expression of a catalytically inactive mutant isoform (Cyt-PTPε-D245A) (Flint et al., 1997; Peretz et al., 2000) did not (Fig. 9B). Cyt-PTPε expression also strongly inhibited elevated K^+ currents in Kv2.1(S800D)-expressing CHO cells (Fig. 10A,B). Importantly, manipulation of Y124 phosphorylation, first via src inhibition (Fig. 7A, B) and now Cyt-PTPε overexpression, blocks the apoptotic K^+ current surge. These results show not only that Y124 is required, but it must be phosphorylated for the apoptotic Kv2.1-mediated current surge.

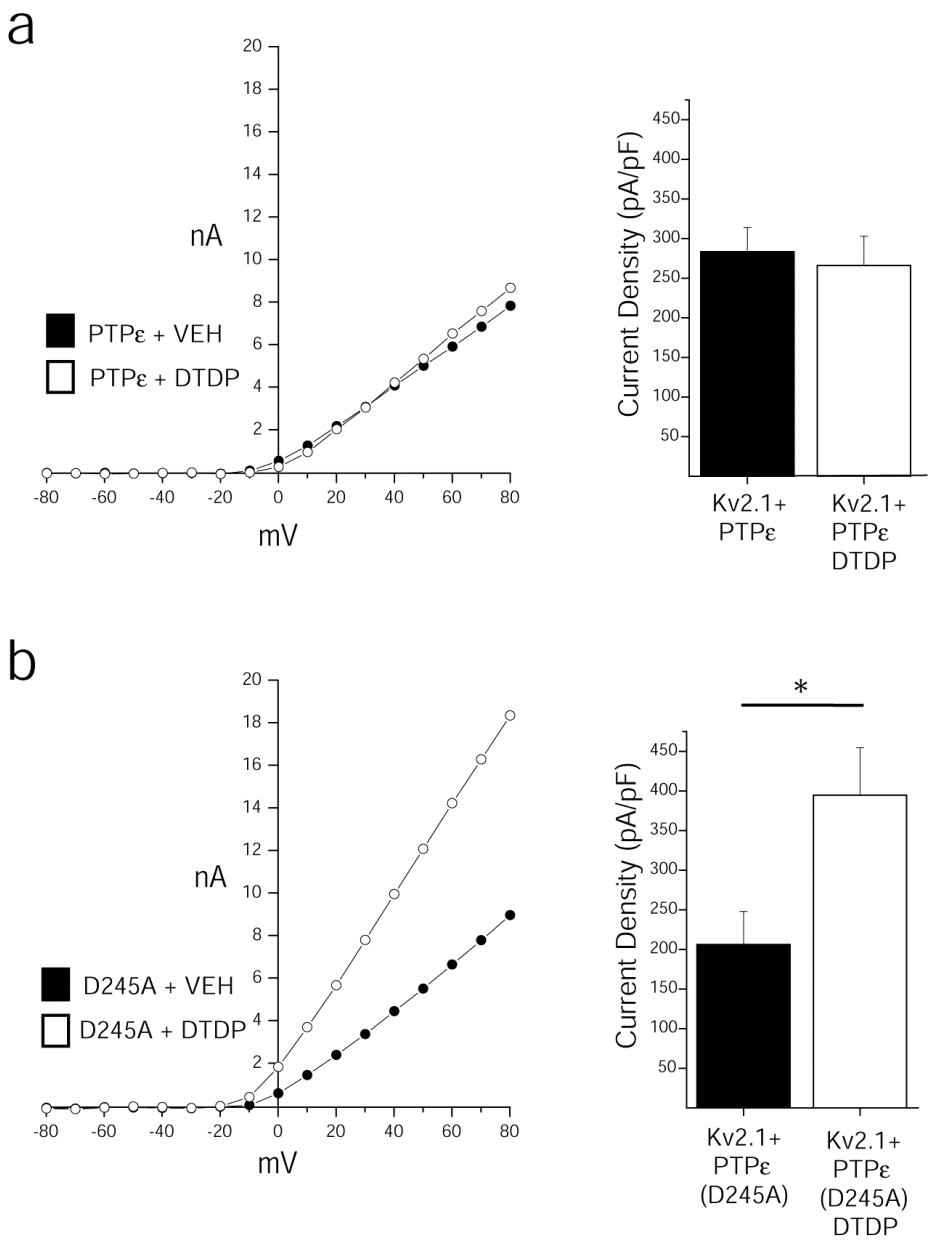
a
nA
mV
PTPε + VEH
PTPε + DTDP
Current Density (pA/pF)
Kv2.1+ PTPε
Kv2.1+ PTPε DTDP
b
nA
mV
D245A + VEH
D245A + DTDP
*
Current Density (pA/pF)
Kv2.1+ PTPε (D245A)
Kv2.1+ PTPε (D245A) DTDP

Figure 9. Cyt-PTPε activity blocks apoptotic K^+ current enhancement. *(a)* Cyt-PTPε and Kv2.1 co-expression blocks apoptotic K^+ current densities in CHO cells. *(Left)* Representative steady state current/voltage relationship of Kv2.1- and Cyt-PTPε-expressing CHO cells recorded following vehicle (*black)* and DTDP treatment (*white)* conditions (30μM for 5min). Currents were obtained 3 h post oxidative injury. *(Right)* Mean ± SEM current densities from Kv2.1- and Cyt-PTPε-expressing CHO cells recorded under control (n=16, *black*) and DTDP treatment (n=16, *white*) conditions. *(b)* Enzymatic activity of Cyt-PTPε is required for inhibition of apoptotic K^+ current enhancement. *(Left)* Representative steady state current/voltage relationship of Kv2.1- and Cyt-PTPε(D245A)-expressing CHO cells recorded under control (*black*) and DTDP treatment (*white)* conditions. *(Right)* Mean ± SEM current densities from Kv2.1- and Cyt-PTPε(D245A)-expressing CHO cells recorded under control (n=16, *black*) and DTDP treatment (n=16, *white*) conditions (*$P<0.01$; 2-tailed *t*-test). Current density was calculated as the steady state K^+ current evoked by a single voltage step to +10mV from a holding potential of -80mV normalized to cell capacitance.

3.4.4 Intracellular Zn^{2+} regulates the apoptotic K^+ current surge. As mentioned earlier, overexpression of Cyt-PTPε inhibited elevated K^+ currents in Kv2.1(S800D)-expressing CHO cells (Fig. 10A,B), indicating that the current surge requires phosphorylation of both Y124 and S800. However, following DTDP exposure we observed that Kv2.1(S800D)-mediated K^+ currents were elevated even in phosphatase-overexpressing cells (Fig. 10A,B). This suggests that Y124 remains phosphorylated during oxidative injury in Kv2.1(S800D)-expressing cells. Since DTDP exposure induces a dramatic rise in free intracellular Zn^{2+} (McLaughlin et al., 2001; Bossy-Wetzel et al., 2004; Redman et al., 2007), we evaluated whether this metal was responsible for the apoptotic K^+ current surge in DTDP treated Kv2.1(S800D)-expressing cells. We thus exposed CHO cells expressing Kv2.1(S800D) and Cyt-PTPε to DTDP in the presence of the Zn^{2+} chelator tetrakis-(2-pyridylmethyl)ethylenediamine (TPEN; 10μM). Under these conditions, Kv2.1(S800D)-mediated current densities were no longer enhanced (Fig. 10A, B), suggesting that Y124 phosphorylation is facilitated by Zn^{2+}. Treating Kv2.1(S800D) and Cyt-PTPε-expressing cells with TPEN alone resulted in no significant changes in current density compared to control conditions (data not shown). To confirm that the TPEN-elicited block of K^+ current enhancement was specific to Zn^{2+} chelation, we treated Kv2.1(S800D) and Cyt-PTPε-expressing cells with DTDP and equimolar concentrations of TPEN and $ZnCl_2$ (10μM). By preloading TPEN with Zn^{2+}, we eliminated TPEN's ability to chelate any DTDP-liberated Zn^{2+} because its metal binding sites are already occupied. These cells showed a pronounced K^+ current enhancement (Fig. 10A, B), again strongly suggesting a Zn^{2+}-dependent modulation of Y124. Since TPEN can also chelate iron, we treated Kv2.1(S800D)- and Cyt-PTPε-expressing cells with DTDP and equimolar concentrations of TPEN and $FeCl_2$ (10μM). In this experiment, any free Zn^{2+} would displace Fe^{2+} from TPEN, reducing the cytoplasmic free [Zn^{2+}] while

increasing the free [Fe^{2+}], as TPEN has a higher affinity for Zn^{2+} than for Fe^{2+} (Zn^{2+}, K_D=2.6x10^{-16} Fe^{2+}, K_D=2.4x10^{-15}). As anticipated, these cells displayed no K^+ current surge (Fig. 10A, B), confirming that Zn^{2+} is the metal species most likely responsible for ensuring Y124 phosphorylation. Because Cyt-PTPε overexpression did not prevent the K^+ current surge in Kv2.1(S800D)-expressing cells when intracellular Zn^{2+} was available, Zn^{2+} inhibition of Cyt-PTPε may potentially be the molecular mechanism leading to elevated K^+ currents.

a

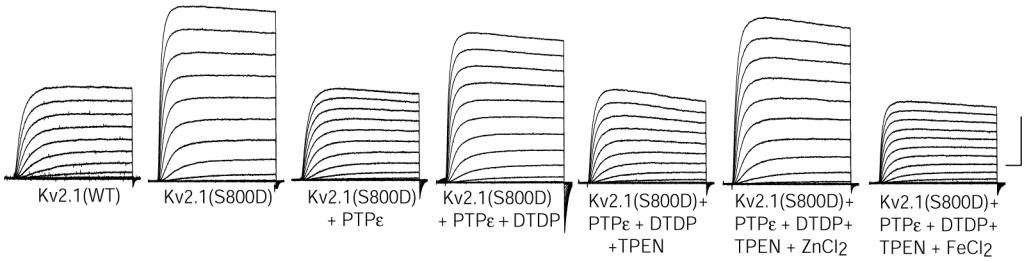

b

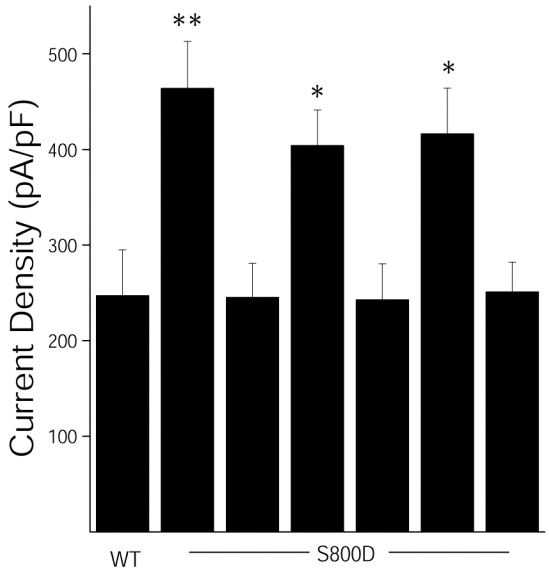

PTPε	–	–	+	+	+	+	+
DTDP	–	–	–	+	+	+	+
TPEN	–	–	–	–	+	+	+
$ZnCl_2$	–	–	–	–	–	+	–
$FeCl_2$	–	–	–	–	–	–	+

Figure 10. K^+ current surge is regulated by intracellular Zn^{2+}. *(a)* Representative whole-cell K+ currents from wild-type (wt) Kv2.1-, Kv2.1(S800D)- and Cyt-PTPε-expressing CHO cells recorded under control and DTDP treatment conditions (30μM for 5min). Other cell groups were treated with tetrakis-(2-pyridylmethyl)ethylenediamine (TPEN) alone (10μM) or in equimolar solutions (10μM) with $FeCl_2$ or $ZnCl_2$ in both the DTDP-treatment and post-treatment medium. Currents were obtained 24h post-transfection, 3h post oxidative injury, and evoked by sequential 10mV voltage steps to +80mV from a holding potential of -80mV. Calibration: 5nA, 25ms. *(b)* Mean ± SEM current densities from wt Kv2.1- (n=14), Kv2.1(S800D)- (n=11), or Kv2.1(S800D) and Cyt-PTPε-expressing CHO cells treated with vehicle (n=15), DTDP (n=18), DTDP + TPEN (n=16), DTDP + equimolar TPEN and $FeCl_2$ (n=20), or DTDP + equimolar TPEN and $ZnCl_2$ (n=19) (significantly different from vehicle-treated WT Kv2.1-expressing cells, **P<0.01; *P<0.05; ANOVA/Dunnett).

3.4.5 Zn^{2+} inhibits catalytic activity of Cyt-PTPε. To test whether Cyt-PTPε enzymatic activity is directly inhibited by Zn^{2+}, we performed an *in vitro* phosphatase assay (Promega, Madison, WI) using immunopurified Cyt-PTPε expressed in CHO cells. As shown in Fig. 11, we observed a 50% inhibition in activity of Cyt-PTPε isolated from cells previously treated with 100μM extracellular Zn^{2+} and 1μM of the Zn^{2+}-selective ionophore pyrithione. This stimulus was used, rather than oxidative injury, as we found it difficult to recover sufficient amounts of active protein from DTDP-treated cells. The effect was reversed in Cyt-PTPε isolated from cells co-treated with 100μM Zn^{2+}, 1μM pyrithione and 10μM TPEN (Fig. 11). Moreover, a consistent increase in phosphatase activity was observed in Cyt-PTPε isolated from cells treated with TPEN alone (Fig. 11). These data thus indicate that basal, endogenous levels of Zn^{2+} inhibit Cyt-PTPε enzymatic activity, which may explain the large current densities observed in Kv2.1(S800D)-expressing cells. Importantly, these results also suggest that disruption of Cyt-PTPε activity operates in parallel with src and p38 (McLaughlin et al., 2001) activation, pinpointing the liberation of intracellular Zn^{2+} as the critical upstream signaling event required for Y124 and S800 phosphorylation during apoptosis (Fig. 13).

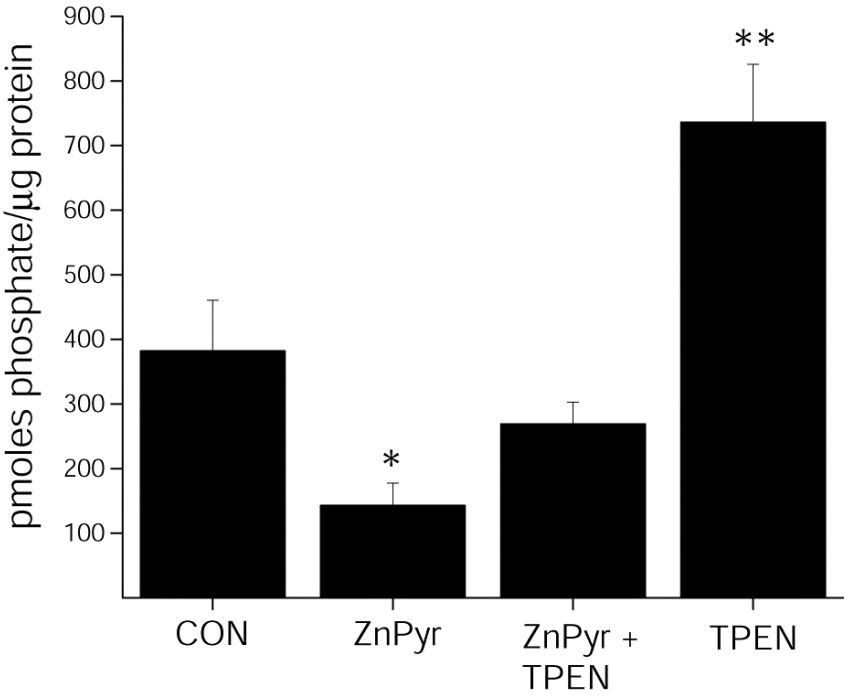
pmoles phosphate/µg protein
900
800
700
600
500
400
300
200
100
*
**
CON
ZnPyr
ZnPyr +
TPEN
TPEN

Figure 11. Cyt-PTPε catalytic activity is inhibited by Zn^{2+}. Cyt-PTPε was purified by immunoprecipitation from whole CHO cell lysates treated with either vehicle, Zn^{2+} (100μM) + pyrithione (1μM), Zn^{2+} + pyrithione+ TPEN (10μM), or TPEN, and added to a phosphatase assay containing 2 synthetic phosphotyrosine peptide substrates. Activity was normalized to Cyt-PTPε recovered following immunoprecipitation and elution and is expressed as pmoles phosphate generated per μg protein (mean±S.E.M., n=6, significantly different from control, *P<0.05, **P<0.01, ANOVA/Dunnett).

3.4.6 Overexpression of Cyt-PTPε attenuates neuronal cell death. To confirm that Cyt-PTPε can modify endogenous Kv2.1-encoded channels, we performed recordings in vehicle- and DTDP-treated cortical neurons transfected with either empty vector or Cyt-PTPε. While vector transfected neurons exhibited a robust, characteristic K^+ current surge following DTDP treatment (Fig. 12A), Cyt-PTPε transfected neurons exhibited no K^+ current increase (Fig. 12B). Since overexpression of the phosphatase blocks the K^+ current surge we evaluated whether it also affects the viability of cortical neurons exposed to activated microglia (Boeckman and Aizenman, 1996; Pal et al., 2003; Aras et al., 2008). Activated microglia can mediate cell death in cortical neurons via a Zn^{2+} and K^+ channel-dependent process *in vitro* (Knoch et al., 2008). Cyt-PTPε -expressing neurons displayed an approximate 2-fold increase in viability compared to vector-expressing neurons exposed to activated microglia (Fig. 12C), almost identical to the rescue we observed in previous studies using Kv2.1 dominant negative isoforms (Pal et al., 2003; Knoch et al., 2008). Taken together, these data suggest that Cyt-PTPε overexpression confers neuroprotection by its actions on Y124 and inhibition of the K^+ current surge following an apoptotic insult.

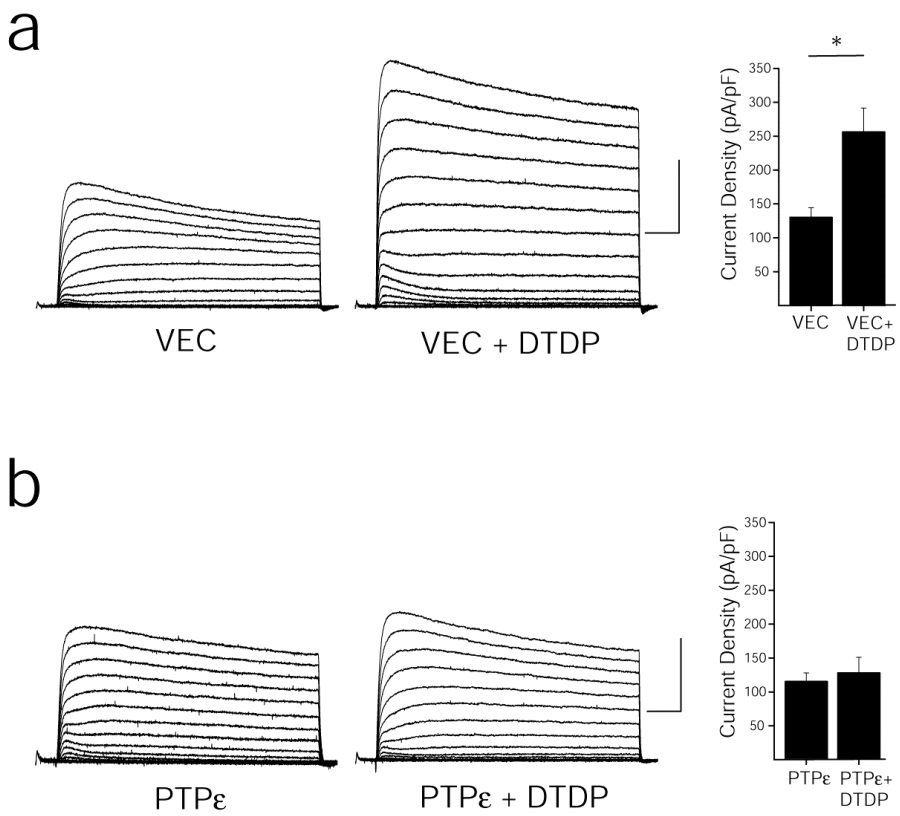
a
VEC
VEC + DTDP
*
Current Density (pA/pF)
350
300
250
200
150
100
50
VEC
VEC+ DTDP
b
PTPε
PTPε + DTDP
Current Density (pA/pF)
350
300
250
200
150
100
50
PTPε
PTPε+ DTDP
c
Δ
***
**
Viability (Luciferase units)
1400
1200
1000
800
600
400
200
CON
AMG
CON
AMG
VEC
PTPε

Figure 12. Overexpression of Cyt-PTPε blocks Kv2.1-mediated neuronal cell death. *(a)* K^+ currents are enhanced in vector-expressing cortical neurons following oxidative injury. *(Left)* Representative whole-cell K^+ currents from cortical neurons co-transfected with empty pRBG4-vector eGFP recorded following vehicle and DTDP treatment conditions (30μM for 10min). Calibration: 5nA, 25ms. *(Right)* Mean ± SEM current densities from empty pRBG4-vector- and eGFP-expressing cortical neurons recorded under control (n=11) and DTDP (n=10) treatment conditions (*P<0.01; 2-tailed *t*-test). Current density was calculated as the steady state K^+ current evoked by a single voltage step to +10mV from a holding potential of -80mV normalized to cell capacitance. *(b)* Overexpression of Cyt-PTPε blocks apoptotic K^+ current densities in cortical neurons. *(Left)* Representative whole-cell K^+ currents from Cyt-PTPε- and eGFP-expressing cortical neurons recorded under control and DTDP treatment conditions. Calibration: 5nA, 25ms. *(Right)* Mean ± SEM current densities from Cyt-PTPε- and eGFP-expressing cortical neurons recorded under control (n=10) and DTDP (n=10) treatment conditions. *(c)* Cyt-PTPε overexpression blocks neuronal cell death following exposure to activated microglia. (Experiments performed by Karen Hartnett). Viability was assayed 24 h post-treatment by luciferase activity and expressed as luciferase units. Values represent the mean ± SEM viability from each condition performed in triplicate and are representative of six separate, independent experiments. (***P<0.001,**P<0.01, ANOVA/Tukey).

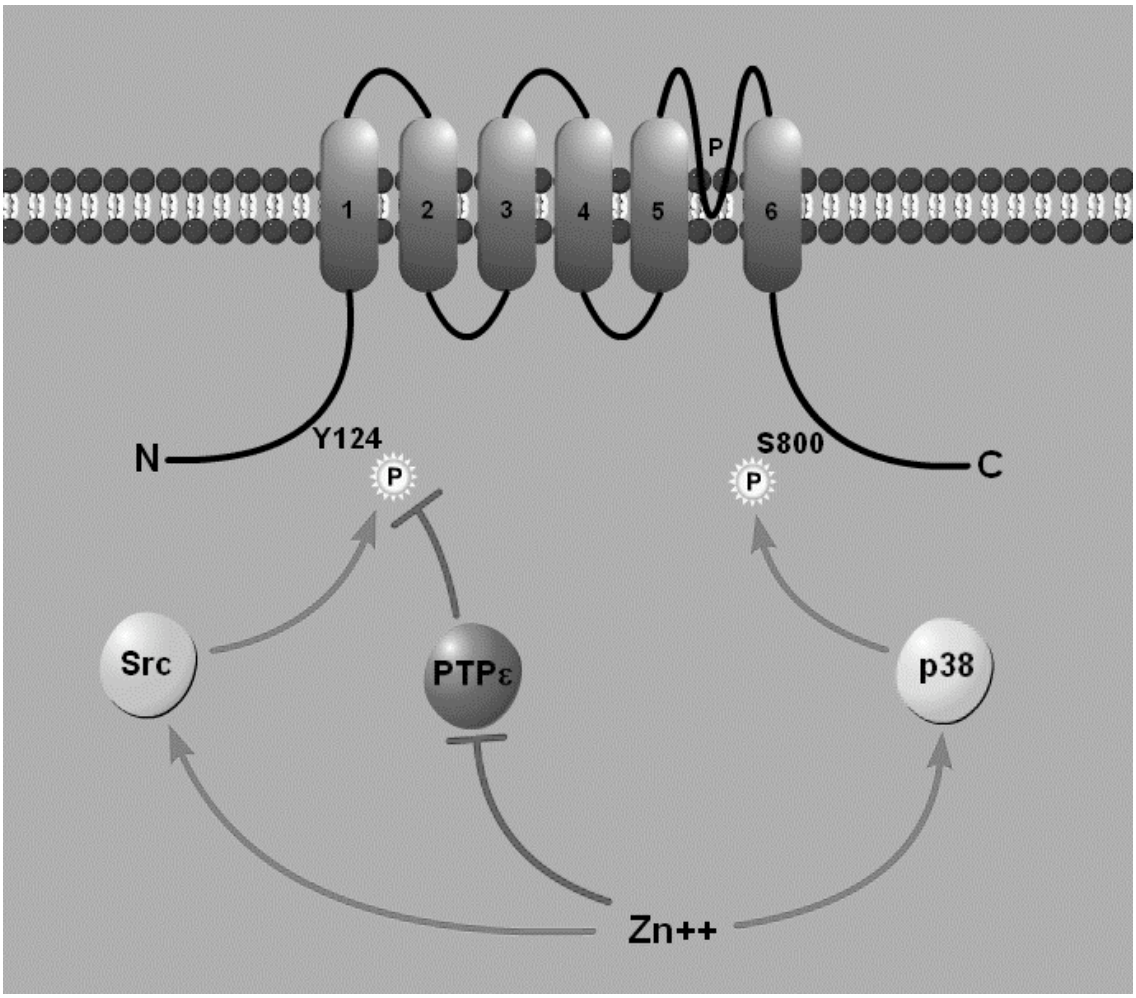

Figure 13. Schematic of Kv2.1 illustrating the proposed effect of intracellular Zn^{2+} on the checkpoint-modifying enzymes src, Cyt-PTPε and p38. The apoptotic K^+ current surge observed in neuronal apoptosis is mediated by surface delivery of Kv2.1-encoded ion channels when intracellular residues Y124 and S800 are phosphorylated. The dual phosphorylation state is achieved following intracellular Zn^{2+} liberation, which increases kinase activity while inhibiting phosphatase activity.

3.5 Discussion

The results presented here demonstrate that two different phosphorylation targets on Kv2.1, namely Y124 and S800, work in concert to regulate the apoptotic surge of K^+ currents. Until now, direct p38 phosphorylation of Kv2.1 residue S800 was thought to be sufficient to account for the apoptotic K^+ current surge mediating death of cortical neurons (Redman et al., 2007). Unlike S800, the majority of phosphorylation and dephosphorylation sites described for Kv2.1 modify channel gating properties (Park et al., 2006). However, oxidative apoptotic injury does not alter the voltage-dependent gating of membrane-resident Kv2.1 channels (Yu et al., 1997), as has been demonstrated in several non-injurious cellular environments (Misonou et al., 2004; Misonou et al., 2005a). In these latter instances, the Ca^{2+} activated phosphatase calcineurin mediates the dephosphorylation of numerous intracellular sites that cooperate in the graded regulation of channel activation and inactivation (Park et al., 2006). Importantly, Y124 and S800 are not calcineurin targets, and thus these sites do not participate in Kv2.1 gating during non-apoptotic conditions. The present findings indicate that phosphorylation of previously characterized S800 (Redman et al., 2007) is not sufficient, and Y124 phosphorylation is required, for Kv2.1-mediated current enhancement during apoptosis. Therefore, Y124 and S800 act as molecular checkpoints mediating the apoptotic K^+ current surge and can strongly influence neuronal viability. Remarkably, the cation ultimately controlling Kv2.1 channel phosphorylation at these sites and subsequent cell death is Zn^{2+}, not Ca^{2+}.

Earlier studies by Elson and colleagues (Tiran et al., 2003) identified Y124 as a novel substrate for direct phosphorylation and dephosphorylation reactions by src and Cyt-PTPε, respectively. However, the role of Y124 on apoptosis had not been evaluated. Src phosphorylation of Kv2.1 does not affect channel activation kinetics under normal conditions (Tiran et al., 2003), and single Kv2.1 channel analysis suggests that the K^+ current enhancement observed in PTPε null mice are not due to differences in channel open probability (Peretz et al., 2000; Tiran et al., 2006). These findings, combined with the present data, indicate that the Y124 phosphorylation dependent K^+ current surge occurs by increasing the number of active membrane-resident channels during apoptosis (Pal et al., 2006). Y124 phosphorylation is therefore critical to support the obligatory K^+ current enhancement in dying cortical neurons, and can be achieved via a combination of src activation and/or Cyt-PTPε inhibition. Nonetheless Y124 phosphorylation is required and must work in concert with p38 phosphorylation of S800, as a serine to alanine point mutation is sufficient to abolish the current surge (Redman et al., 2007).

Although src is activated by endogenous Zn^{2+} liberation (Wu et al., 2002), Zn^{2+}-activated src can not account for enhanced K^+ currents observed under all conditions, as CHO cells expressing Kv2.1(S800D) mutant channels exhibit elevated currents without DTDP treatment (Fig. 8C, Fig. 10). This apparent discrepancy could be explained by basal levels of src activity leading to Y124 phosphorylation. Indeed, this would account for the decreased current densities observed in Kv2.1(S800D)-expressing cells transfected with Cyt-PTPε (Fig. 10). Alternatively, Kv2.1 could be more efficiently phosphorylated by src at Y124 with the S800 checkpoint already fulfilled by pseudo-phosphorylation. However, as pharmacological inhibition of src was

sufficient to block injury-dependent K^+ current surge in cortical neurons (Fig. 7), Zn^{2+}-activated src is likely to be an important component in apoptotic endogenous channel trafficking. Also, recent evidence suggests src tyrosine kinases enhance K^+ currents mediated by hERG (Zhang et al., 2008) and Kv4.3 (Gomes et al., 2008) channels, but direct channel phosphorylation and the nature of K^+ current augmentation has yet to be determined. Although src activity is known to play a neurodegenerative function in various paradigms defined by altered Zn^{2+} homestasis (Paul et al., 2001; Volonte et al., 2001; Khanna et al., 2002; Lennmyr et al., 2004), a novel role for src signaling in a neurodegenerative process has been revealed by the work presented here: regulation of K^+ channel trafficking.

The present study has also established that the balance between Y124 phosphorylation and dephosphorylation is strongly modulated by Zn^{2+}. Our data show the Cyt-PTPε, which targets Y124 on Kv2.1 (Tiran et al., 2003), is inhibited by Zn^{2+}. Protein phosphatases can be inhibited by a number of injury induced cellular processes, including proteolytic cleavage (Gil-Henn et al., 2001), dimerization (Toledano-Katchalski et al., 2003), and oxidation (Meng et al., 2002). There are also reports indicating that phosphatases are inhibited by Zn^{2+} in both cell free preparations (Brautigan et al., 1981; Haase and Maret, 2003, 2005b, a) and following cellular exposure to exogenous Zn^{2+} (Haase and Maret, 2003, 2005b; Kim et al., 2006; Tal et al., 2006). Notably, a recent report demonstrated inhibition of the MAPK phosphatase PP2A by endogenous Zn^{2+} following oxidative injury (Ho et al., 2008). However, the present findings represent, to our knowledge, a novel persistent inhibition of a specific protein tyrosine phosphatase (Cyt-PTPε) by Zn^{2+}. The finding that Zn^{2+} can directly act on the highly conserved active site of protein tyrosine phosphatases at nanomolar concentrations (Haase and Maret, 2003) is highly suggestive

not only that Zn^{2+} may inhibit Cyt-PTPε directly, but may also exert powerful inhibitory effects on all PTPs, including others that may target Y124. We recognize, however, that Zn^{2+} may also be inhibiting Cyt-PTPε by an unknown posttranslational modification or alteration in protein-protein interactions. For instance, Cyt-PTPε forms inactive monomeric and dimeric species under basal conditions that are stabilized during times of increased oxidative stress (Toledano-Katchalski et al., 2003), but the role of Zn^{2+} in this process has yet to be examined.

Although not widely reported in the current literature, convergence of multiple enzymatic signaling pathways mediating different phosphorylation events at membrane resident ion channels has been demonstrated, albeit in non-injurious circumstances. (Moult et al., 2008) showed that p38 and an unspecified protein tyrosine phosphatase co-modify mGLuR2 subunits of AMPARs to mediate receptor internalization and long-term depression in the CA1 region of the rat hippocampus. The present findings, combined with previous work, suggest a concurrent disruption in tyrosine phosphatase activity and enhancement of src and p38 (McLaughlin et al., 2001) activity during apoptosis (Fig. 13). Thus, the liberation of intracellular Zn^{2+} is a common upstream signal determining the phosphorylation both Y124 and S800. With this work, we illustrate an essential regulatory event in the apoptotic program, as separate Zn^{2+}-dependent signaling cascades converge at Kv2.1-encoded ion channels to mediate the apoptotic K^+ current surge and neuronal death.

4. Discussion

Increases in intracellular free Zn^{2+} represent a ubiquitous signal for neuronal injury in neurodegenerative disorders. Dysregulation of Zn^{2+} homeostasis by pathophysiological conditions, especially those in which reactive oxygen and nitrogen species have been implicated, is central to the progression of neuronal injury. In addition, loss of cytoplasmic K^+ appears to be an equally critical cell death catalyst downstream of the initial oxidant-induced Zn^{2+} release. Here, I have summarized the key molecular components that link the Zn^{2+} liberation to the loss of cytoplasmic K^+ in apoptotic neurons. Specifically, I have identified two requisite, Zn^{2+}-dependent phosphorylation events on Kv2.1, at Y124 and S800, that cooperatively mediate apoptotic K^+ current enhancement. Also, I have demonstrated that enzymatic activity of Cyt-PTPε is inhibited by Zn^{2+}. This, in combination with previous observations that Zn^{2+} stimulates src and p38 activity, places this metal as a critical upstream signaling factor governing the dual phosphorylation checkpoint on Kv2.1 (Fig. 13). By characterizing the signaling pathway linking these two events I have helped to elucidate essential mechanistic events that mediate neuronal cell death. In this final chapter I will discuss some of the questions that arise from the present findings and how my results can be incorporated into the overall picture that is emerging for neuronal apoptosis.

4.1 The Zn^{2+}-K^+ continuum: a conserved cell death pathway?

There is now evidence strongly suggesting that the apoptotic Zn^{2+}-K^+ continuum characterized in this study may be widespread in other cell death programs. For instance, in addition to direct exposure to injurious oxidants (McLaughlin et al., 2001; Pal et al., 2004; Zhang et al., 2004), intraneuronal Zn^{2+} liberation is also a defining characteristic in acute neurodegenerative conditions such as epilepsy (Lee et al., 2000; Lavoie et al., 2007), and cerebral ischemia (Calderone et al., 2004). Along these lines, our group has recently detected the release of intracellular Zn^{2+} followed by an apoptotic surge in K^+ currents in cortical neurons exposed to oxygen-glucose deprivation (OGD) (Supplementary Fig. 3, 4). Also, Zn^{2+} dysregulation and K^+ current enhancement have been implicated in the two most prevalent chronic neurodegenerative conditions: Alzheimer's disease (AD) and Parkinson's disease (PD). Importantly, this continuum of ionic dysregulation is not limited to neurodegenerative disease, as both intracellular Zn^{2+} release and K^+ current enhancement are also characteristics of neurodevelopmental cell death (Hribar et al., 2004; Lee et al., 2006). In the following section, I will discuss in greater detail how AD and PD, two disorders historically defined by distinct pathophysiology, share similar features of the apoptotic continuum of Zn^{2+} and K^+ dysregulation.

In the context of AD, significant Zn^{2+} elevations have been found in brain regions displaying severe pathological alterations in the diseased brain, such as the hippocampus (Cuajungco and Faget, 2003). A defining feature of AD pathology is the accumulation of beta

amyloid (Aβ) comprised neuritic plaques, which are proteinacious deposits hypothesized to contribute to neurotoxicity. Studies *in vitro* (Forloni et al., 1993) and *in vivo* (LaFerla et al., 1995) have demonstrated that Aβ is neurotoxic, albeit by poorly defined mechanisms. Zn^{2+} co-localizes with beta amyloid (Aβ) plaques in transgenic mouse models of AD (Lee et al., 1999) and in human diseased brain tissue (Danscher et al., 1997; Suh et al., 2000), while chelation of Zn^{2+} facilitates plaque dissolution (Cherny et al., 1999; Regland et al., 2001; Ritchie et al., 2003; Friedlich et al., 2004) and solubilizes Aβ from deposits in post-mortem tissue from Alzheimer's disease patients (Hensley et al., 1995). Synaptically released Zn^{2+} significantly contributes to Aβ aggregation and toxicity *in vivo*, as transgenic mice lacking synaptic Zn^{2+} display an amelioration of Aβ pathology (Lee et al., 2002). Zn^{2+} has been shown to promote Aβ-induced ROS generation (Huang et al., 1999) although it must be noted that other redox active metal ions, such as copper and iron, have also been shown to potentiate Aβ-induced ROS generation and toxicity (Cuajungco et al., 2000). Because Zn^{2+} is not redox active, Zn^{2+} may be acting to coordinate Aβ aggregation, while downstream toxic ROS generation might be purely dependent on copper and iron. In either case, Aβ-mediated ROS production may also be functioning as a positive feedback mechanism, leading to further Zn^{2+} liberation from intracellular metal-binding proteins. As p38 activation has also been shown in the AD brain (Hensley et al., 1999), and following introduction of exogenous Aβ (Giovannini et al., 2002), Zn^{2+}-mediated ROS generation via Aβ could, in theory, lead to apoptotic p38 activation. In fact, this putative signaling pathway closely resembles the Zn^{2+}-mediated ROS generation by mitochondria and 12-LOX leading to p38 activation following oxidant exposure (McLaughlin et al., 2001; Sensi and Jeng, 2004; Zhang et al., 2004). Moreover, other putative Aβ signaling pathways may involve src family kinases, as mice deficient in fyn are resistant to Aβ-induced neurotoxicity (Lambert et al., 1998), further

suggesting that Zn^{2+}-activated signaling pathways are a common component of apoptotic excecution.

In addition to Zn^{2+} dysregulation, K^+ channel dysfunction has also been implicated in the neurodegenerative processes of AD. In rat cortical neurons exposed to Aβ, a selective enhancement in both transient and delayed rectifyer voltage-gated potassium current is detected prior to completion of the apoptotic program (Yu et al., 1998; Yu et al., 2006). Very recently, another group provided evidence implicating Kv3.4 and accessory subunit MiRP2 as the molecular gateway responsible for the increased transient K^+ current observed following Aβ exposure (Pannaccione et al., 2007). The investigators observed a nuclear factor κB (NF-κB)-dependent transcriptional co-upregulation of Kv3.4 and MiRP2, followed by increased channel membrane insertion prior to caspase activation and cell death (Pannaccione et al., 2007). The mechanism and Kv channel leading to elevated delayed rectifying currents was not identified, but the results from the present study suggest that Kv2.1 surface delivery via dual phosphorylation is most likely responsible, especially since oxidative stress, and Zn^{2+} dysregulation seem to be central to Aβ toxicity. Importantly, blocking both the transient and delayed rectifying K^+ current surge with selective antagonists was neuroprotective (Pannaccione et al., 2007; Yu et al., 2006), indicating that K^+ efflux is also a critical event in Aβ-induced neuronal cell death.

Relevant to Parkinson's disease, several *in vitro* and *in vivo* models have demonstrated characteristics of a Zn^{2+}-K^+ continuum leading to neuronal death. Parkinson's disease pathology is characterized by dopaminergic cell death in the striatum and substantia nigra, and for the most

part, pre-clinical models of have made use of neurotoxins that selectively target dopaminergic neurons in these two brain regions. For instance, the dopaminergic neurotoxin 6-hydroxydopamine- (6-OHDA) has recently been shown to affect Zn^{2+} and K^+ regulation. 6-OHDA is transported into dopaminergic neurons by the dopamine transporter (DAT), where it has been suggested to mediate toxicity via oxidative signaling processes (Blum et al., 2001) and caspase-dependent apoptosis (Choi et al., 2004). A considerable elevation in cellular Zn^{2+} levels has been observed in dopaminergic neurons in the 6-OHDA-induced rodent model of Parkinson's disease (Tarohda et al., 2005), while 6-OHDA induced neurotoxicity is significantly exacerbated in mice lacking two out of three metallothionein isofoms expressed in the brain (MT-1 and MT-II null mice) (Asanuma et al., 2002). Also, a significant increase in p38-dependent, Kv2.1-mediated K^+ currents was detected in dopaminergic neurons exposed to 6-OHDA *in vitro* (Appendix; Redman et al., 2006), suggesting that the specific signal transduction pathway delineated in the present study is mediating apoptosis. However, it was also recently demonstrated that activation of ATP-sensitive potassium channels (K-ATP) participates in dopaminergic cell death in the substantia nigra following exposure to the dopaminerginc toxins rotenone and MPTP (Liss et al., 2005). K-ATP channels are activated in response to the convergence of cellular energy depletion and increased ROS generation induced by mitochondrial disuptions. Along with K-ATP channel activation, metallothionein levels are significantly reduced in the substantia nigra of mice following a single neurotoxic injection of (MPTP) (Dhanasekaran et al., 2007). Thus, a potential rise in intracellular Zn^{2+} resulting from removal of this metal-buffering protein may contribute to subsequent ROS generation and K^+ channel activation. Still, the molecular link between K-ATP activation and dopaminergic cell death following MPTP treatment has not been established. It is quite possible that K-ATP

channels are facilitating an apoptotic K^+ efflux similar to the requisite event mediated by Kv2.1 in dopaminergic neurons exposed to 6-OHDA *in vitro* (Appendix; Redman et al., 2006). On the other hand, because some K-ATP channels are localized at mitochondria, they represent additional putative targets of Zn^{2+}-dependent mitochondrial disruption, in addition to Zn^{2+} activation of mitochondrial multi-conductance channels associated with cell death signaling molecules (Bonanni et al., 2006). Therefore, Kv2.1-encoded channels are more likely mediating death via K^+ efflux downstream of K-ATP-mediated neurotoxic signaling pathways.

In summary, sequential disruption in Zn^{2+} and K^+ homeostasis is associated with a range of neuronal cell death conditions, including chronic neurodegenerative disorders associated with oxidative stress, mitochondrial impairment and Aβ. Although different disease states will undoubtedly involve multiple pathways participating in toxicity, if the Zn^{2+}-regulated signaling molecules described in the present study are activated, they will likely participate through modulation of Kv2.1. Also, it is possible that different K^+ channels are able to provide multiple gates for K^+ efflux, even in the same cell type, depending on the nature of the injury. Thus, blocking the appropriate K^+ channel population, like has been demonstrated here with Kv2.1, will be necessary to rescue cells from different neurotoxic insults.

4.2 Mechanism of Cyt-PTPε inhibition by Zn^{2+}

The experiments presented in Chapter 2 indicate that Cyt-PTPε is inhibited by Zn^{2+}, but the specific mechanism of Zn^{2+} inhibition remains unknown. In this section, I will explore potential mechanisms regulating the Cyt-PTPε inhibition that was observed following treatment

of CHO cells with Zn^{2+} and immunopurification of the phosphatase. Because Cyt-PTPε activity was measured as the function of the free phosphate generated after cellular Zn^{2+} exposure, cell lysis, and immunoprecipitation procedures, the inhibition of Cyt-PTPε by Zn^{2+} must be long lasting and highly resilient. Recently, Ho et al. (2008) demonstrated a similar sustained inhibition of PP2A by endogenous Zn^{2+} following oxidative injury using an *in vitro* phosphatase assay, although the mechanism of inhibition was not explored. As discussed earlier, protein phosphatases can be inhibited by oxidation-induced dimerization (Toledano-Katchalski et al., 2003), oxidation of the catalytic cysteine residue (Meng et al., 2002), and posttranslational modifications (Toledano-Katchalski et al., 2003). Because Zn^{2+} can enter mitochondria and induce the production of ROS (Manev et al., 1997), Zn^{2+} may inhibit Cyt-PTPε via an oxidative mechanism. Indeed, a short (5 min) exposure to 100 μM Zn^{2+} during activation of Zn^{2+}-permeable ion channels was sufficient to induce mitochondrial ROS generation in neurons (Sensi et al., 1999). Thus, the 30 min exposure to 100 μM Zn^{2+} and 1 μM pyrithione used in this study could potentially be inducing similar mitochondrial ROS generation capable of phosphatase inhibition. However, either reversible oxidation of the active site or reversible oxidation induced dimerization are unlikely, due to the high concentration of the reducing agent dithiothreitol (DTT) present in the phosphatase assay buffer. DTT was necessary to keep the immunopurified phosphatase active, and phosphatase activity was decreased with lower DTT concentrations (data not shown). On the other hand, the catalytic cysteine sulfydryl group could have undergone *irreversible* oxidation to either a sulfinic or sulfonic acid, a modification that has been demonstrated with PTP 1B (Haase and Maret, 2005) and would be resistant to reduction and hence catalytic reactivation by DTT. Thus, if Zn^{2+}-induced ROS generation is responsible for

the prolonged inhibition in Cyt-PTPε, it is likely the result of irreversible oxidation of the catalytic domain.

The finding that Zn^{2+} effectively inhibits T-cell PTP at nanomolar concentrations (Haase and Maret, 2003) by binding to the highly conserved catalytic domain suggests that a direct inhibitory effect of Zn^{2+} is also quite possible, especially at the concentrations used in this study (100 μM). Interestingly, direct Zn^{2+} binding has been suggested to mediate sustained inhibition of purified dual specificity phosphatases exposed to oxidant-liberated Zn^{2+} (Ho et al., 2008). Because DTT has been shown to form a complex with free or readily accessible Zn^{2+} ions (Cornell and Crivaro, 1972), I was unable to examine direct inhibition by simply adding Zn^{2+} to the purified phosphatase reaction. Moreover, Zn^{2+} inhibition of Cyt-PTPε would need to be resistant to DTT. This situation may be possible, as Zn^{2+} chelators are ineffective at recovering catalytic activity once the purified protein is bound by Zn^{2+} in other systems (Zhuo and Dixon, 1997). Thus, DTT chelation of the inhibitory Zn^{2+} ion and reactivation of purified Cyt-PTPε is unlikely to be a confounding factor if Zn^{2+} is binding and inhibiting Cyt-PTPε during CHO cell exposure, further supporting the notion that the sustained inhibition of Cyt-PTPε observed in this study could also be the result of a direct Zn^{2+} interaction.

Another possible scenario mediating Cyt-PTPε inhibition is a Zn^{2+}-mediated post-translational structural modification, such as phosphorylation, resulting in a protein subject to immunoprecipitation while retaining a catalytically inactive conformation. Indeed, Zn^{2+}-mediated phosphorylation is responsible for the prolonged alteration in catalytic activity that has been demonstrated previously with PTP 1B (Haase and Maret, 2005). Interestingly, the

alteration in PTP 1B signaling is regulated by several kinases, including protein kinase C (PKC) (Haase and Maret, 2005), an enzyme known to be activated by Zn^{2+} (Noh et al., 1999). Thus, a Zn^{2+}-dependent PKC phosphorylation event could, in theory, be modifying Cyt-PTPε leading to sustained inhibition, particularly if Zn^{2+}-dependent phosphatase inhibition is widespread and the phosphatase that normally reverses the PKC phosphate addition is inactive. Regardless of the molecular mechanism, the data suggest a sustained Cyt-PTPε inhibition by Zn^{2+}, which in the context of oxidant-induced neuronal cell death would act as an effective cellular strategy for supporting Y124 phosphorylation, Kv2.1 surface delivery, and apoptosis.

4.3 Signal transduction pathways from Zn^{2+} to Kv2.1: other considerations.

The results presented in this dissertation, in addition to previous work, suggest the following model connecting oxidative Zn^{2+} liberation to the loss of cytoplasmic K^+ in apoptotic neurons: Zn^{2+} stimulates src and p38 activity while inhibiting Cyt-PTPε, thus facilitating the dual phosphorylation of Kv2.1 at Y124 and S800, followed by channel surface delivery and apoptotic K^+ efflux (Fig. 13). However, further studies are required to determine the specific molecular interactions between p38, src, Cyt-PTPε and Kv2.1, as well as other apoptotic signaling molecules implicated in Zn^{2+} and K^+ dysregulation and neuronal cell death. Certainly, the literature suggests additional possibilities of p38, src and PTPε interactions that may be regulating the neuronal apoptotic program.

Different Kv2.1-targeting PTP isoforms may regulate apoptotic channel surface delivery by modulating other proteins in the proposed pathway, in addition to Y124 phosphorylation.

Along with Cyt-PTPε, Y124 is also a substrate of RPTPε and RPTPα (Tiran et al., 2006). Both RPTPε and RPTPα, but not Cyt-PTPε, have been shown to activate src *in vitro* and *in vivo* via dephosphorylation of the inhibitory tyrosine 527 (Tiran et al., 2006). As such, perhaps RPTPα or RPTPε mediated basal src activation is the reason for elevated currents observed in Kv2.1(S800D)-expressing CHO cells (Fig.10). Nevertheless, the fact that RPTPε and RPTPα can both activate src and block the Y124 checkpoint, while Cyt-PTPε only targets Y124, suggests that different PTP isoforms perform distinct and overlapping roles in Kv2.1 modulation during neuronal apoptosis.

Interestingly, Cyt-PTPε expression strongly inhibits activity of downstream reporters of p38 MAPK activation during non-injurious conditions (i.e. transcription factor CHOP; Toledano-Katchalski et al., 2003b), although direct p38 inhibition has not been tested. As Cyt-PTPε directly inactivates ERK1/2 MAPK (Toledano-Katchalski et al., 2003a), it is not unreasonable to propose p38 as an additional potential target for Cyt-PTPε activity, thereby negatively regulating both Kv2.1 and p38 activity. There is also evidence indicating that src can activate p38 by an unknown mechanism following cellular glutathione depletion (Cuadrado et al., 2003). Thus, like Kv2.1, p38 activity may also be regulated by the balance between src-mediated phosphorylation and Cyt-PTPε-mediated dephosphorylation. Furthermore, Cyt-PTPε may be responsible for inhibiting channel surface expression by dephosphorylating both Kv2.1 and p38, effectively blocking both N- and C-terminal checkpoints during non-injurious conditions through direct and indirect phosphatase signaling.

Along with evidence indicating src and p38 are both regulated by PTPε, functional interactions have also been demonstrated between src and p38 kinase pathways. As mentioned above, src is known to activate p38 (Cuadrado et al., 2003), while reciprocal activation of src by p38 has also been demonstrated (Volonte et al., 2001). Because both kinase pathways are activated by Zn^{2+} and converge at Kv2.1, the function of reciprocal activation in the proposed model would serve to amplify the current enhancement even more. This interaction of Zn^{2+}-dependent pathways prior to convergence at Kv2.1 might serve to activate both src and p38 proteins that are localized in a Zn^{2+}-deficient subcellular domain. Even so, if Zn^{2+} is present at the appropriate subcellular localization and concentration, it could rapidly modulate all of the signaling enzymes in the vicinity. For instance, metallothionein proteins could be positioned in close proximity to p38, src and Cyt-PTPε, effectively releasing Zn^{2+} to readily influence nearby signaling molecules following an oxidative insult. Such a scenario has been reported with calcineurin regulation of Kv2.1, as channel clusters lie in close proximity to endoplasmic reticulum derived subsurface cisternae rich in ryanodine Ca^{2+} channels (Misonou et al., 2005). Also, as Zn^{2+}-induced injury has shown to be blocked by antagonists of Zn^{2+} influx, such as Ca^{2+}-permeable voltage- and glutamate-gated ion channels (Colvin et al., 2003), exogenous Zn^{2+} influx could function to modulate enzymes localized at the plasma membrane. This is particularly applicable to the Zn^{2+}-K^+ neuronal cell death pathway, as Zn^{2+} may be inhibiting the other membrane localized PTPs that share functional redundancy to Cyt-PTPε and target Kv2.1, namely RPTPε and RPTPα (Tiran et al., 2006), in addition to activating src and p38. Perhaps the most efficient system for achieving dual Kv2.1 phosphorylation via localized Zn^{2+} signaling would be the consolidation of relevant signaling enzymes with the channel into a Zn^{2+}-accessible protein complex. Such a "macro-molecular" signaling complex has been demonstrated before

containing the K^+ channel Kv7.1, the auxillary subunit MinK, protein kinase A and protein phosphatase 1, and is required for channel modulation via phosphorylation and dephosphorylation (Marx et al., 2002).

4.4 How does phosphorylation lead to channel insertion?

Another issue that requires further experimentation is the mechanism K^+ current enhancement following dual Kv2.1 phosphorylation. Previous observations from our laboratory indicate that cleavage of the SNARE proteins SNAP-25 and syntaxin is sufficient to block the apoptotic K^+ current enhancement (Pal et al., 2006). SNAP-25 forms a direct physical association with the cytoplasmic N-terminal (MacDonald et al., 2002), while syntaxin and syntaxin/SNAP25 t-SNARE complex directly interact with a membrane proximal region of the intracellular C-terminal of Kv2.1, defined as the C1a region (Leung et al., 2003; Tsuk et al., 2005). Recent findings indicate that Kv2.1 also interacts with the vesicular SNARE (v-SNARE) protein VAMP2 in brain membranes and *Xenopus* oocytes (Lvov et al., 2008). However, the interaction of individual SNARE proteins with Kv2.1 is eliminated upon construction of the full SNARE complex (syntaxin/SNAP-25/VAMP2) (Tsuk et al., 2008). In addition, overexpression of syntaxin 1A and Kv2.1 can inhibit channel surfacing leading to a decrease in Kv2.1-mediated current density (Leung et al., 2003). Very recently, it has been demonstrated that the Kv2.1 C-terminal association with syntaxin 1A directly facilitates an increase in dense-core vesicle exocytosis following elevation in cytoplasmic Ca^{2+} (Singer-Lahat et al., 2007). These various observations suggest that changes in phosphorylation state of Y124 and S800 lead to changes in association of the exocytotic SNARE protein machinery with the channel. A similar

"biochemical switch" situation has been observed in other systems, where phosphorylation of N-type Ca^{2+} channels by PKC or CAMKII leads to inhibition of binding with both syntaxin and SNAP-25 (Yokoyama et al., 1997), although the physiological significance of this switch is not known.

Because the effect of sytnaxin 1A binding on phosphorylation-mediated Kv2.1 trafficking has not been examined extensively, it represents an important subject for future studies. For instance, whether the phosphorylation state of Y124 and S800 is responsible for Kv2.1 association with syntaxin 1A could easily be assayed in a recombinant expression system using Kv2.1 mutant channels and syntaxin 1A overexpression, followed by immunoprecipitation. Also, whether the C1a syntaxin binding domain is necessary for p38 phosphorylation of S800 could be determined in a recombinant expression system overexpressing channels lacking C1a followed by cell lysis and immunostaining with our phospho-S800 antibody.

Changes in physical association with other proteins known to interact with Kv2.1 may also play a role in surface delivery following phosphorylation. For instance, association between Kv2.1 and an undefined retention scaffolding protein associated with the actin cytoskeleton is hypothesized to regulate lateral diffusion of channels between their well characterized clustered subcellular distribution in neurons (O'Connell et al., 2006), and changes in intracellular termini phosphorylation state are thought to determine this association. Whether unclustering accompanies phosphorylation-dependent apoptotic surface delivery in our paradigm is unknown. Along these lines, disruption in the actin cytoskeleton prevents the apoptotic K^+ loss and subsequent loss in cell volume and DNA fragmentation in Jurkat-T cells following Fas-L or UV

exposure (Bortner et al., 2008). As such, regulation of channel trafficking and gating may be dependent on maintenance of cytoskeletal architecture as well. Also, K^+ channel β-subunits can control trafficking and surface expression of K^+ channel α subunits, in addition to modulating channel activity (Shi et al., 1996). Although only Kv1 and Kv4 channel subfamilies have historically been associated with β subunits, there is some evidence that Kv2.1 forms endogenous heteromeric associations with Kv9.3 (Coma et al., 2002). As mentioned above, intracellular N- and C-termini of Kv2.1 have been shown to interact physically (Kobrinsky et al., 2006; Mohapatra et al., 2008), and this interaction is required for efficient channel trafficking to the plasma membrane (Mohapatra et al., 2008). It has been demonstrated that a 17 amino acid sequence located within the N-terminal T1 domain (residues 55-71), the region corresponding to the β subunit binding site in Kv1 and Kv4 channels, is required for both N- and C-terminal interaction and Kv2.1 channel surface expression (Mohapatra et al., 2008). It is thus also probable that conformational changes in intracellular N- and C- termini, mediated by Y124 and S800 phosphorylation, determine Kv2.1 trafficking during apoptosis, similar to the changes in Kv2.1 channel activity mediated by altered intracellular associations between termini (Kobrinsky et al., 2006).

The molecular consequence of dual phosphorylation of Kv2.1 may be similar to the regulation of src, where one phosphorylation event initiates a steric shift that allows a second kinase access to its phosphorylation site. It should be possible to probe whether p38 phosphorylation of S800 is dependent on src phosphorylation of Y124 by using our phospho-S800 antibody in combination with wild-type Kv2.1 and Kv2.1(Y124F) mutant channels. Also, probing whether src phosphorylation of Kv2.1 is dependent on the p38 phosphorylation event

could be achieved, in theory, by using wild-type Kv2.1, Kv2.1(S800A) and Kv2.1(S800D) mutant channels in combination with the Cyt-PTPε(D245A) substrate trapping mutant. Elson and colleagues have shown that Cyt-PTPε(D245A) is less likely to bind a dephosphorylated Y124 (Tiran et al., 2003), and thus the mutant phosphatase could be used as an assay for Y124 phosphorylation by looking for changes in association between channel and phosphatase. In other words, future studies could determine if the phosphorylation sites are inderdependent, and whether the order of phosphorylation events is a critical factor for channel surface delivery.

4.5 Concluding remarks

In this dissertation, I have characterized an important signaling pathway regulating neuronal cell death by identifying key molecular components that link oxidant-induced Zn^{2+} liberation to the loss of cytoplasmic K^+ in apoptotic neurons. Specifically, I have identified two essential phosphorylation sites on Kv2.1, at Y124 and S800, that cooperatively mediate the apoptotic K^+ current surge and neuronal cell death. Also, I have demonstrated that enzymatic activity of Cyt-PTPε is inhibited by Zn^{2+}. As Zn^{2+} has also been demonstrated to activate src and p38, this cation is an important signaling factor governing the dual phosphorylation of Kv2.1. The work presented here provides a more complete understanding of neuronal apoptotic processes by highlighting the importance of intracellular signaling cascades accompanying ionic dysregulation. As these processes may be widespread, this work also provides possible novel therapeutic targets for a range of neurodegenerative disorders.

APPENDIX

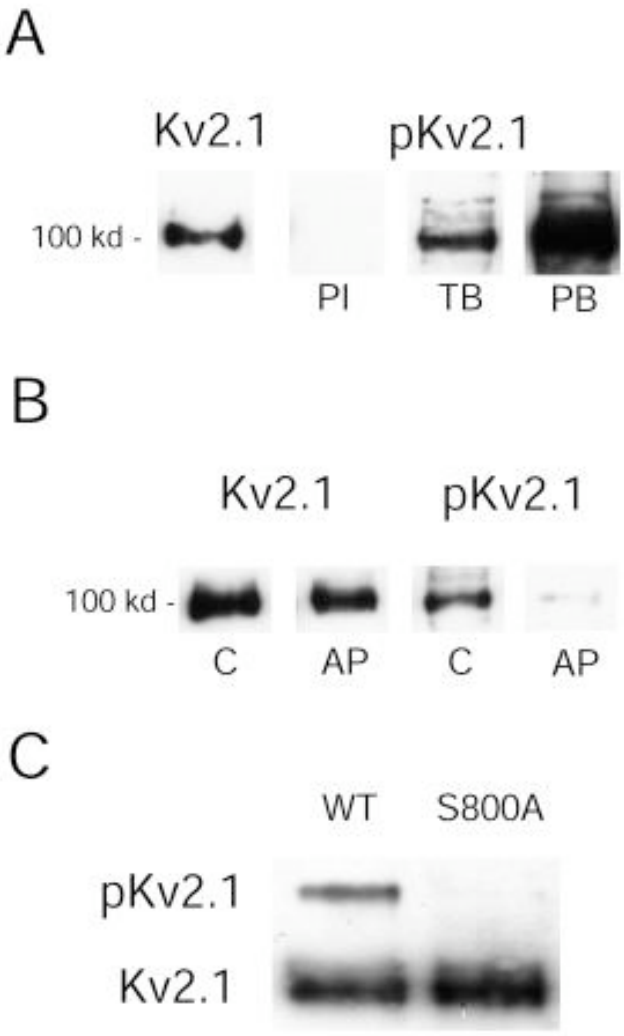
A
Kv2.1
pKv2.1
100 kd -
PI
TB
PB
B
Kv2.1
pKv2.1
100 kd -
C
AP
C
AP
C
WT
S800A
pKv2.1
Kv2.1

Supplementary Figure 1. Generation of phospho-specific antibody. Antisera specific for the phosphorylated p38 MAPK consensus sequence of Kv2.1 (pKv2.1) was produced in rabbits immunized with a keyhole limpet hemocyanin-conjugated peptide with the sequence C-KNHFESSPLPTS(p)PKFLR. Protein samples were generated from CHO cells expressing either WT Kv2.1 or the mutant Kv2.1(S800A). Cells were treated with 25 mM DTDP (5 min) 3 h before harvesting. (A) Immunoblots probed with a commercial Kv2.1 antibody (Alomone; 1:3,000) or serum from immunized rabbits (pKv2.1). PI, preimmune serum (1:3,000); TB, test bleed (1:3,000); PB, production bleed (1:3,000). (B) Immunoblots probed with either Kv2.1 (1:3,000) or pKv2.1 (1:12,000) antibodies under control conditions (C), or after an overnight incubation of the nitrocellulose membrane with alkaline phosphatase (AP; 100 units/ml) containing buffer (50 mM Tris-HCl, 1 mM $MgCl_2$, 0.1 mM $ZnCl_2$, 0.1 mM EDTA, 45% glycerol, pH 8.5) at 36°C. Note that the signal for the phospho-specific antibody is abolished by the phosphatase treatment. (C) Immunoblots probed with either Kv2.1 (1:3,000) or pKv2.1 (1:12,000) antibodies on protein samples from CHO cells expressing either Kv2.1 or Kv2.1(S800A). Note the lack of phospho-specific signal for the mutant channel.

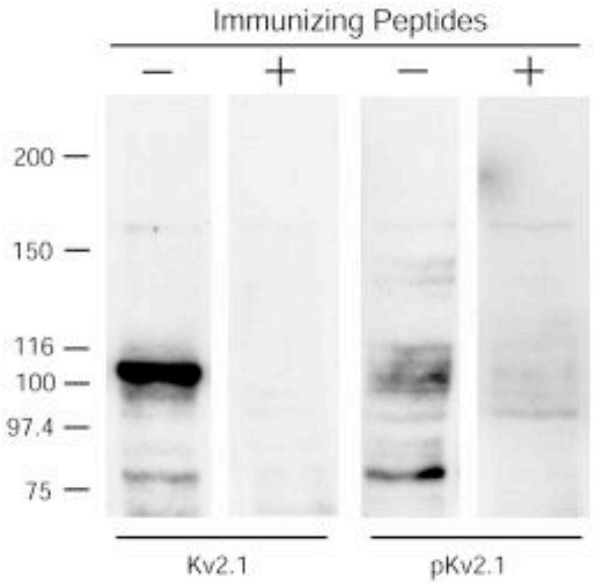

Supplementary Figure 2. Immunodetection of neuronal Kv2.1 protein. Equal amounts of protein were separated by 6% reducing SDS/PAGE and transferred to nitrocellulose membranes. The resulting blots were probed with affinity-purified rabbit polyclonal antibodies specific for either the C terminus of Kv2.1 (Alomone Labs) or pS800 of Kv2.1. Both antibodies reacted with the 80-kDa band as well a diffuse band with a molecular mass of »100 kDa. Preincubation of the two antibodies with their respective synthetic immunizing peptides eliminated both immunoreactive signals.

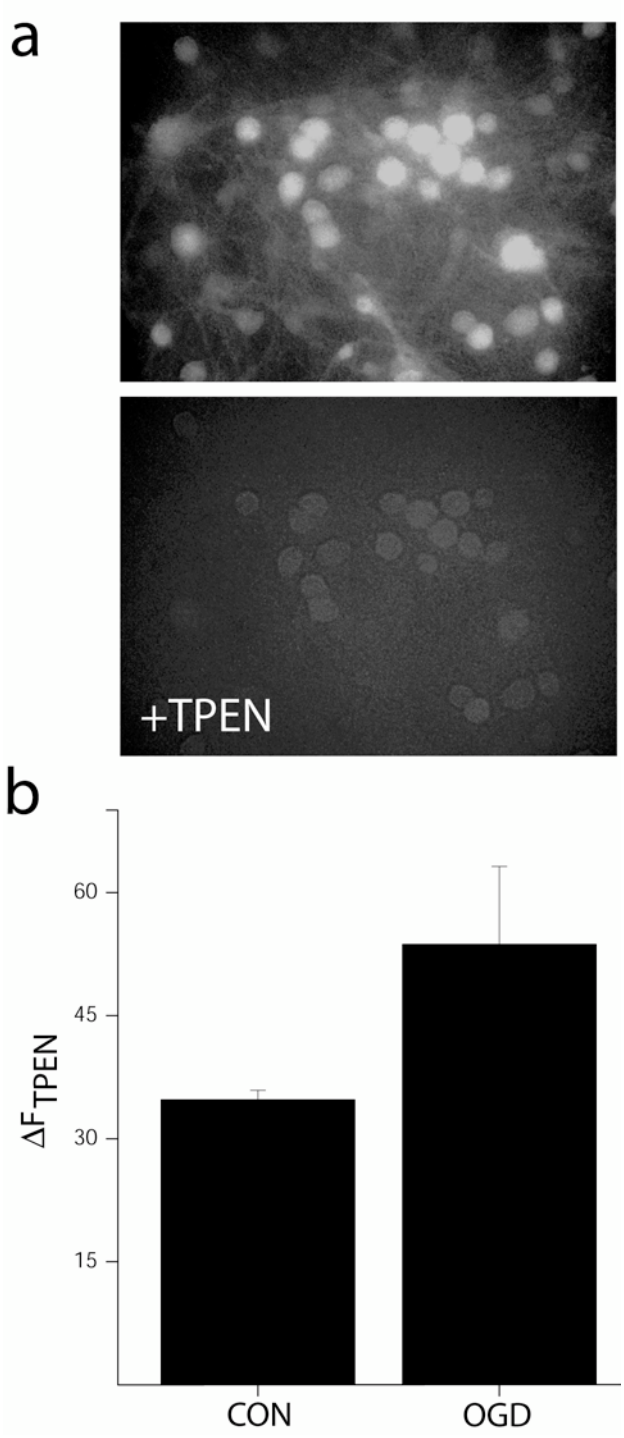
a
+TPEN
b
60
45
30
15
ΔF TPEN
CON
OGD

Supplementary Figure 3. Oxidative injury induces intracellular zinc release. Experiments completed by Megan Knoch, Ph.D. Cortical neurons were loaded with the Zn^{2+}-sensitive fluorescent reporter Fluozin-3 AM (5μM for 30min) and then perfused with DTDP (100μM for 5min). Images were acquired with a 485 nm excitation light *(top)*. Following DTDP exposure, cells were treated with 20μM TPEN to chelate free intracellular Zn^{2+} and images were again acquired at 485 nm (*bottom)*. *(b)* Zn^{2+} release following an ischemic insult. Data represents TPEN sensitive intraneuronal Zn^{2+} 4 hours after 30 minutes of oxygen-glucose deprivation (OGD; n=3) or 30 minutes non-OGD control exposure (glucose-containing salt solution; n=3). Following OGD, neurons were loaded with the Zn^{2+}-sensitive fluorescent reporter Fluozin-3 AM (5μM for 30min). Images were then acquired with 485 nm excitation light. Baseline images were acquired and then cells were treated with 20μM TPEN to chelate free intracellular Zn^{2+}. Relative Zn^{2+} fluorescence for all neurons was determined by subtracting the Fluozin-3 AM signal after TPEN application from the baseline Fluozin-3 AM signal (ΔF_{TPEN}). Data represent pooled (Mean±SEM) TPEN sensitive Zn^{2+} fluorescence measurements from 3 coverslips, each containing 5-15 cortical neurons.

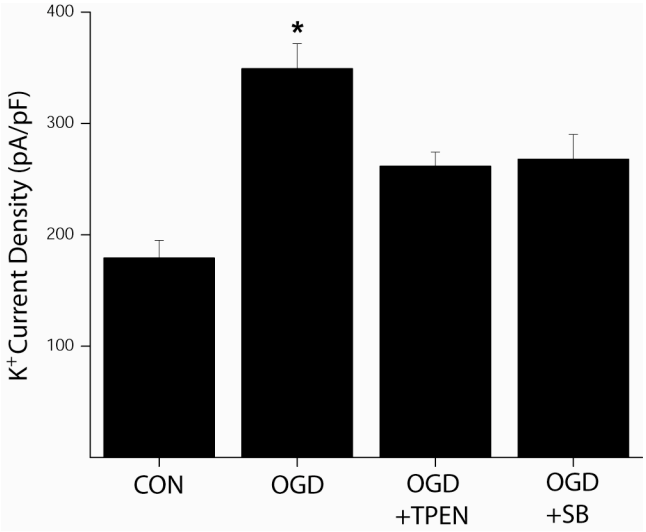

Supplementary Figure 4. OGD induces an apoptosis-associated K^+ current enhancement. Experiments completed by Megan Knoch, Ph.D. Whole cell potassium currents were obtained from non-OGD exposed control cortical neurons (n=10), cortical neurons following 105 minutes of OGD (n=22), cortical neurons following 105 minutes of OGD in 25μM TPEN (n=12), and cortical neurons following 105 minutes of OGD in 20μM SB293063 (n=15). Recordings were performed 3 hours after each treatment condition, as at this time point the apoptotic K^+ current enhancement is reliably detected. Potassium currents were evoked by a single voltage step to +10mV from a holding potential of -80mV. Current amplitudes were normalized to cell capacitance. Mean ± SEM; *P<0.001, (ANOVA followed by Tukey-Kramer multiple comparisons test).

A VITAL ROLE FOR Kv CHANNELS IN DOPAMINE TRANSPORTER-MEDIATED 6-HYDROXYDOPAMINE NEUROTOXICITY

Patrick T. Redman,[1] Bahiyyah S. Jefferson,[1] Chandra B. Ziegler,[2] Ole V. Mortensen,[1] Gonzalo E. Torres,[1] Edwin S. Levitan[2] and Elias Aizenman[1*]

[1]Departments of Neurobiology and [2]Pharmacology, University of Pittsburgh School of Medicine, Pittsburgh, PA 15261

ABSTRACT

6-hydroxydopamine (6-OHDA), a neurotoxic substrate of the dopamine transporter (DAT), is widely used in Parkinson's disease models. However, the molecular mechanisms underlying 6-OHDA's selectivity for dopamine neurons and the injurious sequelae that it triggers are not well understood. We tested whether ectopic expression of DAT induces sensitivity to 6-OHDA in non-dopaminergic cortical neurons and evaluated the contribution of Kv channel-dependent apoptosis to the toxicity of this compound in cortical and midbrain dopamine neurons. Cortical neurons expressing DAT accumulated dopamine and were highly vulnerable to 6-OHDA. Pharmacological inhibition of DAT completely blocked this toxicity. We also observed a p38-dependent Kv current surge in DAT-expressing cortical neurons exposed to 6-OHDA, and p38 antagonists and Kv channel blockers were neuroprotective in this model. Thus, DAT-mediated uptake of 6-OHDA recruited the oxidant-induced Kv channel dependent cell death pathway present in cortical neurons. Finally, we report that 6-OHDA also increased Kv currents in cultured midbrain dopamine neurons and this toxicity was blocked with Kv channel

antagonists. We conclude that native DAT expression accounts for the dopamine neuron specific toxicity of 6-OHDA. Following uptake, 6-OHDA triggers the oxidant-associated Kv channel-dependent cell death pathway that is conserved in non-dopaminergic cortical neurons and midbrain dopamine neurons.

INTRODUCTION

Parkinson's disease is characterized by the loss of midbrain dopaminergic neurons. For over 35 years, the catecholamine-derived neurotoxin 6-hydroxydopamine (6-OHDA) has been used to induce dopaminergic cell death in various models of this disorder (Przedborski and Ischiropoulos, 2005). However, at sufficiently high concentrations all catecholamine derivatives, including dopamine and norepinephrine, induce non-selective cell death due to the generation of reactive oxygen species and reactive quinones following auto-oxidation (Heikkila and Cohen, 1972; Rosenberg, 1988). As such, the selectivity of 6-OHDA for dopaminergic neurons, under the right experimental circumstances, may be due to the distinct neurochemical properties of this cell type and/or the fact that the catecholaminergic toxin acts as a substrate for the dopamine transporter (DAT), unique to these cells (Blum et al., 2001). Nonetheless, in spite the widespread use of 6-OHDA, the precise molecular mechanism by which this toxin destroys dopaminergic neurons has not been fully delineated, although many mechanisms have been proposed (Blum et al., 2001). Here, we first examined whether DAT expression in non-dopaminergic neurons would be sufficient to render these cells selectively sensitive to 6-OHDA toxicity. In addition, the molecular mechanism of 6-OHDA-induced cell death in this artificial system was later confirmed to exist in dopaminergic neurons, revealing a potentially new neuroprotective strategy for Parkinson's disease and related disorders.

EXPERIMENTAL PROCEDURES

Green enhanced fluorescent protein, GFP, was from Clontech (Palo Alto, CA). GFP-DAT cDNA was kindly provided by Dr. S. Amara (Pittsburgh, PA, USA). Luciferase, pUHC13-3, was from Dr. H. Bujard (Heidelberg, Germany). Tyrosine hydroxylase antibody was from Chemicon (Temecula, CA, USA). Stromatoxin was purchased from Alomone (Jerusalem, Israel). Freshly prepared 6-OHDA (Sigma Chemical Co., St. Louis, MO, USA) stocks (10 mM) were prepared in 0.15% ascorbate and kept at –80^{o}C until ready to use. Exposure vehicle consisted of minimum essential medium (without phenol red) with 25 mM HEPES and 0.01% bovine serum albumin. Solutions of 100 μM 6-OHDA in the exposure vehicle were prepared immediately (<1 min) prior to use, as they auto-oxidized at neutral pH at a rate of approximately 30% per minute at room temperature, as measured spectrophotometrically (490 nm). No further auto-oxidation products were noted beyond 6-7 minutes. Cortical cultures were prepared from E16 rat embryos as previously described (Hartnett et al., 1997). Cultures were transfected at 18-22 DIV with Lipofectamine 2000 (Invitrogen, Carlsbad, CA, USA; Pal et al., 2003; ~5% transfection efficiency). Cells were maintained for 24 to 48 hours at 37^{o}C, 5% CO_2 prior to recording and toxicity assays. [^{3}H]-Dopamine (DA) uptake assays were performed as described in Prasad and Amara (2001). Uptake was performed for 5 minutes at room temperature in Ringer's solution containing 1 μM catechol-O-methyltransferase inhibitor Ro 41-0960 (Sigma), and 50 nM ^{3}H-dopamine (60 Ci/mmol; PerkinElmer, Wellesley, MA, USA). Ventral mesencephalic cultures were established from postnatal day 1 rat (Cardozo and Bean, 1995). Briefly, dissected tissue was dissociated with 20 U/ml papain (Worthington Biochemicals, Lakewood, NJ, USA) and triturated. The cell suspension was layered onto Basal Medium Eagle solution containing 10 mg/ml trypsin inhibitor 10 mg/ml bovine serum albumin and spun for 8

min at 200 g. The pellet was resuspended and cells plated at a density of 35,000 cells per 31 mm poly-L-lysine-coated glass coverslip. Cultures were fed twice weekly with Basal Medium Eagle with N2 supplement (Gibco, Carlsbad, CA, USA), penicillin/streptomycin, 2% rat serum, 0.6 mM glutamine, 10 mM glucose, and 10 mM HEPES; pH 7.3. Electrophysiological and toxicity experiments were performed at >12 DIV. At this *in vitro* age, functional expression of the DAT is well established (Valchar and Hanbauer, 1995) and, in our hands, the cells become highly vulnerable to 6-OHDA. We compared the sensitivity of dopaminergic neurons to 6-OHDA toxicity (100 μM, 15 min exposure) at two developmental stages, 8 DIV (n=5) and 15 DIV (n=9). We observed that viability of the younger cells was much grater than in the older cells following the toxin exposure (84.7 ± 15.4% at 8 DIV vs. 44.2 ± 5% at 15 DIV; $p<0.01$).

Recordings were conducted using the whole-cell configuration of the patch-clamp technique as described previously (McLaughlin et al., 2001). The extracellular solution contained (in mM): 115 NaCl, 2.5 KCl, 2.0 MgCl2, 10 HEPES, 10 D-glucose, pH 7.2, 0.1 mM tetrodotoxin. The electrode solution contained (in mM): 120 K-gluconate, 11 EGTA, 10 KCl, 1 $MgCl_2$, 1 $CaCl_2$,10 HEPES, 0.22 ATP; pH 7.2 and osmolarity adjusted to 280 mOsm with sucrose. Measurements were obtained under voltage clamp with an Axopatch 200 amplifier (Axon Instruments, Foster City, CA) and pClamp software (Axon Instruments) using 2 MΩ electrodes. Partial compensation (80%) for series resistance was always performed. Currents were filtered at 2 kHz and digitized at 10 kHz (Digidata; Axon Instruments). Potassium currents were evoked with a series of incremental positive voltage steps from a negative holding potential. Steady-state current amplitudes were leak-subtracted (P/N protocol), and normalized to cell capacitance. Capacitive transients were subtracted manually with the amplifier built-in

circuits. Transfected cortical neurons were identified by GFP fluorescence. DA neurons were identified by fluorescence by 5,7-dihydroxytryptamine (Cardozo and Bean, 1995). We found that 5,7-dihydroxytryptamine incubation could diminish the neurotoxic consequences of 6-OHDA exposure. As such, 6-OHDA treatments always preceded labeling.

Toxicity assays in cortical neurons were conducted at 48 hours post-transfection in parallel with electrophysiological recordings, but in luciferase co-transfected cells (Boeckman and Aizenman, 1996; Pal et al., 2003), or, in untransfected cells by a lactate dehydrogenase release assay (Hartnett et al., 1997). Cells were rinsed immediately prior to drug treatment. Cells were exposed to either vehicle or 6-OHDA for 15 min at 37^{o}C, 5% CO_2. Luciferase activity as an index of cell viability (Boeckman and Aizenman, 1996) was measured using the GeneLux Kit (Perkin Elmer, Boston, MA, USA) in a Victor2 Multilabel Counter (Perkin Elmer). Since we found that the potassium channel blocker tetraethylammonium (TEA) interfered with luciferase expression, toxicity assays involving this drug were quantified by cell counting of GFP-positive neurons. Counts were obtained from 30 fields of a 40X objective per condition, in triplicate. Toxicity in mesencephalic cultures (15 DIV) was determined by cell counts of tyrosine hydroxylase positive cells 24 hours after 6-OHDA treatments. Counts were conducted by determining the total number of TH positive cells in the entire culture dish, with at least 2-3 culture dishes per condition, using a 20X objective.

RESULTS

We first provide evidence of a functional separation between dopaminergic neuronal phenotype and DAT function in the toxicity of 6-OHDA. Non-dopaminergic rat cortical neurons

in culture were transfected with a plasmid encoding a GFP-DAT fusion protein (Fig. 1A), and its functional expression confirmed by [^{3}H]-dopamine uptake. We observed a significant increase in [^{3}H]-DA uptake in GFP-DAT expressing cells, when compared to neurons transfected with a GFP-only expression vector (Fig. 1B). We then tested whether the catecholaminergic neurotoxin 6-OHDA would preferentially injure the GFP-DAT-expressing cortical neurons. A 15 min exposure to 100 μM 6-OHDA, which was relatively innocuous to untransfected cortical neurons (Fig. 1C), or cortical neurons expressing GFP-only vector (Fig. 1D), was sufficient to kill approximately 50% of the GFP-DAT expressing cortical neurons (Fig. 1D). In contrast, the glutamatergic toxin N-methyl-D-aspartate (200 μM, 15 min) killed neurons equally well, regardless of the expression of GFP-DAT (Fig. 1D). The toxicity of 6-OHDA in GFP-DAT-expressing cortical neurons was dependent on the activity of the transporter as it was completely blocked by the DAT inhibitor GBR12909 (Fig. 1E). This situation is highly reminiscent of the conditions necessary to induce 50% apoptotic cell death in dopaminergic neurons in vitro (Ding et al., 2004). As such, the expression of DAT is necessary and sufficient to render non-dopaminergic neurons selectively susceptible to 6-OHDA toxicity under conditions where the extracellular auto-oxidation of the toxin induces little or no non-specific injury.

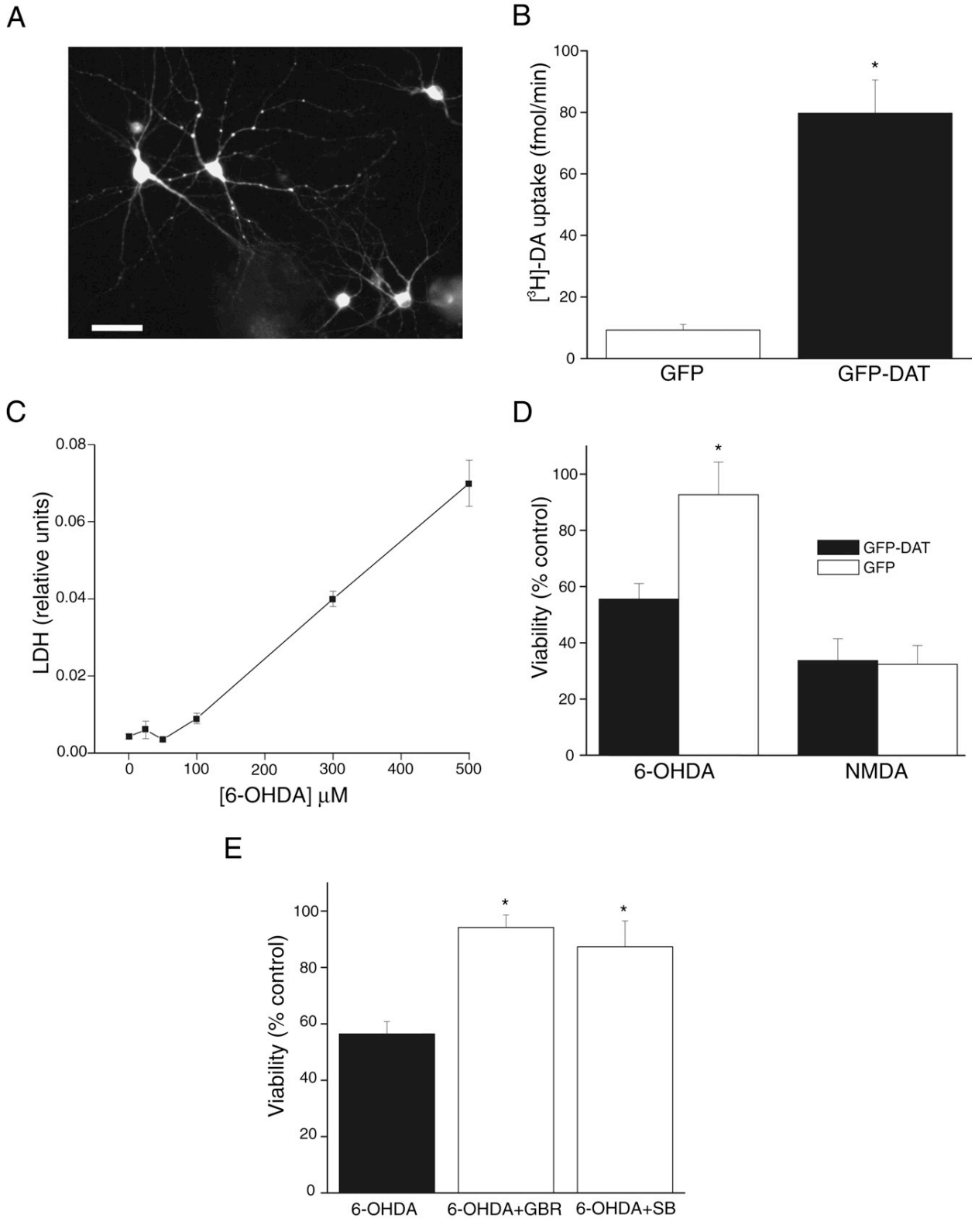
A
B
[3H]-DA uptake (fmol/min)
100
80
60
40
20
0
*
GFP
GFP-DAT
C
LDH (relative units)
0.08
0.06
0.04
0.02
0.00
0
100
200
300
400
500
[6-OHDA] μM
D
Viability (% control)
100
80
60
40
20
0
*
GFP-DAT
GFP
6-OHDA
NMDA
E
Viability (% control)
100
80
60
40
20
0
*
*
6-OHDA
6-OHDA+GBR
6-OHDA+SB

Figure 1. DAT renders non-dopaminergic neurons sensitive to 6-OHDA. ***A,*** Micrograph showing the expression of GFP-DAT in transfected cortical neurons (bar, 80 μm). ***B***, Expression of GFP-DAT in cultured cortical neurons leads to functional expression of the transporter as measured by [^{3}H]dopamine (DA) uptake, which is not observed in GFP vector alone-expressing cultures. Values represent the m ± s.e.m.uptake (fmol/min) in three independent experiments (*p < 0.005; t-test). Inset: GFP-DAT expressing neuron. ***C***, Concentration-toxicity relationship for naïve, untransfected cortical neurons exposed to increasing levels of 6-OHDA for 15 min. Toxicity was measured by a lactate dehydrogenase (LDH) release assay (n=4). ***D***, 6-OHDA is toxic to GFP-DAT expressing cortical neurons. GFP-DAT and GFP expressing cortical neurons were exposed to 6-OHDA (100 μM, 15 min) or to NMDA (200 μM, 15 min). Viability was assayed by a luciferase cell survival assay 24 hr. later and expressed as a percent of vehicle-treated control (n=6-10). Note that 6OHDA induced 50% cell death in GFP-DAT expressing neurons but was not lethal to GFP-expressing cells. In contrast, NMDA was equally toxic to both types of neurons (*p<0.001; t-test). ***E***, 6-OHDA toxicity in GFP-DAT expressing cortical neurons is blocked by a DAT uptake inhibitor and by a p38-MAPK antagonist. GFP-DAT expressing cortical neurons were exposed 100 μM 6OHDA (15 min) in the absence or presence of either 10 μM GBR12909 (a DA uptake inhibitor) or 20 μM SB29063 (a p38 inhibitor). Viability was assayed by a luciferase cell survival assay. Note that both these drugs prevented 6OHDA toxicity (n= 4-13; *p<0.01; ANOVA/Dunnet).

Dopaminergic neurons treated with 6-OHDA undergo caspase-dependent cell death following the phosphorylation of the mitogen-activated protein kinase (MAPK) p38 (Choi et al., 2004). As such, we tested whether the p38 antagonist SB239063 could block 6-OHDA-induced toxicity in GFP-DAT expressing cortical neurons. We observed that SB239063 was indeed very effective in preventing cell death induced by the neurotoxin (Fig. 1E). We have previously reported that oxidative stress in cortical neurons leads to a p38-dependent enhancement of voltage-dependent K^+ currents (McLaughlin et al., 2001). This K^+ current surge, mediated by the membrane insertion of Kv2.1-encoded K^+ channels, is required for apoptosis to occur, and precedes caspase activation (McLaughlin et al., 2001; Pal et al., 2003; Pal et al., 2006). Therefore, we investigated if 6-OHDA activated a similar, p38-dependent pathway in GFP-DAT expressing cortical neurons. A pronounced, toxin-induced K^+ current surge was observed in these cells, which was completely suppressed by SB239063 (Fig. 2A). More critically, the K^+ channel blocker tetraethylammonium (TEA; Fig. 2B) was neuroprotective against 6-OHDA in GFP-DAT expressing cortical neurons, similar to what we have observed for other oxidant stressors (McLaughlin et al., 2001). These data show that DAT-dependent 6-OHDA toxicity can activate a cell death pathway that is very similar to that triggered by other oxidants in cortical neurons.

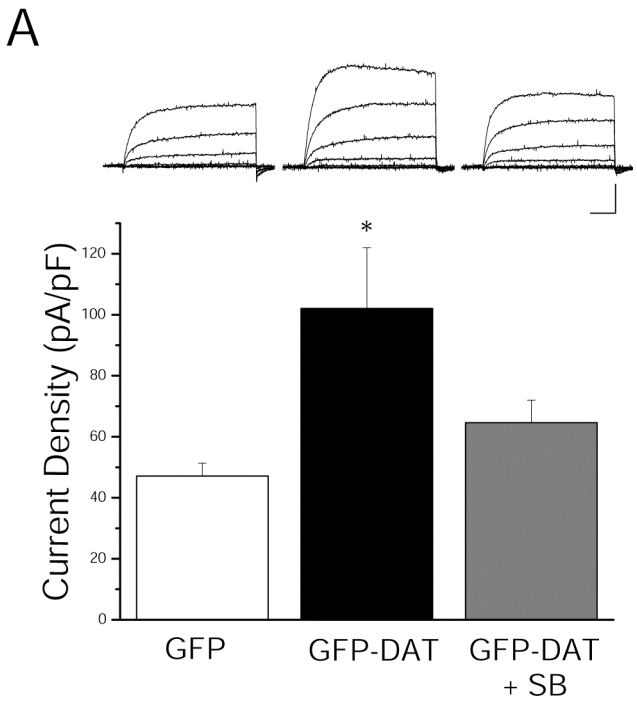
A
Current Density (pA/pF)
0
20
40
60
80
100
120
*
GFP
GFP-DAT
GFP-DAT
+ SB

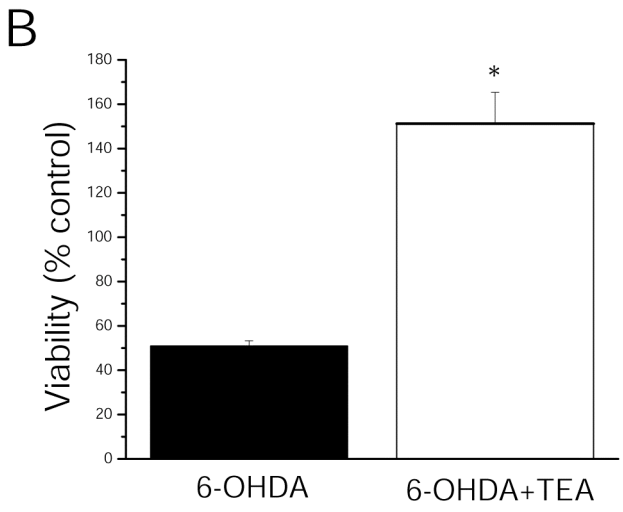
B
Viability (% control)
0
20
40
60
80
100
120
140
160
180
*
6-OHDA
6-OHDA+TEA

Figure 2. Critical role of Kv channels in 6-OHDA toxicity in GFP-DAT expressing cortical neurons. ***A***, 6-OHDA enhances voltage-dependent K^+ currents in GFP-DAT expressing cortical neurons. Bottom, mean current densities in wild type cortical neurons (left; n = 21), GFP-DAT expressing cortical neurons (middle; n = 16) and GFP-DAT expressing cortical neurons pretreated with the p38 inhibitor SB293063 (20 μM, right; n = 10). All cells were treated with 30 μM 6-OHDA for 15 min prior to recording (100 μM of the toxin led to very unstable recordings in GFP-DAT expressing neurons). Currents were evoked by a voltage-step to +5 mV from a holding potential of –70 mV and normalized to cell capacitance (*$p<0.05$; ANOVA/Dunnet). Top, representative whole-cell recordings from all three treatment groups. Currents were evoked by a series of 15 mV voltage steps to +35 mV from –70 mV. Each set of traces is directly above its corresponding treatment group displayed in the bar graph. Calibration: 5nA, 15ms Note that the 6-OHDA-induced current surge could be blocked by the p38 inhibitor. ***B***, 6-OHDA toxicity in GFP-DAT-expressing cortical neurons can be blocked by a K^+ channel inhibitor. GFP-DAT expressing cortical neurons were exposed 100 μM 6OHDA (15 min) in the absence or presence of either 10 mM TEA. TEA treatment continued following toxin exposure. Viability was assayed by cell counting (GFP-positive cells) 24 hr. later as TEA interfered with the luciferase expression assay utilized above. Note TEA protected cells from 6OHDA toxicity (n=3; *$p<0.005$, t-test).

Given these results, we investigated whether 6-OHDA could induce a K^+ current surge in dopaminergic neurons, which express DAT endogenously. In addition we tested whether K^+ channel antagonists could prevent 6-OHDA toxicity in these cells. Similar to what was observed in GFP-DAT expressing cortical neurons, 6-OHDA induced approximately a 2-fold increase in voltage-dependent K^+ currents in dopaminergic neurons obtained from rat mesencephalic cultures (Figs. 3A and B). In addition, this toxin (100 μM, 15 min) produced, approximately, 50% dopaminergic neuronal cell death (Fig. 3C). Importantly, 6-OHDA toxicity to dopaminergic neurons could be completely abrogated by 10 mM TEA (Fig. 3C). We also observed nearly complete neuroprotection by the Kv2.1-selective blocker stromatoxin (ScTX, 100 nM; Shiau et al., 2003; Grishin et al., 2005; Fig. 3C), but not by the K-ATP channel antagonist glibenclamide (1 μM; not shown). These results indicate that 6-OHDA toxicity in dopaminergic cells activates a K^+ current surge, reminiscent to what has been reported many cell types undergoing apoptosis (Yu, 2003; Bortner and Cidlowski, 2004). Additionally, blocking K^+ channels was neuroprotective, suggesting their critical role in the cell death process.

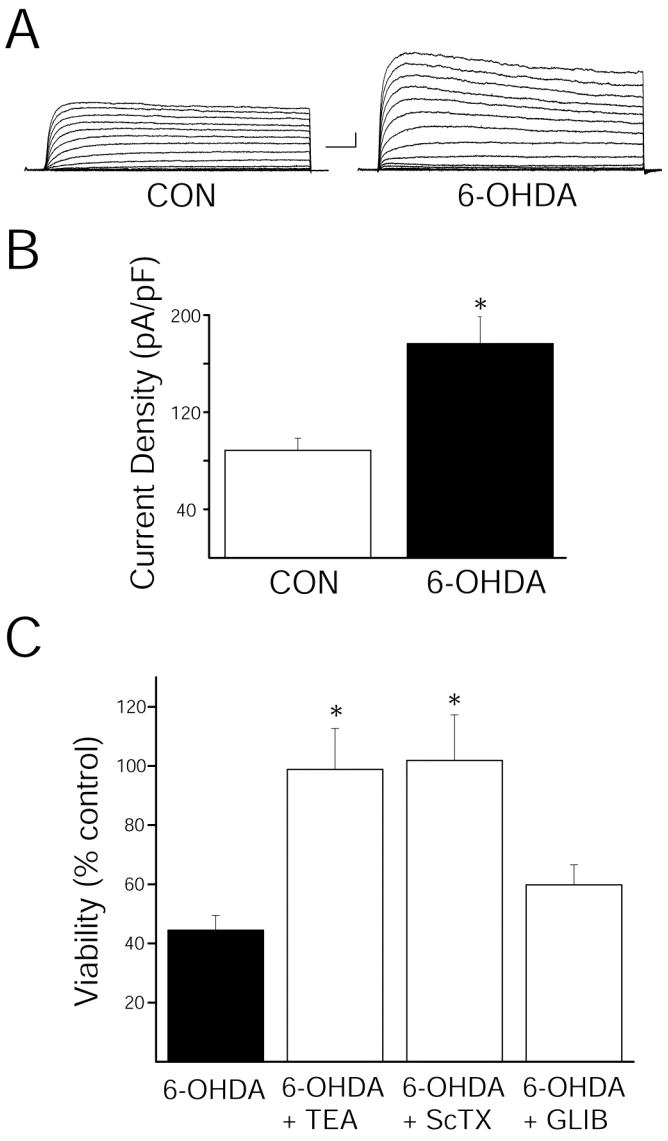
A
CON
6-OHDA
B
Current Density (pA/pF)
200
120
40
*
CON
6-OHDA
C
Viability (% control)
120
100
80
60
40
20
*
*
6-OHDA
6-OHDA + TEA
6-OHDA + ScTX
6-OHDA + GLIB

Figure 3. Kv channels mediate 6-OHDA toxicity in dopaminergic neurons. ***A,*** 6-OHDA enhances voltage-dependent K^+ currents in mesencephalic dopaminergic neurons. Currents were evoked from 13 DIV dopaminergic cells in mesencephalic cultures by a series of 10 mV voltage steps to +80 mV from a holding voltage of –80 mV under control conditions and following a 15 min treatment with 30 μM 6-OHDA. ***B***, Mean ± s.e.m. current densities under control (n =10) and 6-OHDA treatment (n = 6) conditions. Currents were evoked by a voltage step to +10 mV from a holding potential of –80 mV and normalized to cell capacitance (*p<0.001; t-test). (**g**) 6-OHDA toxicity in dopaminergic neurons can be blocked by TEA and stromatoxin, but not glibenclamide. Mesencephalic cultures (15 DIV) were treated with 100 μM 6OHDA (15 min) in the absence or presence of 10 mM TEA, 100 nM stromatoxin (ScTX), or 1 μM glibenclamide (GLIB). TEA, ScTX and GLB treatments continued following toxin exposure. Cultures were fixed and immunostained for the presence of tyrosine hydroxylase (TH) 24 hours later. TH positive cells were then counted to assay DA cell survival. Note TEA and STR, but not GLIB, protected cells from 6-OHDA toxicity (n=3-9; *p<0.01; ANOVA/Dunnet). TEA, STR, and GLIB alone did not affect their viability (not shown).

DISCUSSION

The selectivity of 6-OHDA for catecholaminergic neurons, and, especially, dopaminergic neurons, has been the subject of much debate due to the fact that this substance, and indeed all catecholaminergic-derived compounds, can auto-oxidize in physiological solutions to generate highly reactive quinones, as well as free radicals (Heikkila and Cohen, 1972; Rosenberg, 1988). Nonetheless, as early as 1970, it was suggested that 6-OHDA could selectively damage dopaminergic neurons *in vivo* due to the long-term depletion of central dopamine following intracerebral injections of the toxin (Uretsky and Iversen, 1970). The sparing of 6-OHDA-treated cultured dopaminergic neurons by DAT inhibitors provided unequivocal evidence that, at least under certain conditions, the selectivity of the toxin could be accounted by cellular uptake systems (Cerruti et al., 1993). The results presented in this study corroborate this finding and indicate that under conditions where extracellular auto oxidation of 6-OHDA is not sufficient to induce non-selective injury (Hanrott et al., 2006), the presence of DAT activity can render the catecholaminergic derivative toxic, even in neurons not having an otherwise dopaminergic phenotype. As such, DAT expression is not only sufficient, but a decisive component for the manifestation of selective 6-OHDA toxicity.

Cellular K^+ efflux is a requisite step for apoptosis to proceed in a variety cell death paradigms (Yu, 2003; Bortner and Cidlowski, 2004). The enhancement of potassium currents during the apoptotic process leads to a decrease in the concentration of this cation in the cytoplasm, which acts as a permissive cell death signal (Yu, 2003; Bortner and Cidlowski, 2004).

Our group has demonstrated that the K^+ efflux accompanying oxidant-induced apoptosis is mediated by an enhancement of voltage-gated K^+ currents (McLaughlin et al., 2001). This phenomenon is triggered by the oxidative liberation of intraneuronal Zn^{2+}, which leads to a p38-mediated exocytotic insertion of Kv2.1-encoded channels (Aizenman et al., 2000; McLaughlin et al., 2001; Pal et al., 2003; Pal et al., 2006). Recently, however, it was demonstrated that activation of ATP-sensitive potassium channels (K-ATP) was critical for the selective vulnerability of nigral dopaminergic neurons to the mitochondrial complex I inhibitors rotenone and 1-methyl-4-phenylpyridinium (Liss et al., 2005). However, the molecular link between K-ATP channel activation and cell death pathways was not established, nor was it demonstrated whether these channels were also associated with 6-OHDA-induced toxicity. The lack of neuroprotection by the K-ATP channel blocker glibenclamide observed in our studies indicates that these channels are not directly involved in the neurotoxicity induced by 6-OHDA in mesencephalic cultures. Nonetheless, it is entirely plausible that different K^+ channels are able to provide various exit routes for the cation, even in the same cell type, depending on the injurious stimulus. While metabolically-sensitive K-ATP channels may be ideally suited to detect alterations in mitochondrial function by complex 1 inhibitors (Liss et al., 2005), voltage-gated channels like Kv2.1, which are directly linked to oxidative signaling processes (Pal et al., 2004), mediate 6-OHDA toxicity, and possibly the toxicity of other oxidants. It is noteworthy that the general term "oxidative stress" is commonly and intimately associated with nigral cell death in the Parkinson's disease literature (Abou-Sleiman et al., 2006). The neuroprotective actions of ScTX, a Kv2.1-selective blocker, observed here, suggest that this channel mediates K^+ efflux in dopaminergic neurons undergoing apoptosis, just like it does in cortical cells (Pal et al., 2003). Interestingly, Kv2.1 has recently been shown to be a major binding partner of DAT

(Maiya et al., 2006). Our data strongly indicates that K^+ channels may provide novel therapeutic targets for neuroprotection in Parkinson's disease and related disorders.

References

Abou-Sleiman PM, Muqit MM, Wood NW (2006) Expanding insights of mitochondrial dysfunction in Parkinson's disease. Nat Rev Neurosci 7:207-219.

Adams JP, Anderson AE, Varga AW, Dineley KT, Cook RG, Pfaffinger PJ, Sweatt JD (2000) The A-type potassium channel Kv4.2 is a substrate for the mitogen-activated protein kinase ERK. J Neurochem 75:2277-2287.

Ahn YH, Kim YH, Hong SH, Koh JY (1998) Depletion of intracellular zinc induces protein synthesis-dependent neuronal apoptosis in mouse cortical culture. Exp Neurol 154:47-56.

Aizenman E, Sinor JD, Brimecombe JC, Herin GA (2000a) Alterations of N-methyl-D-aspartate receptor properties after chemical ischemia. J Pharmacol Exp Ther 295:572-577.

Aizenman E, Stout AK, Hartnett KA, Dineley KE, McLaughlin B, Reynolds IJ (2000b) Induction of neuronal apoptosis by thiol oxidation: putative role of intracellular zinc release. J Neurochem 75:1878-1888.

Aras MA, Aizenman E (2005) Obligatory role of ASK1 in the apoptotic surge of K+ currents. Neurosci Lett 387:136-140.

Aras MA, Hartnett KA, Aizenman E (2008) Assessment of cell viability in primary neuronal cultures. Curr Protoc Neurosci Chapter 7:Unit 7 18.

Asanuma M, Miyazaki I, Higashi Y, Tanaka K, Haque ME, Fujita N, Ogawa N (2002) Aggravation of 6-hydroxydopamine-induced dopaminergic lesions in metallothionein-I and -II knock-out mouse brain. Neurosci Lett 327:61-65.

Barone FC, Irving EA, Ray AM, Lee JC, Kassis S, Kumar S, Badger AM, White RF, McVey MJ, Legos JJ, Erhardt JA, Nelson AH, Ohlstein EH, Hunter AJ, Ward K, Smith BR, Adams JL, Parsons AA (2001) SB 239063, a second-generation p38 mitogen-activated protein kinase inhibitor, reduces brain injury and neurological deficits in cerebral focal ischemia. J Pharmacol Exp Ther 296:312-321.

Berman-Golan D, Granot-Attas S, Elson A (2008) Protein tyrosine phosphatase epsilon and Neu-induced mammary tumorigenesis. Cancer Metastasis Rev 27:193-203.

Blum D, Torch S, Lambeng N, Nissou M, Benabid AL, Sadoul R, Verna JM (2001) Molecular pathways involved in the neurotoxicity of 6-OHDA, dopamine and MPTP: contribution to the apoptotic theory in Parkinson's disease. Prog Neurobiol 65:135-172.

Boeckman FA, Aizenman E (1996) Pharmacological properties of acquired excitotoxicity in Chinese hamster ovary cells transfected with N-methyl-D-aspartate receptor subunits. J Pharmacol Exp Ther 279:515-523.

Bonanni L, Chachar M, Jover-Mengual T, Li H, Jones A, Yokota H, Ofengeim D, Flannery RJ, Miyawaki T, Cho CH, Polster BM, Pypaert M, Hardwick JM, Sensi SL, Zukin RS, Jonas EA (2006) Zinc-dependent multi-conductance channel activity in mitochondria isolated from ischemic brain. J Neurosci 26:6851-6862.

Bortner CD, Cidlowski JA (1999) Caspase independent/dependent regulation of K(+), cell shrinkage, and mitochondrial membrane potential during lymphocyte apoptosis. J Biol Chem 274:21953-21962.

Bortner CD, Cidlowski JA (2004) The role of apoptotic volume decrease and ionic homeostasis in the activation and repression of apoptosis. Pflugers Arch 448:313-318.

Bortner CD, Cidlowski JA (2007) Cell shrinkage and monovalent cation fluxes: role in apoptosis. Arch Biochem Biophys 462:176-188.

Bortner CD, Hughes FM, Jr., Cidlowski JA (1997) A primary role for K+ and Na+ efflux in the activation of apoptosis. J Biol Chem 272:32436-32442.
Bortner CD, Sifre MI, Cidlowski JA (2008) Cationic gradient reversal and cytoskeleton-independent volume regulatory pathways define an early stage of apoptosis. J Biol Chem 283:7219-7229.
Bossy-Wetzel E, Talantova MV, Lee WD, Scholzke MN, Harrop A, Mathews E, Gotz T, Han J, Ellisman MH, Perkins GA, Lipton SA (2004) Crosstalk between nitric oxide and zinc pathways to neuronal cell death involving mitochondrial dysfunction and p38-activated K+ channels. Neuron 41:351-365.
Brautigan DL, Bornstein P, Gallis B (1981) Phosphotyrosyl-protein phosphatase. Specific inhibition by Zn. J Biol Chem 256:6519-6522.
Brevnova EE, Platoshyn O, Zhang S, Yuan JX (2004) Overexpression of human KCNA5 increases IK V and enhances apoptosis. Am J Physiol Cell Physiol 287:C715-722.
Buist A, Zhang YL, Keng YF, Wu L, Zhang ZY, den Hertog J (1999) Restoration of potent protein-tyrosine phosphatase activity into the membrane-distal domain of receptor protein-tyrosine phosphatase alpha. Biochemistry 38:914-922.
Burg ED, Remillard CV, Yuan JX (2006) K+ channels in apoptosis. J Membr Biol 209:3-20.
Cain K, Langlais C, Sun XM, Brown DG, Cohen GM (2001) Physiological concentrations of K+ inhibit cytochrome c-dependent formation of the apoptosome. J Biol Chem 276:41985-41990.
Calderone A, Jover T, Mashiko T, Noh KM, Tanaka H, Bennett MV, Zukin RS (2004) Late calcium EDTA rescues hippocampal CA1 neurons from global ischemia-induced death. J Neurosci 24:9903-9913.
Capasso M, Jeng JM, Malavolta M, Mocchegiani E, Sensi SL (2005) Zinc dyshomeostasis: a key modulator of neuronal injury. J Alzheimers Dis 8:93-108; discussion 209-115.
Cardozo DL, Bean BP (1995) Voltage-dependent calcium channels in rat midbrain dopamine neurons: modulation by dopamine and GABAB receptors. J Neurophysiol 74:1137-1148.
Cerruti C, Drian MJ, Kamenka JM, Privat A (1993) Protection by BTCP of cultured dopaminergic neurons exposed to neurotoxins. Brain Res 617:138-142.
Cha A, Snyder GE, Selvin PR, Bezanilla F (1999) Atomic scale movement of the voltage-sensing region in a potassium channel measured via spectroscopy. Nature 402:809-813.
Cherny RA, Legg JT, McLean CA, Fairlie DP, Huang X, Atwood CS, Beyreuther K, Tanzi RE, Masters CL, Bush AI (1999) Aqueous dissolution of Alzheimer's disease Abeta amyloid deposits by biometal depletion. J Biol Chem 274:23223-23228.
Choe S (2002) Potassium channel structures. Nat Rev Neurosci 3:115-121.
Choi DW (1995) Calcium: still center-stage in hypoxic-ischemic neuronal death. Trends Neurosci 18:58-60.
Choi DW, Koh JY (1998) Zinc and brain injury. Annu Rev Neurosci 21:347-375.
Choi DW, Yokoyama M, Koh J (1988) Zinc neurotoxicity in cortical cell culture. Neuroscience 24:67-79.
Choi SM, Choi KO, Lee N, Oh M, Park H (2006) The zinc chelator, N,N,N',N'-tetrakis (2-pyridylmethyl) ethylenediamine, increases the level of nonfunctional HIF-1alpha protein in normoxic cells. Biochem Biophys Res Commun 343:1002-1008.
Choi WS, Eom DS, Han BS, Kim WK, Han BH, Choi EJ, Oh TH, Markelonis GJ, Cho JW, Oh YJ (2004) Phosphorylation of p38 MAPK induced by oxidative stress is linked to

activation of both caspase-8- and -9-mediated apoptotic pathways in dopaminergic neurons. J Biol Chem 279:20451-20460.
Chung JJ, Li M (2005) Biochemical characterization of the native Kv2.1 potassium channel. FEBS J 272:3743-3755.
Cockerill SL, Tobin AB, Torrecilla I, Willars GB, Standen NB, Mitcheson JS (2007) Modulation of hERG potassium currents in HEK-293 cells by protein kinase C. Evidence for direct phosphorylation of pore forming subunits. J Physiol 581:479-493.
Colvin RA, Fontaine CP, Laskowski M, Thomas D (2003) Zn2+ transporters and Zn2+ homeostasis in neurons. Eur J Pharmacol 479:171-185.
Coma M, Vicente R, Tsevi I, Grande M, Tamkun MM, Felipe A (2002) Different Kv2.1/Kv9.3 heteromer expression during brain and lung post-natal development in the rat. J Physiol Biochem 58:195-203.
Cornell NW, Crivaro KE (1972) Stability constant for the zinc-dithiothreitol complex. Anal Biochem 47:203-208.
Creagh EM, Conroy H, Martin SJ (2003) Caspase-activation pathways in apoptosis and immunity. Immunol Rev 193:10-21.
Cuadrado A, Garcia-Fernandez LF, Gonzalez L, Suarez Y, Losada A, Alcaide V, Martinez T, Fernandez-Sousa JM, Sanchez-Puelles JM, Munoz A (2003) Aplidin induces apoptosis in human cancer cells via glutathione depletion and sustained activation of the epidermal growth factor receptor, Src, JNK, and p38 MAPK. J Biol Chem 278:241-250.
Cuajungco MP, Faget KY (2003) Zinc takes the center stage: its paradoxical role in Alzheimer's disease. Brain Res Brain Res Rev 41:44-56.
Cuajungco MP, Faget KY, Huang X, Tanzi RE, Bush AI (2000) Metal chelation as a potential therapy for Alzheimer's disease. Ann N Y Acad Sci 920:292-304.
Cuenda A, Rousseau S (2007) p38 MAP-kinases pathway regulation, function and role in human diseases. Biochim Biophys Acta 1773:1358-1375.
Danscher G, Jensen KB, Frederickson CJ, Kemp K, Andreasen A, Juhl S, Stoltenberg M, Ravid R (1997) Increased amount of zinc in the hippocampus and amygdala of Alzheimer's diseased brains: a proton-induced X-ray emission spectroscopic analysis of cryostat sections from autopsy material. J Neurosci Methods 76:53-59.
Daum G, Solca F, Diltz CD, Zhao Z, Cool DE, Fischer EH (1993) A general peptide substrate for protein tyrosine phosphatases. Anal Biochem 211:50-54.
Dhanasekaran M, Albano CB, Pellet L, Karuppagounder SS, Uthayathas S, Suppiramaniam V, Brown-Borg H, Ebadi M (2007) Role of Lipoamide Dehydrogenase and Metallothionein on 1-Methyl-4-phenyl-1,2,3,6- tetrahydropyridine-induced Neurotoxicity. Neurochem Res.
Di Matteo V, Esposito E (2003) Biochemical and therapeutic effects of antioxidants in the treatment of Alzheimer's disease, Parkinson's disease, and amyotrophic lateral sclerosis. Curr Drug Targets CNS Neurol Disord 2:95-107.
Dikalov SI, Mason RP (2001) Spin trapping of polyunsaturated fatty acid-derived peroxyl radicals: reassignment to alkoxyl radical adducts. Free Radic Biol Med 30:187-197.
Du J, Tao-Cheng JH, Zerfas P, McBain CJ (1998) The K+ channel, Kv2.1, is apposed to astrocytic processes and is associated with inhibitory postsynaptic membranes in hippocampal and cortical principal neurons and inhibitory interneurons. Neuroscience 84:37-48.

Du J, Haak LL, Phillips-Tansey E, Russell JT, McBain CJ (2000) Frequency-dependent regulation of rat hippocampal somato-dendritic excitability by the K+ channel subunit Kv2.1. J Physiol 522 Pt 1:19-31.
Du S, McLaughlin B, Pal S, Aizenman E (2002) In vitro neurotoxicity of methylisothiazolinone, a commonly used industrial and household biocide, proceeds via a zinc and extracellular signal-regulated kinase mitogen-activated protein kinase-dependent pathway. J Neurosci 22:7408-7416.
Elson A, Leder P (1995) Protein-tyrosine phosphatase epsilon. An isoform specifically expressed in mouse mammary tumors initiated by v-Ha-ras OR neu. J Biol Chem 270:26116-26122.
Flint AJ, Tiganis T, Barford D, Tonks NK (1997) Development of "substrate-trapping" mutants to identify physiological substrates of protein tyrosine phosphatases. Proc Natl Acad Sci U S A 94:1680-1685.
Forloni G, Chiesa R, Smiroldo S, Verga L, Salmona M, Tagliavini F, Angeretti N (1993) Apoptosis mediated neurotoxicity induced by chronic application of beta amyloid fragment 25-35. Neuroreport 4:523-526.
Fraker PJ, Telford WG (1997) A reappraisal of the role of zinc in life and death decisions of cells. Proc Soc Exp Biol Med 215:229-236.
Frederickson CJ, Bush AI (2001) Synaptically released zinc: physiological functions and pathological effects. Biometals 14:353-366.
Frederickson CJ, Hernandez MD, McGinty JF (1989) Translocation of zinc may contribute to seizure-induced death of neurons. Brain Res 480:317-321.
Frederickson CJ, Maret W, Cuajungco MP (2004) Zinc and excitotoxic brain injury: a new model. Neuroscientist 10:18-25.
Frederickson CJ, Koh JY, Bush AI (2005) The neurobiology of zinc in health and disease. Nat Rev Neurosci 6:449-462.
Frederickson CJ, Rampy BA, Reamy-Rampy S, Howell GA (1992) Distribution of histochemically reactive zinc in the forebrain of the rat. J Chem Neuroanat 5:521-530.
Frederickson CJ, Cuajungco MP, LaBuda CJ, Suh SW (2002) Nitric oxide causes apparent release of zinc from presynaptic boutons. Neuroscience 115:471-474.
Friedlich AL, Lee JY, van Groen T, Cherny RA, Volitakis I, Cole TB, Palmiter RD, Koh JY, Bush AI (2004) Neuronal zinc exchange with the blood vessel wall promotes cerebral amyloid angiopathy in an animal model of Alzheimer's disease. J Neurosci 24:3453-3459.
Gil-Henn H, Volohonsky G, Elson A (2001) Regulation of protein-tyrosine phosphatases alpha and epsilon by calpain-mediated proteolytic cleavage. J Biol Chem 276:31772-31779.
Gil-Henn H, Volohonsky G, Toledano-Katchalski H, Gandre S, Elson A (2000) Generation of novel cytoplasmic forms of protein tyrosine phosphatase epsilon by proteolytic processing and translational control. Oncogene 19:4375-4384.
Giovannini MG, Scali C, Prosperi C, Bellucci A, Vannucchi MG, Rosi S, Pepeu G, Casamenti F (2002) Beta-amyloid-induced inflammation and cholinergic hypofunction in the rat brain in vivo: involvement of the p38MAPK pathway. Neurobiol Dis 11:257-274.
Gomes P, Saito T, Del Corsso C, Alioua A, Eghbali M, Toro L, Stefani E (2008) Identification of a functional interaction between Kv4.3 channels and c-Src tyrosine kinase. Biochim Biophys Acta.

Grishin A, Ford H, Wang J, Li H, Salvador-Recatala V, Levitan ES, Zaks-Makhina E (2005) Attenuation of apoptosis in enterocytes by blockade of potassium channels. Am J Physiol Gastrointest Liver Physiol 289:G815-821.
Gutman GA, Chandy KG, Grissmer S, Lazdunski M, McKinnon D, Pardo LA, Robertson GA, Rudy B, Sanguinetti MC, Stuhmer W, Wang X (2005) International Union of Pharmacology. LIII. Nomenclature and molecular relationships of voltage-gated potassium channels. Pharmacol Rev 57:473-508.
Haase H, Maret W (2003) Intracellular zinc fluctuations modulate protein tyrosine phosphatase activity in insulin/insulin-like growth factor-1 signaling. Exp Cell Res 291:289-298.
Haase H, Maret W (2005) Protein tyrosine phosphatases as targets of the combined insulinomimetic effects of zinc and oxidants. Biometals 18:333-338.
Han J, Lee JD, Bibbs L, Ulevitch RJ (1994) A MAP kinase targeted by endotoxin and hyperosmolarity in mammalian cells. Science 265:808-811.
Han J, Lee JD, Jiang Y, Li Z, Feng L, Ulevitch RJ (1996) Characterization of the structure and function of a novel MAP kinase kinase (MKK6). J Biol Chem 271:2886-2891.
Hanrott K, Gudmunsen L, O'Neill MJ, Wonnacott S (2006) 6-hydroxydopamine-induced apoptosis is mediated via extracellular auto-oxidation and caspase 3-dependent activation of protein kinase Cdelta. J Biol Chem 281:5373-5382.
Hao Q, Maret W (2006) Aldehydes release zinc from proteins. A pathway from oxidative stress/lipid peroxidation to cellular functions of zinc. FEBS J 273:4300-4310.
Hartnett KA, Stout AK, Rajdev S, Rosenberg PA, Reynolds IJ, Aizenman E (1997) NMDA receptor-mediated neurotoxicity: a paradoxical requirement for extracellular Mg2+ in Na+/Ca2+-free solutions in rat cortical neurons in vitro. J Neurochem 68:1836-1845.
Hegle AP, Marble DD, Wilson GF (2006) A voltage-driven switch for ion-independent signaling by ether-a-go-go K+ channels. Proc Natl Acad Sci U S A 103:2886-2891.
Heikkila R, Cohen G (1972) Further studies on the generation of hydrogen peroxide by 6-hydroxydopamine. Potentiation by ascorbic acid. Mol Pharmacol 8:241-248.
Hensley K, Hall N, Subramaniam R, Cole P, Harris M, Aksenov M, Aksenova M, Gabbita SP, Wu JF, Carney JM, et al. (1995) Brain regional correspondence between Alzheimer's disease histopathology and biomarkers of protein oxidation. J Neurochem 65:2146-2156.
Hensley K, Floyd RA, Zheng NY, Nael R, Robinson KA, Nguyen X, Pye QN, Stewart CA, Geddes J, Markesbery WR, Patel E, Johnson GV, Bing G (1999) p38 kinase is activated in the Alzheimer's disease brain. J Neurochem 72:2053-2058.
Hershfinkel M, Silverman WF, Sekler I (2007) The zinc sensing receptor, a link between zinc and cell signaling. Mol Med 13:331-336.
Hershfinkel M, Moran A, Grossman N, Sekler I (2001) A zinc-sensing receptor triggers the release of intracellular Ca2+ and regulates ion transport. Proc Natl Acad Sci U S A 98:11749-11754.
Ho Y, Samarasinghe R, Knoch ME, Lewis M, Aizenman E, Defranco DB (2008) Selective Inhibition of MAPK Phosphatases by Zinc Accounts for ERK1/2-dependent Oxidative Neuronal Cell Death. Mol Pharmacol.
Hribar M, Bloc A, Medilanski J, Nusch L, Eder-Colli L (2004) Voltage-gated K+ current: a marker for apoptosis in differentiating neuronal progenitor cells? Eur J Neurosci 20:635-648.
Huang X, Atwood CS, Hartshorn MA, Multhaup G, Goldstein LE, Scarpa RC, Cuajungco MP, Gray DN, Lim J, Moir RD, Tanzi RE, Bush AI (1999) The A beta peptide of Alzheimer's

disease directly produces hydrogen peroxide through metal ion reduction. Biochemistry 38:7609-7616.
Huang XY, Morielli AD, Peralta EG (1994) Molecular basis of cardiac potassium channel stimulation by protein kinase A. Proc Natl Acad Sci U S A 91:624-628.
Huang YZ, Pan E, Xiong ZQ, McNamara JO (2008) Zinc-mediated transactivation of TrkB potentiates the hippocampal mossy fiber-CA3 pyramid synapse. Neuron 57:546-558.
Hughes FM, Jr., Cidlowski JA (1999) Potassium is a critical regulator of apoptotic enzymes in vitro and in vivo. Adv Enzyme Regul 39:157-171.
Hughes FM, Jr., Bortner CD, Purdy GD, Cidlowski JA (1997) Intracellular K+ suppresses the activation of apoptosis in lymphocytes. J Biol Chem 272:30567-30576.
Ichijo H, Nishida E, Irie K, ten Dijke P, Saitoh M, Moriguchi T, Takagi M, Matsumoto K, Miyazono K, Gotoh Y (1997) Induction of apoptosis by ASK1, a mammalian MAPKKK that activates SAPK/JNK and p38 signaling pathways. Science 275:90-94.
Ingley E (2008) Src family kinases: regulation of their activities, levels and identification of new pathways. Biochim Biophys Acta 1784:56-65.
Ingraham CA, Cox ME, Ward DC, Fults DW, Maness PF (1989) c-src and other proto-oncogenes implicated in neuronal differentiation. Mol Chem Neuropathol 10:1-14.
Ishizawar R, Parsons SJ (2004) c-Src and cooperating partners in human cancer. Cancer Cell 6:209-214.
Jiang D, Sullivan PG, Sensi SL, Steward O, Weiss JH (2001) Zn(2+) induces permeability transition pore opening and release of pro-apoptotic peptides from neuronal mitochondria. J Biol Chem 276:47524-47529.
Jin X, Gereau RWt (2006) Acute p38-mediated modulation of tetrodotoxin-resistant sodium channels in mouse sensory neurons by tumor necrosis factor-alpha. J Neurosci 26:246-255.
Kay AR (2003) Evidence for chelatable zinc in the extracellular space of the hippocampus, but little evidence for synaptic release of Zn. J Neurosci 23:6847-6855.
Kerr JF, Wyllie AH, Currie AR (1972) Apoptosis: a basic biological phenomenon with wide-ranging implications in tissue kinetics. Br J Cancer 26:239-257.
Khanna S, Venojarvi M, Roy S, Sen CK (2002) Glutamate-induced c-Src activation in neuronal cells. Methods Enzymol 352:191-198.
Kim YH, Kim EY, Gwag BJ, Sohn S, Koh JY (1999) Zinc-induced cortical neuronal death with features of apoptosis and necrosis: mediation by free radicals. Neuroscience 89:175-182.
Kim YM, Reed W, Wu W, Bromberg PA, Graves LM, Samet JM (2006) Zn2+-induced IL-8 expression involves AP-1, JNK, and ERK activities in human airway epithelial cells. Am J Physiol Lung Cell Mol Physiol 290:L1028-1035.
Kleiner D (1974) The effect of Zn2+ ions on mitochondrial electron transport. Arch Biochem Biophys 165:121-125.
Knoch ME, Hartnett KA, Hara H, Kandler K, Aizenman E (2008) Microglia induce neurotoxicity via intraneuronal Zn(2+) release and a K(+) current surge. Glia 56:89-96.
Kobrinsky E, Stevens L, Kazmi Y, Wray D, Soldatov NM (2006) Molecular rearrangements of the Kv2.1 potassium channel termini associated with voltage gating. J Biol Chem 281:19233-19240.
Korichneva I (2006) Zinc dynamics in the myocardial redox signaling network. Antioxid Redox Signal 8:1707-1721.

Kudo I, Murakami M (2002) Phospholipase A2 enzymes. Prostaglandins Other Lipid Mediat 68-69:3-58.
Kurz LL, Zuhlke RD, Zhang HJ, Joho RH (1995) Side-chain accessibilities in the pore of a K+ channel probed by sulfhydryl-specific reagents after cysteine-scanning mutagenesis. Biophys J 68:900-905.
Lambert MP, Barlow AK, Chromy BA, Edwards C, Freed R, Liosatos M, Morgan TE, Rozovsky I, Trommer B, Viola KL, Wals P, Zhang C, Finch CE, Krafft GA, Klein WL (1998) Diffusible, nonfibrillar ligands derived from Abeta1-42 are potent central nervous system neurotoxins. Proc Natl Acad Sci U S A 95:6448-6453.
Lau AF (2005) c-Src: bridging the gap between phosphorylation- and acidification-induced gap junction channel closure. Sci STKE 2005:pe33.
Lauritzen I, De Weille JR, Lazdunski M (1997) The potassium channel opener (-)-cromakalim prevents glutamate-induced cell death in hippocampal neurons. J Neurochem 69:1570-1579.
Lavoie N, Peralta MR, 3rd, Chiasson M, Lafortune K, Pellegrini L, Seress L, Toth K (2007) Extracellular chelation of zinc does not affect hippocampal excitability and seizure-induced cell death in rats. J Physiol 578:275-289.
Lee JC, Laydon JT, McDonnell PC, Gallagher TF, Kumar S, Green D, McNulty D, Blumenthal MJ, Heys JR, Landvatter SW, et al. (1994) A protein kinase involved in the regulation of inflammatory cytokine biosynthesis. Nature 372:739-746.
Lee JY, Mook-Jung I, Koh JY (1999) Histochemically reactive zinc in plaques of the Swedish mutant beta-amyloid precursor protein transgenic mice. J Neurosci 19:RC10.
Lee JY, Cole TB, Palmiter RD, Koh JY (2000) Accumulation of zinc in degenerating hippocampal neurons of ZnT3-null mice after seizures: evidence against synaptic vesicle origin. J Neurosci 20:RC79.
Lee JY, Kim JH, Palmiter RD, Koh JY (2003) Zinc released from metallothionein-iii may contribute to hippocampal CA1 and thalamic neuronal death following acute brain injury. Exp Neurol 184:337-347.
Lee JY, Hwang JJ, Park MH, Koh JY (2006) Cytosolic labile zinc: a marker for apoptosis in the developing rat brain. Eur J Neurosci 23:435-442.
Lee JY, Cole TB, Palmiter RD, Suh SW, Koh JY (2002) Contribution by synaptic zinc to the gender-disparate plaque formation in human Swedish mutant APP transgenic mice. Proc Natl Acad Sci U S A 99:7705-7710.
Lennmyr F, Ericsson A, Gerwins P, Akterin S, Ahlstrom H, Terent A (2004) Src family kinase-inhibitor PP2 reduces focal ischemic brain injury. Acta Neurol Scand 110:175-179.
Leung YM, Kang Y, Gao X, Xia F, Xie H, Sheu L, Tsuk S, Lotan I, Tsushima RG, Gaisano HY (2003) Syntaxin 1A binds to the cytoplasmic C terminus of Kv2.1 to regulate channel gating and trafficking. J Biol Chem 278:17532-17538.
Levinson AD, Oppermann H, Levintow L, Varmus HE, Bishop JM (1978) Evidence that the transforming gene of avian sarcoma virus encodes a protein kinase associated with a phosphoprotein. Cell 15:561-572.
Li Y, Um SY, McDonald TV (2006) Voltage-gated potassium channels: regulation by accessory subunits. Neuroscientist 12:199-210.
Liss B, Haeckel O, Wildmann J, Miki T, Seino S, Roeper J (2005) K-ATP channels promote the differential degeneration of dopaminergic midbrain neurons. Nat Neurosci 8:1742-1751.

Liu Y, Min W (2002) Thioredoxin promotes ASK1 ubiquitination and degradation to inhibit ASK1-mediated apoptosis in a redox activity-independent manner. Circ Res 90:1259-1266.
Long SB, Campbell EB, Mackinnon R (2005) Crystal structure of a mammalian voltage-dependent Shaker family K+ channel. Science 309:897-903.
Lvov A, Chikvashvili D, Michaelevski I, Lotan I (2008) VAMP2 interacts directly with the N terminus of Kv2.1 to enhance channel inactivation. Pflugers Arch.
MacDonald PE, Wang G, Tsuk S, Dodo C, Kang Y, Tang L, Wheeler MB, Cattral MS, Lakey JR, Salapatek AM, Lotan I, Gaisano HY (2002) Synaptosome-associated protein of 25 kilodaltons modulates Kv2.1 voltage-dependent K(+) channels in neuroendocrine islet beta-cells through an interaction with the channel N terminus. Mol Endocrinol 16:2452-2461.
Malaiyandi LM, Honick AS, Rintoul GL, Wang QJ, Reynolds IJ (2005) Zn2+ inhibits mitochondrial movement in neurons by phosphatidylinositol 3-kinase activation. J Neurosci 25:9507-9514.
Malin SA, Nerbonne JM (2002) Delayed rectifier K+ currents, IK, are encoded by Kv2 alpha-subunits and regulate tonic firing in mammalian sympathetic neurons. J Neurosci 22:10094-10105.
Maness PF, Aubry M, Shores CG, Frame L, Pfenninger KH (1988) c-src gene product in developing rat brain is enriched in nerve growth cone membranes. Proc Natl Acad Sci U S A 85:5001-5005.
Manev H, Kharlamov E, Uz T, Mason RP, Cagnoli CM (1997) Characterization of zinc-induced neuronal death in primary cultures of rat cerebellar granule cells. Exp Neurol 146:171-178.
Maret W (1994) Oxidative metal release from metallothionein via zinc-thiol/disulfide interchange. Proc Natl Acad Sci U S A 91:237-241.
Maret W (2006) Zinc coordination environments in proteins as redox sensors and signal transducers. Antioxid Redox Signal 8:1419-1441.
Maret W, Vallee BL (1998) Thiolate ligands in metallothionein confer redox activity on zinc clusters. Proc Natl Acad Sci U S A 95:3478-3482.
Maret W, Krezel A (2007) Cellular zinc and redox buffering capacity of metallothionein/thionein in health and disease. Mol Med 13:371-375.
Martin GS (2001) The hunting of the Src. Nat Rev Mol Cell Biol 2:467-475.
Martin SJ, Reutelingsperger CP, McGahon AJ, Rader JA, van Schie RC, LaFace DM, Green DR (1995) Early redistribution of plasma membrane phosphatidylserine is a general feature of apoptosis regardless of the initiating stimulus: inhibition by overexpression of Bcl-2 and Abl. J Exp Med 182:1545-1556.
Matsukawa J, Matsuzawa A, Takeda K, Ichijo H (2004) The ASK1-MAP kinase cascades in mammalian stress response. J Biochem 136:261-265.
McLaughlin B, Pal S, Tran MP, Parsons AA, Barone FC, Erhardt JA, Aizenman E (2001) p38 activation is required upstream of potassium current enhancement and caspase cleavage in thiol oxidant-induced neuronal apoptosis. J Neurosci 21:3303-3311.
Michaelevski I, Chikvashvili D, Tsuk S, Singer-Lahat D, Kang Y, Linial M, Gaisano HY, Fili O, Lotan I (2003) Direct interaction of target SNAREs with the Kv2.1 channel. Modal regulation of channel activation and inactivation gating. J Biol Chem 278:34320-34330.

Misonou H, Mohapatra DP, Trimmer JS (2005a) Kv2.1: a voltage-gated k+ channel critical to dynamic control of neuronal excitability. Neurotoxicology 26:743-752.
Misonou H, Mohapatra DP, Menegola M, Trimmer JS (2005b) Calcium- and metabolic state-dependent modulation of the voltage-dependent Kv2.1 channel regulates neuronal excitability in response to ischemia. J Neurosci 25:11184-11193.
Misonou H, Mohapatra DP, Park EW, Leung V, Zhen D, Misonou K, Anderson AE, Trimmer JS (2004) Regulation of ion channel localization and phosphorylation by neuronal activity. Nat Neurosci 7:711-718.
Mohapatra DP, Park KS, Trimmer JS (2007) Dynamic regulation of the voltage-gated Kv2.1 potassium channel by multisite phosphorylation. Biochem Soc Trans 35:1064-1068.
Mohapatra DP, Siino DF, Trimmer JS (2008) Interdomain cytoplasmic interactions govern the intracellular trafficking, gating, and modulation of the Kv2.1 channel. J Neurosci 28:4982-4994.
Moult PR, Correa SA, Collingridge GL, Fitzjohn SM, Bashir ZI (2008) Co-activation of p38 mitogen-activated protein kinase and protein tyrosine phosphatase underlies metabotropic glutamate receptor-dependent long-term depression. J Physiol 586:2499-2510.
Murakoshi H, Trimmer JS (1999) Identification of the Kv2.1 K+ channel as a major component of the delayed rectifier K+ current in rat hippocampal neurons. J Neurosci 19:1728-1735.
Murphy TH, Miyamoto M, Sastre A, Schnaar RL, Coyle JT (1989) Glutamate toxicity in a neuronal cell line involves inhibition of cystine transport leading to oxidative stress. Neuron 2:1547-1558.
Noh KM, Koh JY (2000) Induction and activation by zinc of NADPH oxidase in cultured cortical neurons and astrocytes. J Neurosci 20:RC111.
Noh KM, Kim YH, Koh JY (1999) Mediation by membrane protein kinase C of zinc-induced oxidative neuronal injury in mouse cortical cultures. J Neurochem 72:1609-1616.
O'Connell KM, Tamkun MM (2005) Targeting of voltage-gated potassium channel isoforms to distinct cell surface microdomains. J Cell Sci 118:2155-2166.
O'Connell KM, Rolig AS, Whitesell JD, Tamkun MM (2006) Kv2.1 potassium channels are retained within dynamic cell surface microdomains that are defined by a perimeter fence. J Neurosci 26:9609-9618.
Obenauer JC, Cantley LC, Yaffe MB (2003) Scansite 2.0: Proteome-wide prediction of cell signaling interactions using short sequence motifs. Nucleic Acids Res 31:3635-3641.
Pal S, He K, Aizenman E (2004) Nitrosative stress and potassium channel-mediated neuronal apoptosis: is zinc the link? Pflugers Arch 448:296-303.
Pal S, Hartnett KA, Nerbonne JM, Levitan ES, Aizenman E (2003) Mediation of neuronal apoptosis by Kv2.1-encoded potassium channels. J Neurosci 23:4798-4802.
Pal SK, Takimoto K, Aizenman E, Levitan ES (2006) Apoptotic surface delivery of K+ channels. Cell Death Differ 13:661-667.
Panayiotidis MI, Bortner CD, Cidlowski JA (2006) On the mechanism of ionic regulation of apoptosis: would the Na+/K+-ATPase please stand up? Acta Physiol (Oxf) 187:205-215.
Pannaccione A, Boscia F, Scorziello A, Adornetto A, Castaldo P, Sirabella R, Taglialatela M, Di Renzo GF, Annunziato L (2007) Up-regulation and increased activity of KV3.4 channels and their accessory subunit MinK-related peptide 2 induced by amyloid peptide are involved in apoptotic neuronal death. Mol Pharmacol 72:665-673.
Papazian DM (1999) Potassium channels: some assembly required. Neuron 23:7-10.

Pardo LA, Contreras-Jurado C, Zientkowska M, Alves F, Stuhmer W (2005) Role of voltage-gated potassium channels in cancer. J Membr Biol 205:115-124.
Park JA, Koh JY (1999) Induction of an immediate early gene egr-1 by zinc through extracellular signal-regulated kinase activation in cortical culture: its role in zinc-induced neuronal death. J Neurochem 73:450-456.
Park KS, Mohapatra DP, Misonou H, Trimmer JS (2006) Graded regulation of the Kv2.1 potassium channel by variable phosphorylation. Science 313:976-979.
Paul R, Zhang ZG, Eliceiri BP, Jiang Q, Boccia AD, Zhang RL, Chopp M, Cheresh DA (2001) Src deficiency or blockade of Src activity in mice provides cerebral protection following stroke. Nat Med 7:222-227.
Pearce LL, Wasserloos K, St Croix CM, Gandley R, Levitan ES, Pitt BR (2000) Metallothionein, nitric oxide and zinc homeostasis in vascular endothelial cells. J Nutr 130:1467S-1470S.
Peretz A, Gil-Henn H, Sobko A, Shinder V, Attali B, Elson A (2000) Hypomyelination and increased activity of voltage-gated K(+) channels in mice lacking protein tyrosine phosphatase epsilon. EMBO J 19:4036-4045.
Pongs O, Leicher T, Berger M, Roeper J, Bahring R, Wray D, Giese KP, Silva AJ, Storm JF (1999) Functional and molecular aspects of voltage-gated K+ channel beta subunits. Ann N Y Acad Sci 868:344-355.
Przedborski S, Ischiropoulos H (2005) Reactive oxygen and nitrogen species: weapons of neuronal destruction in models of Parkinson's disease. Antioxid Redox Signal 7:685-693.
Redman PT, Jefferson BS, Ziegler CB, Mortensen OV, Torres GE, Levitan ES, Aizenman E (2006) A vital role for voltage-dependent potassium channels in dopamine transporter-mediated 6-hydroxydopamine neurotoxicity. Neuroscience 143:1-6.
Redman PT, He K, Hartnett KA, Jefferson BS, Hu L, Rosenberg PA, Levitan ES, Aizenman E (2007) Apoptotic surge of potassium currents is mediated by p38 phosphorylation of Kv2.1. Proc Natl Acad Sci U S A 104:3568-3573.
Regland B, Lehmann W, Abedini I, Blennow K, Jonsson M, Karlsson I, Sjogren M, Wallin A, Xilinas M, Gottfries CG (2001) Treatment of Alzheimer's disease with clioquinol. Dement Geriatr Cogn Disord 12:408-414.
Riedl SJ, Salvesen GS (2007) The apoptosome: signalling platform of cell death. Nat Rev Mol Cell Biol 8:405-413.
Ritchie CW, Bush AI, Mackinnon A, Macfarlane S, Mastwyk M, MacGregor L, Kiers L, Cherny R, Li QX, Tammer A, Carrington D, Mavros C, Volitakis I, Xilinas M, Ames D, Davis S, Beyreuther K, Tanzi RE, Masters CL (2003) Metal-protein attenuation with iodochlorhydroxyquin (clioquinol) targeting Abeta amyloid deposition and toxicity in Alzheimer disease: a pilot phase 2 clinical trial. Arch Neurol 60:1685-1691.
Roder K, Koren G (2006) The K+ channel gene, Kcnb1: genomic structure and characterization of its 5'-regulatory region as part of an overlapping gene group. Biol Chem 387:1237-1246.
Rosenberg PA (1988) Catecholamine toxicity in cerebral cortex in dissociated cell culture. J Neurosci 8:2887-2894.
Santos S, Aizenman E (2002) Functional expression of muscle-type nicotinic acetylcholine receptors in rat forebrain neurons in vitro. Methods Find Exp Clin Pharmacol 24:63-66.
Scannevin RH, Murakoshi H, Rhodes KJ, Trimmer JS (1996) Identification of a cytoplasmic domain important in the polarized expression and clustering of the Kv2.1 K+ channel. J Cell Biol 135:1619-1632.

Schrader LA, Birnbaum SG, Nadin BM, Ren Y, Bui D, Anderson AE, Sweatt JD (2006) ERK/MAPK regulates the Kv4.2 potassium channel by direct phosphorylation of the pore-forming subunit. Am J Physiol Cell Physiol 290:C852-861.
Sekler I, Sensi SL, Hershfinkel M, Silverman WF (2007) Mechanism and regulation of cellular zinc transport. Mol Med 13:337-343.
Sensi SL, Jeng JM (2004) Rethinking the excitotoxic ionic milieu: the emerging role of Zn(2+) in ischemic neuronal injury. Curr Mol Med 4:87-111.
Sensi SL, Yin HZ, Carriedo SG, Rao SS, Weiss JH (1999) Preferential Zn2+ influx through Ca2+-permeable AMPA/kainate channels triggers prolonged mitochondrial superoxide production. Proc Natl Acad Sci U S A 96:2414-2419.
Sensi SL, Ton-That D, Weiss JH, Rothe A, Gee KR (2003) A new mitochondrial fluorescent zinc sensor. Cell Calcium 34:281-284.
Sensi SL, Canzoniero LM, Yu SP, Ying HS, Koh JY, Kerchner GA, Choi DW (1997) Measurement of intracellular free zinc in living cortical neurons: routes of entry. J Neurosci 17:9554-9564.
Sheline CT, Behrens MM, Choi DW (2000) Zinc-induced cortical neuronal death: contribution of energy failure attributable to loss of NAD(+) and inhibition of glycolysis. J Neurosci 20:3139-3146.
Shi G, Nakahira K, Hammond S, Rhodes KJ, Schechter LE, Trimmer JS (1996) Beta subunits promote K+ channel surface expression through effects early in biosynthesis. Neuron 16:843-852.
Shibata N, Kobayashi M (2008) [The role for oxidative stress in neurodegenerative diseases]. Brain Nerve 60:157-170.
Shimizu T, Wolfe LS (1990) Arachidonic acid cascade and signal transduction. J Neurochem 55:1-15.
Shornick LP, Holtzman MJ (1993) A cryptic, microsomal-type arachidonate 12-lipoxygenase is tonically inactivated by oxidation-reduction conditions in cultured epithelial cells. J Biol Chem 268:371-376.
Sines T, Granot-Attas S, Weisman-Welcher S, Elson A (2007) Association of tyrosine phosphatase epsilon with microtubules inhibits phosphatase activity and is regulated by the epidermal growth factor receptor. Mol Cell Biol 27:7102-7112.
Singer-Lahat D, Sheinin A, Chikvashvili D, Tsuk S, Greitzer D, Friedrich R, Feinshreiber L, Ashery U, Benveniste M, Levitan ES, Lotan I (2007) K+ channel facilitation of exocytosis by dynamic interaction with syntaxin. J Neurosci 27:1651-1658.
Soriano P, Montgomery C, Geske R, Bradley A (1991) Targeted disruption of the c-src proto-oncogene leads to osteopetrosis in mice. Cell 64:693-702.
Stork CJ, Li YV (2006) Intracellular zinc elevation measured with a "calcium-specific" indicator during ischemia and reperfusion in rat hippocampus: a question on calcium overload. J Neurosci 26:10430-10437.
Suh SW, Chen JW, Motamedi M, Bell B, Listiak K, Pons NF, Danscher G, Frederickson CJ (2000) Evidence that synaptically-released zinc contributes to neuronal injury after traumatic brain injury. Brain Res 852:268-273.
Sun H, Shikano S, Xiong Q, Li M (2004) Function recovery after chemobleaching (FRAC): evidence for activity silent membrane receptors on cell surface. Proc Natl Acad Sci U S A 101:16964-16969.

Surmeier DJ, Foehring R (2004) A mechanism for homeostatic plasticity. Nat Neurosci 7:691-692.
Tal TL, Graves LM, Silbajoris R, Bromberg PA, Wu W, Samet JM (2006) Inhibition of protein tyrosine phosphatase activity mediates epidermal growth factor receptor signaling in human airway epithelial cells exposed to Zn2+. Toxicol Appl Pharmacol 214:16-23.
Tamkun MM, O'Connell K M, Rolig AS (2007) A cytoskeletal-based perimeter fence selectively corrals a sub-population of cell surface Kv2.1 channels. J Cell Sci 120:2413-2423.
Tanuma N, Nakamura K, Kikuchi K (1999) Distinct promoters control transmembrane and cytosolic protein tyrosine phosphatase epsilon expression during macrophage differentiation. Eur J Biochem 259:46-54.
Tarohda T, Ishida Y, Kawai K, Yamamoto M, Amano R (2005) Regional distributions of manganese, iron, copper, and zinc in the brains of 6-hydroxydopamine-induced parkinsonian rats. Anal Bioanal Chem 383:224-234.
Tatosyan AG, Mizenina OA (2000) Kinases of the Src family: structure and functions. Biochemistry (Mosc) 65:49-58.
Taylor RC, Cullen SP, Martin SJ (2008) Apoptosis: controlled demolition at the cellular level. Nat Rev Mol Cell Biol 9:231-241.
Tiran Z, Peretz A, Attali B, Elson A (2003) Phosphorylation-dependent regulation of Kv2.1 Channel activity at tyrosine 124 by Src and by protein-tyrosine phosphatase epsilon. J Biol Chem 278:17509-17514.
Tiran Z, Peretz A, Sines T, Shinder V, Sap J, Attali B, Elson A (2006) Tyrosine phosphatases epsilon and alpha perform specific and overlapping functions in regulation of voltage-gated potassium channels in Schwann cells. Mol Biol Cell 17:4330-4342.
Toledano-Katchalski H, Tiran Z, Sines T, Shani G, Granot-Attas S, den Hertog J, Elson A (2003) Dimerization in vivo and inhibition of the nonreceptor form of protein tyrosine phosphatase epsilon. Mol Cell Biol 23:5460-5471.
Tonks NK (2006) Protein tyrosine phosphatases: from genes, to function, to disease. Nat Rev Mol Cell Biol 7:833-846.
Trimmer JS (1991) Immunological identification and characterization of a delayed rectifier K+ channel polypeptide in rat brain. Proc Natl Acad Sci U S A 88:10764-10768.
Trimmer JS (1993) Expression of Kv2.1 delayed rectifier K+ channel isoforms in the developing rat brain. FEBS Lett 324:205-210.
Trimmer JS, Rhodes KJ (2004) Localization of voltage-gated ion channels in mammalian brain. Annu Rev Physiol 66:477-519.
Tsuk S, Lvov A, Michaelevski I, Chikvashvili D, Lotan I (2008) Formation of the full SNARE complex eliminates interactions of its individual protein components with the Kv2.1 channel. Biochemistry 47:8342-8349.
Tsuk S, Michaelevski I, Bentley GN, Joho RH, Chikvashvili D, Lotan I (2005) Kv2.1 channel activation and inactivation is influenced by physical interactions of both syntaxin 1A and the syntaxin 1A/soluble N-ethylmaleimide-sensitive factor-25 (t-SNARE) complex with the C terminus of the channel. Mol Pharmacol 67:480-488.
Uretsky NJ, Iversen LL (1970) Effects of 6-hydroxydopamine on catecholamine containing neurones in the rat brain. J Neurochem 17:269-278.
Valchar M, Hanbauer I (1995) Rat mesencephalic neuronal cells cultured for different periods as a model of dopamine transporter ontogenesis. Mol Neurobiol 11:111-119.

Volonte D, Galbiati F, Pestell RG, Lisanti MP (2001) Cellular stress induces the tyrosine phosphorylation of caveolin-1 (Tyr(14)) via activation of p38 mitogen-activated protein kinase and c-Src kinase. Evidence for caveolae, the actin cytoskeleton, and focal adhesions as mechanical sensors of osmotic stress. J Biol Chem 276:8094-8103.

Wang X, Xiao AY, Ichinose T, Yu SP (2000) Effects of tetraethylammonium analogs on apoptosis and membrane currents in cultured cortical neurons. J Pharmacol Exp Ther 295:524-530.

Wei L, Xiao AY, Jin C, Yang A, Lu ZY, Yu SP (2004) Effects of chloride and potassium channel blockers on apoptotic cell shrinkage and apoptosis in cortical neurons. Pflugers Arch 448:325-334.

Weiss JH, Sensi SL, Koh JY (2000) Zn(2+): a novel ionic mediator of neural injury in brain disease. Trends Pharmacol Sci 21:395-401.

Weiss JH, Hartley DM, Koh JY, Choi DW (1993) AMPA receptor activation potentiates zinc neurotoxicity. Neuron 10:43-49.

Wittmack EK, Rush AM, Hudmon A, Waxman SG, Dib-Hajj SD (2005) Voltage-gated sodium channel Nav1.6 is modulated by p38 mitogen-activated protein kinase. J Neurosci 25:6621-6630.

Wu W, Graves LM, Gill GN, Parsons SJ, Samet JM (2002) Src-dependent phosphorylation of the epidermal growth factor receptor on tyrosine 845 is required for zinc-induced Ras activation. J Biol Chem 277:24252-24257.

Wudarczyk J, Debska G, Lenartowicz E (1999) Zinc as an inducer of the membrane permeability transition in rat liver mitochondria. Arch Biochem Biophys 363:1-8.

Xiao H, Dai X, Mao X (2001) [Inhibition of voltage-activated outward delayed rectifier potassium channel currents in dorsal root ganglion neurons of rats by lead]. Zhonghua Yu Fang Yi Xue Za Zhi 35:108-110.

Yamasaki S, Sakata-Sogawa K, Hasegawa A, Suzuki T, Kabu K, Sato E, Kurosaki T, Yamashita S, Tokunaga M, Nishida K, Hirano T (2007) Zinc is a novel intracellular second messenger. J Cell Biol 177:637-645.

Yokoyama M, Koh J, Choi DW (1986) Brief exposure to zinc is toxic to cortical neurons. Neurosci Lett 71:351-355.

Yu HB, Li ZB, Zhang HX, Wang XL (2006) Role of potassium channels in Abeta(1-40)-activated apoptotic pathway in cultured cortical neurons. J Neurosci Res 84:1475-1484.

Yu SP (2003a) Na(+), K(+)-ATPase: the new face of an old player in pathogenesis and apoptotic/hybrid cell death. Biochem Pharmacol 66:1601-1609.

Yu SP (2003b) Regulation and critical role of potassium homeostasis in apoptosis. Prog Neurobiol 70:363-386.

Yu SP, Kerchner GA (1998) Endogenous voltage-gated potassium channels in human embryonic kidney (HEK293) cells. J Neurosci Res 52:612-617.

Yu SP, Farhangrazi ZS, Ying HS, Yeh CH, Choi DW (1998) Enhancement of outward potassium current may participate in beta-amyloid peptide-induced cortical neuronal death. Neurobiol Dis 5:81-88.

Yu SP, Yeh CH, Gottron F, Wang X, Grabb MC, Choi DW (1999) Role of the outward delayed rectifier K+ current in ceramide-induced caspase activation and apoptosis in cultured cortical neurons. J Neurochem 73:933-941.

Yu SP, Yeh CH, Sensi SL, Gwag BJ, Canzoniero LM, Farhangrazi ZS, Ying HS, Tian M, Dugan LL, Choi DW (1997) Mediation of neuronal apoptosis by enhancement of outward potassium current. Science 278:114-117.

Yuan LL, Adams JP, Swank M, Sweatt JD, Johnston D (2002) Protein kinase modulation of dendritic K+ channels in hippocampus involves a mitogen-activated protein kinase pathway. J Neurosci 22:4860-4868.

Zaks-Makhina E, Kim Y, Aizenman E, Levitan ES (2004) Novel neuroprotective K+ channel inhibitor identified by high-throughput screening in yeast. Mol Pharmacol 65:214-219.

Zhang DY, Wang Y, Lau CP, Tse HF, Li GR (2008) Both EGFR kinase and Src-related tyrosine kinases regulate human ether-a-go-go-related gene potassium channels. Cell Signal.

Zhang HJ, Liu Y, Zuhlke RD, Joho RH (1996) Oxidation of an engineered pore cysteine locks a voltage-gated K+ channel in a nonconducting state. Biophys J 71:3083-3090.

Zhang Y, Aizenman E, DeFranco DB, Rosenberg PA (2007) Intracellular zinc release, 12-lipoxygenase activation and MAPK dependent neuronal and oligodendroglial death. Mol Med 13:350-355.

Zhang Y, Wang H, Li J, Jimenez DA, Levitan ES, Aizenman E, Rosenberg PA (2004) Peroxynitrite-induced neuronal apoptosis is mediated by intracellular zinc release and 12-lipoxygenase activation. J Neurosci 24:10616-10627.

Zhang ZY, Thieme-Sefler AM, Maclean D, McNamara DJ, Dobrusin EM, Sawyer TK, Dixon JE (1993) Substrate specificity of the protein tyrosine phosphatases. Proc Natl Acad Sci U S A 90:4446-4450.

Zhuo S, Dixon JE (1997) Effects of sulfhydryl regents on the activity of lambda Ser/Thr phosphoprotein phosphatase and inhibition of the enzyme by zinc ion. Protein Eng 10:1445-1452.